Università degli Studi della Calabria

Facoltà di Scienze M.F.N.
Dipartimenti di Chimica e di Fisica

Dottorato di Ricerca in
"Scienze e Tecnologie delle Mesofasi e dei Materiali Molecolari"

(STM^3)- Dottorato Internazionale XIX° ciclo

PH.D. Thesis
Organic Thermovoltaic Devices (ORTHEC)

Supervisore

Prof. Giuseppe CHIDICHIMO

Candidato

Dott. Luca D'AGOSTINO

Anno Accademico 2003-2006

Alla mia Famiglia.

"Non bisogna far violenza alla natura, ma persuaderla."
"Nessuno, vedendo il male, lo preferisce, ma ne rimane ingannato, parendogli un bene rispetto al male peggiore.."

Epicureo
(Samo, 341 a.C. – Atene 252 a.C.)

Contents.

Chapter 1

Motivation - Outline.

1.1 Motivation.

To date, the primary source of energy is the combustion of fossil materials such as petroleum, coal or natural gases. The environmental impact of such combustion is dangerous for the planet so, over the past forty years, attempt has been made to discover new technologies and methods to use the power of the elements to produce viable energy. Until today the way to transform wind, water, but first of all solar energy into electrical or thermal energy has been studied. Useful devices apt to convert solar energy are photovoltaic cells, solar ovens and concentrators. In many populous regions of Earth, like Mediterranean area, it is possible to have, for 10 month out of about 12 free energy from the sun [1].

On the other hand, some attempts have been made to have free-pollution energy using biomass fuels, as in Brazil where 29-year-old ethanol fuel program [2] uses cheap sugar cane, mainly bagasse (cane-waste) for process heat and power, and modern equipment, and provides a ~22% ethanol blend used nationwide [3], plus 100% hydrous ethanol for four million cars [4].

Local minor low-pollution sources of energy could be considered geothermal energy and industrial or domestic waste biomass energy as biogas or waste fuels.

In this PhD Thesis nuclear energy will be not taken into account as it is a free-pollution source, but we will consider only those energy conversion processes (eco-compatible or not)in which “co-products” of energy transformation are involved, for example such of combustion of fossil oil or bio-fuel, or radioactive slag [5]. The two focal items that convert an energy transformation process into an eco-compatible one are the time scale in which the “co-products” are absorbed and retransformed from the Earth using its natural methods like decomposition

mechanisms or high temperature and high pressure reaction as occurs in the Earth mantel or core, and their impact on Earth life. As a consequence, the fossil oils or gases and radioactive material, are not renewable polluting materialsbecause the time scale of such regeneration is too long (about one hundred thousand years for fossil oil and several million year ex. for the uranium) and the effects on Heart life are lethal [6].

Until now several problems have come together, focusing on the global energy question; but the increase of the number of people that could access to the "energy" for industrial and domestic purpose is an urgent topic: population growth [7] and energy consumption are inexorably tied together (*Fig. 1.1*).

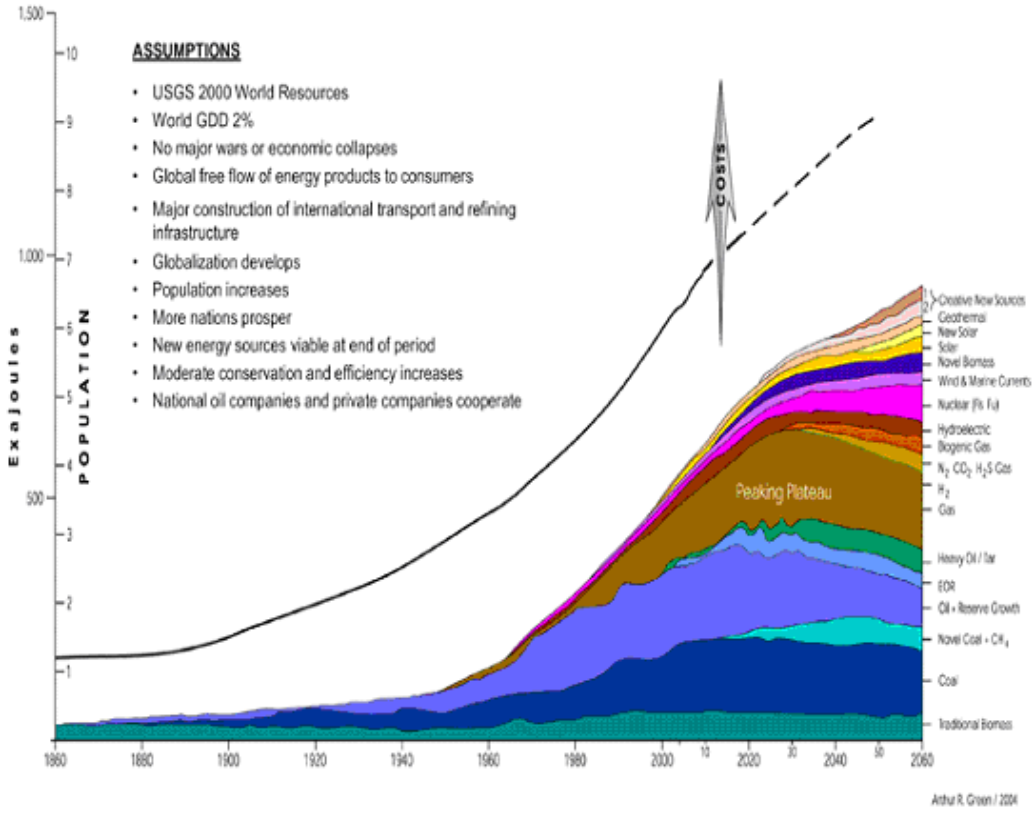

Fig.1.1 *Energy consumption and mix, 1860-2060, along with population growth.*

Thus our heritage to future generation should be a sustainable eco-compatible energy. The high price of oil and gas fossil materials, increasing during last year not only for political and economical purpose but mostly for the prevision of vanishing sources in few decades gives new impulse to free-pollution and suitable energy system production research but, on the other hand, allows the utilization of coil and natural gasses [8] (*Fig.1.2 and 1.3*) to increase.

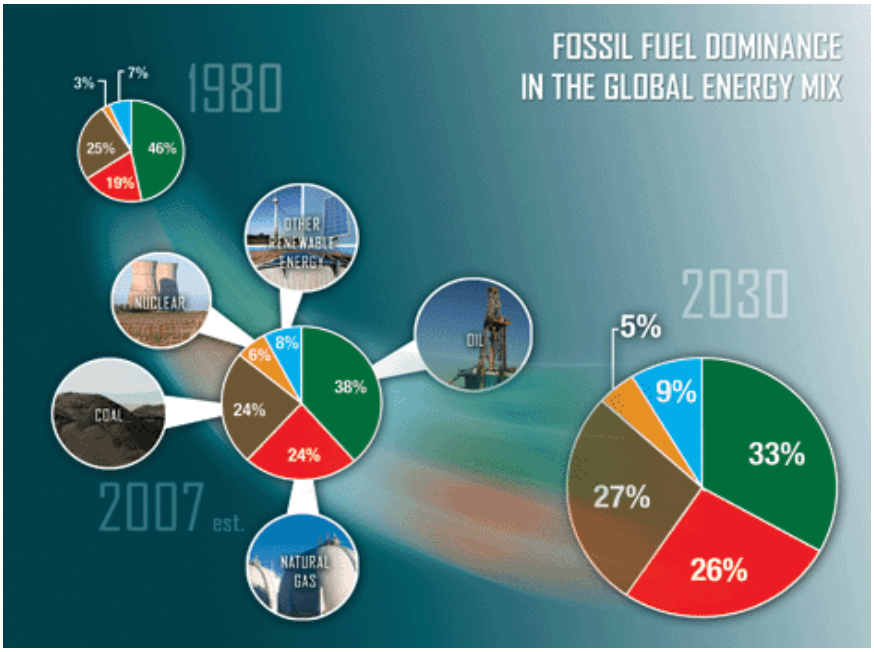

Fig.1.2 *Statistical estimation of global energy sources from 1980 to 2030.*

The exploitation of energy sources involve a large earth pollution, accomplished by an increase of destructive phenomena for the earth ecosystem and dangerous for human life like CO_2 [9], N_xO_y [10], SO_2 [10], tropospheric ozone [11], aromatic compounds, toxic metal and compound fine-powders, emissions.

Population growth (*Fig 1.3*) associated to this badly "global energetic system" will produce unexpected negative effects on our planet and unpredictable consequences for our life.

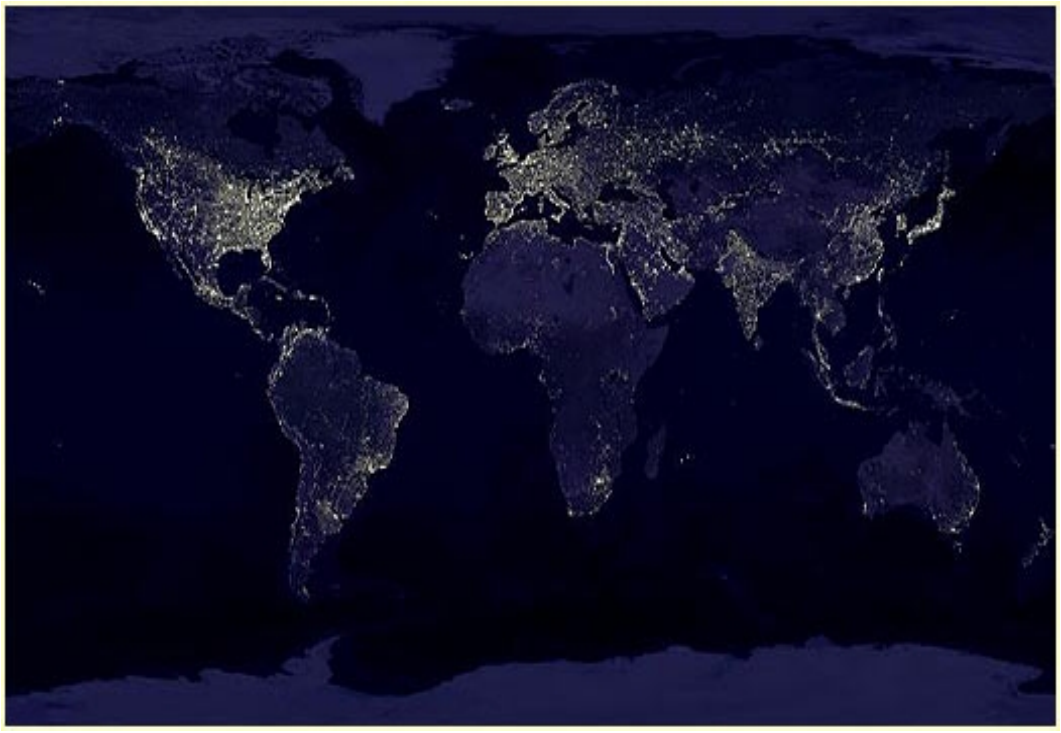

Fig.1.3 *Computer amplification of lights of NASA's picture of the earth by night the 11th September of 2007 .*

Energy consumers, for domestic or industrial purpose, are growing in quasi-exponential trend, because energy manage is strictly connected whit better life conditions. Wherever it is a really positive target especially in some "emerging" planet areas, the earth's energetic resources used to date are not enough for all of us and the "such earth's capacity" or "such renovation time" correlated to the existing energy conversion methods are insufficient.

1.2 The aim of the work

The object of this PhD. thesis work was development and characterization of novel thermal energy conversion devices, which could be used in large scale application as well as in small local applications for domestic or industrial purposes, where a thermal gradient could be available by sun or other sources.

More precisely the main task of the researches has been to develop a novel organic thermovoltaic film and related devices. The adjective "thermovoltaic" it here used to define a devices very structural analogous to Photovoltaic devices, but being thermal energy converters instead of being photon energy converters. Since now thermal energy converters, generating electric power have been mainly defined as thermoelectric (TE) or thermionic (TI), or thermophotovoltaic (TPV) converters.

Thermoelectric materials work by selectively transmitting "hot" (high-energy) electrons from a warm reservoir to a cold reservoir, such that a thermal gradient can drive current flow against a bias voltage V, leading to power generation [12,13]. The major problem which needs to be solved, in these device applications, is to increase their efficiency, which is limited by the fact that thermoelectric materials establishes a direct thermal contact between the hot and the cold reservoir. This mechanism subtracts heat to the hot reservoir just to worm up the cold one. In recent years several authors have made many efforts to reduce this problem by planning special materials which would allow an easy conduction of the electron, preventing at the same time the heat conduction. In this contest it has been recognized that the exact form of the electronic density of states (DOS) in a thermoelectric material has a strong impact on the efficiency of power generation [14-17]. This is because, whereas each electron contributes the same energy eV to the power output, regardless of the electron's initial energy, the efficiency is highest when the electrons that contribute to the current possess only the minimum thermal energy required to surmount the bias voltage. Electrons that leave the hot reservoir with an excess of thermal energy cool the hot reservoir more than necessary, reducing efficiency.

Semiconductor hetero structures grown by modern epitaxial methods are one of the candidate for high-efficiency thermo-electrics because it is possible to

carefully engineer the electronic DOS [14,15,18,19], employing both band offsets and quantum confinement phenomena. Mahan and Sofo pointed out the advantage of delta-like singularities in the electronic DOS and suggested the use of narrow states in rare earth metals [20], and Hicks and Dresselhaus proposed that the reduced dimensionality of superlattices could be used to enhance the electronic density of states in energy ranges near the conduction band edge to improve the efficiency of power generation [12]. An additional advantage of the use of superlattices is the expected reduced thermal conductivity due to increased phonon scattering rates and phonon-localization, such that parasitic heat leaks can be reduced. Indeed, several authors have shown that thermal conductivity in superlattices is much lower than in pure bulk materials and can be lower than the alloy limit [21-23]. The best performing thermoelectric materials demonstrated to date are based on superlattices [24,25]. Heterostructured, low-dimensional materials are therefore thought to be the most promising candidate for broad, economical applications of thermoelectric power generation and heat recovery in the relatively near future, and considerable efforts are being expended to develop and characterize such materials.

A very original research idea, which has been tested in the frame of this thesis work, to improve thermoelectric devices, is to develop a new generation of thermovoltaic devices, by using plastic amorphous semiconductor film, instead of inorganic semiconductors. In this system, due to lack of an ordered lattice, phonon transmission is expected to be very low. On the other hand, work on electrochromic devices conducted at Calabria University [26] has shown that a certain amount of electron conduction can be obtained by inserting specially planned organic molecules in plastic matrices, where the electron conduction is obtained both by intermolecular electron excitations and intramolecular charge transfer jumps. The kind of device which realization was hypothesized at the beginning of this thesis is conceptually represented in *Fig.1.4* and *Fig.1.5*.

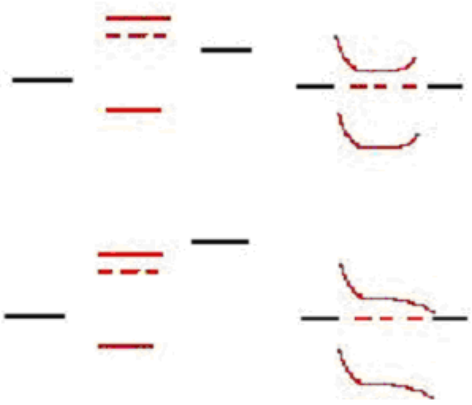

Fig.1.4 *Conceptual representation of the novel thermovoltaic device using a n-type film.*

The scheme reported in the top, left side of the *Fig. 1.4* shows (before contact) the work functions (black lines) of two different metal layers, and the HOMO, LUMO and Fermi level of an organic molecule (red lines). On the top, right side of *Fig.1.4* the possible band configuration obtained after sandwiching the plastic layer of the organic molecule between layers of the two different metals, are shown in an open circuit configuration, and absence of heat flux (equilibrium configuration). The other two schemes reported in the bottom of *Fig.1.4* represents an analogous situation where the second metal layer has an even lower electron extraction work. A blocking contact establishes especially between the higher work function metals and the organic molecule. The base hypothesis we worked with concerns the possibility to promote electron transfer between the highest work function metal to the lower work function metal, across the plastic film of the organic molecule, by using a thermal gradient, with the hot side applied on the left metal layer. The thermoelectric device obtained in this way is expected to have a good efficiency if the barrier created at the left metal /organic contact would not be to high with respect to KT energy at the temperature of the hot reservoir. In practice barriers greater than 0.1 Ev should be avoided (consider that KT is about 0.03 Ev at room temperatures).

In *Fig. 1.4* the central film molecules are supposed to be n-doped. Analogous configuration can be represented in the case of a p-doped central film, as it is shown in *Fig.1.5*:

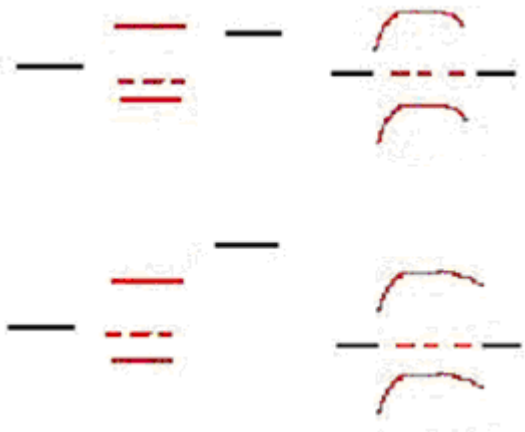

Fig.1.5 *Conceptual representation of the novel thermovoltaic device using a p-type film.*

Organic semiconductors become n-type or p-type as function of the nature of chemical substituents or dopants added to the molecular blend. As a general rule the presence of electron donor groups confers a n-type character to the semiconductor, while acceptor groups or dopants generates p-type semiconductors.

In a practical application the active molecules, having electronic levels compatible with he working strategy reported in *Fig. 1.4*, can be dissolved in a plastic supporting matrix having good mechanical, chemical and thermal properties. Of course such a blend of organic molecules would need to have a sufficient electrical conduction, in order to allow the electron transport from the hot to the cold side, and a low heat conduction in order to guarantee the establishing a the required temperature gradient, without transmitting to much heat from the hot to the cold reservoir.

It has been proved that semiconductor level of electronic currents can be obtained in plastic films by mixing π-conjugated organic oligomers such as poly-tiophenes, poly- vyniles, fullerenes, etc. These systems have been deeply investigated in photovoltaic devices where very tiny layers need to be applied. Recently P.Reddy et al**.** [27] have studied the possibility to build up very small thermoelectric devices, by using benzene-dithyol semiconductor molecules (BDT), sandwiched as very tin layers between two gold metal layers. We will come back on this device in chapter 4, where we use it for comparison. Nevertheless we believe that the idea to use these kind of molecules, as tin layer

semiconductors, in thermoelectric devices does not drive through a real technologic development of thermoelectric conversion , since the heat conduction across tin layers is very high When using plastic semiconductor films in thermoelectric conversion greater thickness of the central semiconductor film is required to avoid direct heat transfer between the hot and the cold reservoirs. For these reason greater specific electron conductivities need to be obtained in the central plastic layers with respect to those used in photo voltaic devices. Fortunately in our case we do not need to worry about electron /hole recombination, so the thickness of the central film can be increased at least up to values of millimetres.

It must be underlined that the thermoelectric plastic layer (or layers) should be blends of a supporting polymer , having good mechanical and chemical properties, with other electron carrier molecules. The supporting polymer matrix can be one of the very stable UV resistant polymer currently used in the manufacture of special glass (automotive front shield, bullet proof glasses) such as poly(vinyl butyral-co-vinyl alcohol-co-vinyl acetate) (PVB), poly(vinyl formal) (PVFM) etc. A limited percentage of these polymer is able to dissolve or disperse in a very homogeneous way big percentages of other molecules. The composite films can be obtained as self supported solid films which are easily laminated between other layers (the metal layers in our case), thus ensuring low cost manufacturing processes. Different kind of active electron carrier molecules can be dissolved in the supporting plastic matrix in order to get the desired LUMO levels (see *Fig.1.4* and *Fig.1.5*) and the required conductivity. By taking into consideration the need of a sufficiently high electron conductivity the best molecules to candidate as charge carriers into the plastic film should again be π-conjugated organic oligomers such as poly-tiophenes, poly- vyniles, fullerenes etc., or blend of these compounds, but we will show in the next that these molecules do not posses the correct LUMO Levels. We will show in the next that the most encouraging results have been obtained by using blends of PVB and PVFM with bipyrimidinium salts.

Although the modern application of heat conversion in electric power seems to cover a niche market, it is obvious that thermal direct production of electric

energy has a very high potential both in large and small scale. How just mentioned above the use of organic materials should improve the device efficiency. In this case the application of low gradient working Thermoelectric devices, will become numerous: they could work a) during the night or in dark conditions b) in cold as well in hot places (they need a ΔT, not an absolute temperature value); and they could be useful in every condition when a thermal gradient is available (ex. sea or lake surfaces).

1.3 Outline

The sequence of the arguments exposed in this thesis work is given in the following.

In the second chapter a brief review of the principal renewable energy conversion systems will be presented, The principal devices on sales all over the world will be mentioned pondering both technologic and economic aspects, and linking positive features and hurdles for each energy conversion process.

Within the third chapter phenomenological laws that route fluxes conversions and stationary states will be mentioned underlining the transformations from heat flow to current. A detailed section will argue the chemical-physic concepts at the origin of the novel thermoelectric devices, and some efficiency parameters will be discussed..

In the fourth chapter novel organic thermovoltaic devices will be discussed, giving working and performance details, also relating phenomenological laws of energy conversion and charge mobility molecular mechanisms the experimental results are presented. Several experimental data have been collected, starting from preliminary experiments, which were carried out to observe an effective stationary state in our devices, to “step up” experiments using several materials and composition ratios. Appropriate experiments to improve and investigate the devices will be mentioned giving an idea of widespread materials applications. Also long-term experiment will be illustrated to evaluate the energetic, theoretical and technological aspects.

Chapter 2

Eco-compatible Energy conversion.

In order to highlight the scientific and practical importance to develop new efficient and low cost thermovoltaic devices, this chapter gives an overview of the most important technologies available to day for chemical, photon and thermal energy conversion.

2.1 Hydrogen and fuel cells

Hydrogen and fuel cells (FCs) [28] have the potential to solve relatively the dependence on petroleum imports, poor air quality, and greenhouse gas emissions (*Fig. 2.1 a,b*). FCs are electrochemical devices that convert the chemical energy of the fuel and oxidant directly into electricity and heat offering high efficiency, low emissions, modularity and quiet operation and they are a promising candidate for powering a wide range of applications, from portable electronics via vehicles to power stations. FCs generate electricity from a simple electrochemical reaction in which oxygen and hydrogen combine to form water. There are several different types of fuel cell but they are all based around a central design which consists of two electrodes, a negative anode and a positive cathode. These are separated by a solid or liquid electrolyte that carries electrically charged particles between the two electrodes. A catalyst, such as platinum, is often used to speed up the reactions at the electrodes.

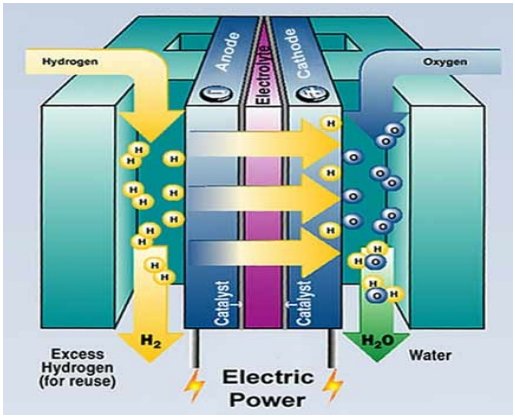

(a)

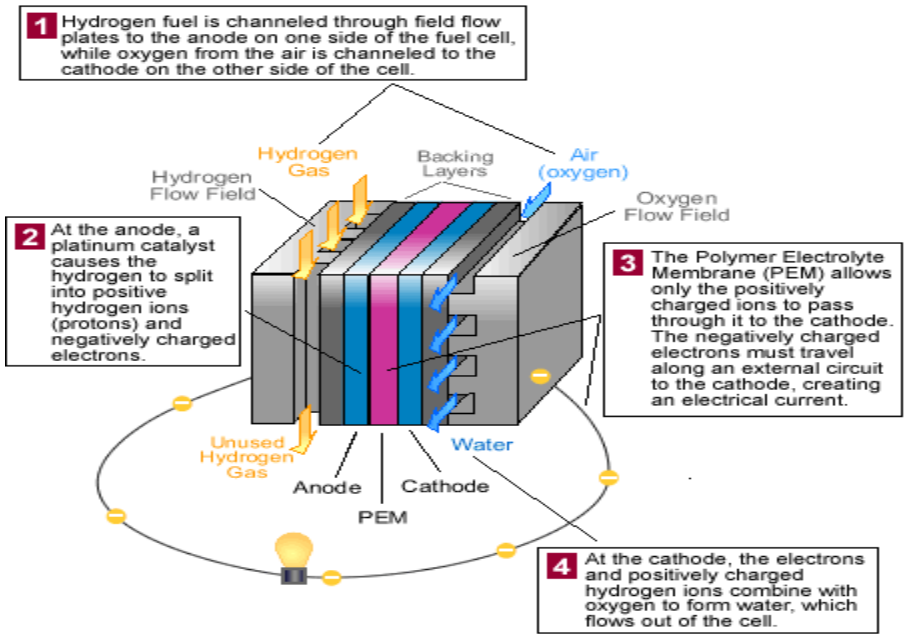

(b)

Fig.2.1 *Standard scheme of individual fuel cell (FC), H_2 fuel and oxidant (oxygen)were used to generate electric power by electrochemical reactions (a), several FC typologies exist according the electrolyte and fuels used: (b) low temperature fuel cell PEMFC.*

FCs are classified according to the nature of the electrolyte and each type requires particular materials and fuels and is suitable for different applications that imply the application in large or small scale: Proton Exchange Membrane Fuel Cells (PEMFC) used by NASA to provide power for the Gemini space project

producing 100W per module; Alkaline Fuel Cells (AFC) Alkaline fuel cells are one of the most developed technologies and have been used to provide power and drinking water to space missions, including the US Space Shuttle; Phosphoric Acid Fuel Cells (PAFC) is currently the most commercially advanced fuel cell technology: currently a number of working units with outputs ranging from 0.2-20MW installed around the world providing power to hospitals, schools and small power stations; Molten Carbonate Fuel Cells (MCFC) that works at too high temperature (650 °C) producing up to 2MW systems; Solid Oxide Fuel Cells (SOFC) work at even higher temperatures than molten carbonate cells (800-1000°C); Direct Methanol Fuel Cells (DMFC); is a variant of the PEMFC which uses methanol directly without prior reforming; Regenerative Fuel Cells (RFC) [29] technology works on the same basis as a conventional cell in that hydrogen and oxygen are used to generate electricity.

Otherwise, one more time, sun, wind and water represent the real effort to renewable energy conversion system (*Fig 2.2*) also using RFC technologies.

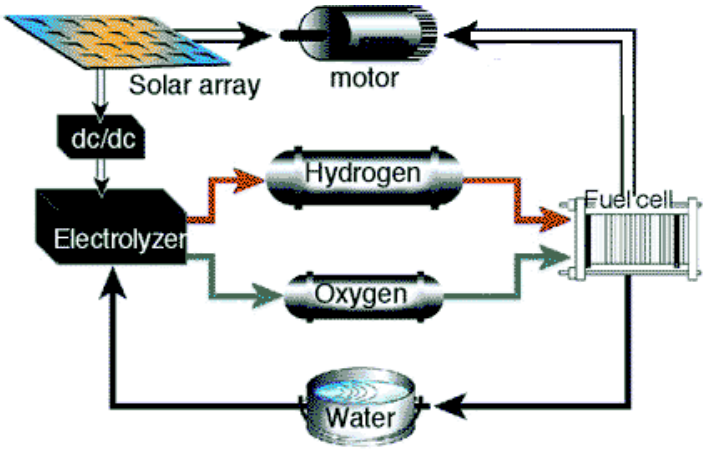

(a)

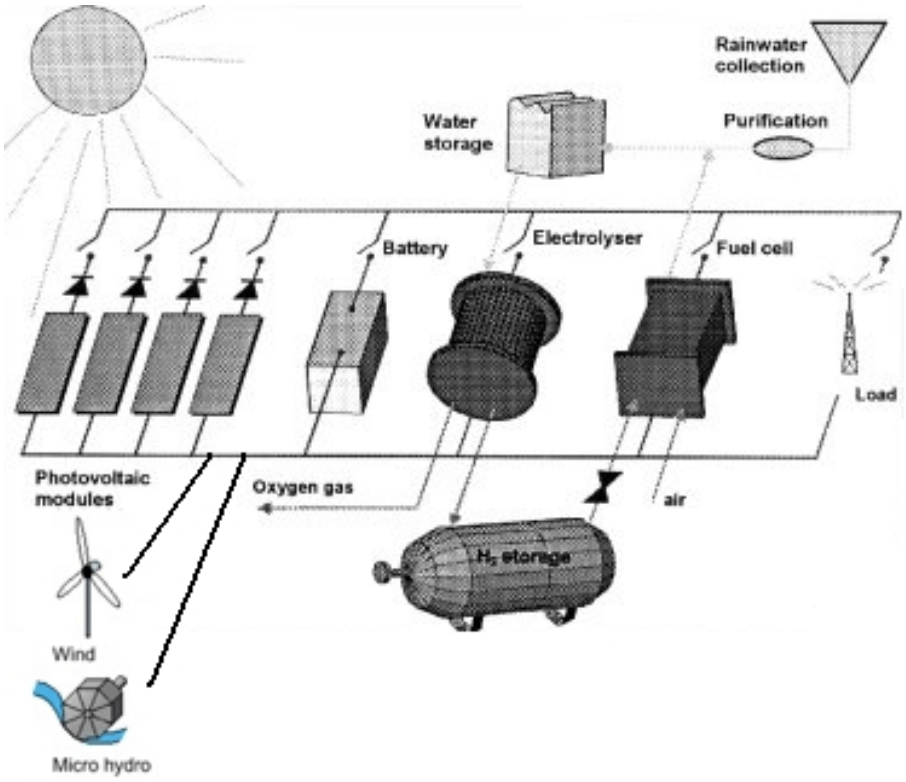

(b)

Fig.2.2 *(a) Scheme of solar RFC cell in which electrolyser works to produce hydrogen and oxygen in sun presence used by FC in sun and dark condition;(b)Scheme of a seasonal energy storage of PV-Hydrogen system.*

The RFCs perform the electrolysis reverse reaction. The water generated in the fuel cell is fed to a solar powered electrolyser where it is separated into its constituent components of hydrogen and oxygen which are then fed back to the fuel cell. In this way a closed system is formed which does not require external hydrogen generation. The development of a commercial system is some way off and there are a number of issues that need to be addressed including cost and the perfecting of a reliable way of harnessing solar and wind power.

However when hydrogen is obtained from renewable energy sources, no global warming gases are emitted. Hydrogen fuel cell systems store intermittent solar and wind power so there is no need for back-up generators powered by fossil fuels.

2.2 Wind and Sun energy conversion systems.

To date the most common sources of renewable energy are **wind** [30] and sun. The first one could be a valid alternative to fossil fuels but the primary obstacle is represented by the high cost of power plant element. Intrinsic building costs of turbines associated with locating a accurate installation place, constantly winded places needed, mean that it is not for a domestic or local use: they need a lot of space considering the turbulence that occurs for each one element (both axial and longitudinal turbines). Otherwise wide use of wind power have to be encouraged by nations government in order to replace a lot of energy from combustion: at the end of 2006, worldwide capacity of wind-powered generators was 73.9 gigawatts; although it currently produces just over 1% of world-wide electricity use, it accounts for approximately 20% of electricity production in Denmark, 9% in Spain, and 7% in Germany. Globally, wind power generation more than quadrupled between 2000 and 2006 [31].

However in the direction of local purpose use (domestic and industrial) and wide range power plant installations, solar energy represent the best alternative to convert free energy in eco-compatible system.

To date the most efficient methods to "harvest" the **sun energy** are the "solar heating systems (SHS)", "concentrating solar power systems (CSP)" and the "photovoltaic systems (PV)"; lees developed methods are "thermophotovoltaic (TPV)", "thermionic (TI)" and "thermoelectric (TE)" energy conversion systems, that represent the next future generation techniques.

SHS [32] harvest the power of the sun to provide solar thermal energy for solar hot water and solar space heating by solar thermal collectors: flat-plate or evacuate tube collectors, adsorbing plates, parabolic collectors and sun-tracking plates are just some example of large literature and patents existing. Also they have some kind of storage system, except solar pool heaters and some industrial systems that use energy "immediately", collecting directly the sun's energy to heat air or a fluid.

Large-scale solar thermal technology is known as CSP [33] (*Fig 2.3*). This research and development focuses on three types of concentrating solar technologies: trough systems, dish/engine systems, and power towers. These solar

technologies are used in CSP plants that use different kinds of mirror configurations to convert the sun's energy into high-temperature heat.

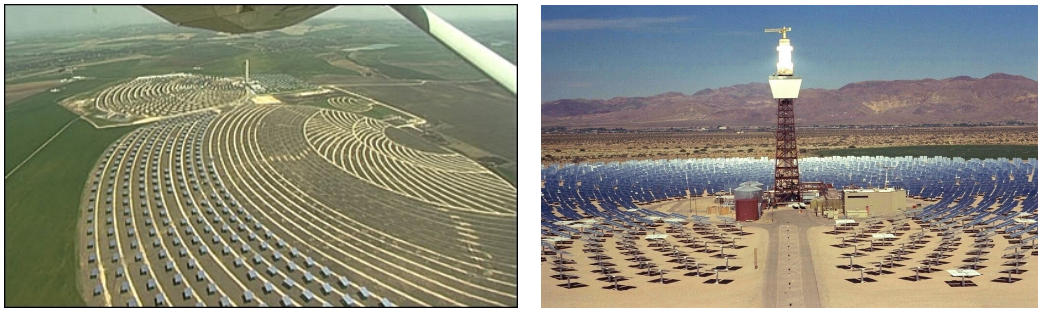

(a) *(b)*

Fig.2.3 *The 11 MWatt CSP plant is located in Seville, Spain have the capacity to produce sufficient energy to let some 180,000 homes consume power from it (a) and the 64MWatt in California, USA Creek (b).*

The heat energy is then usually used to generate electricity in a steam generator, but is it also possible to use TI, TPV or TE devices as shown in the apposite sections in this chapter.

Photovoltaic devices (PV) can be made from various types of semiconductor materials, deposited or arranged in various structures, to produce solar cells that have optimal performance to convert sun light in electrical current. A PVc is the basic building block of a PV (or solar electric) system. An individual PVc is usually quite small, typically producing about 1 or 2 watts of power. To boost the power output of PVcs, they were connected together to form larger units called modules. Modules, in turn, can be connected to form even larger units called arrays (*Fig. 2.4*), which can be interconnected to produce more power, and so on. In this way, we can build PV systems able to meet almost any electric power need, whether small or large.

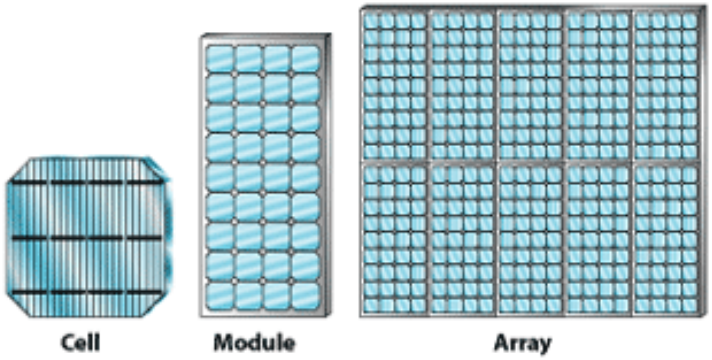

Fig.2.4 *Photovoltaic cell, module and array.*

By themselves, modules or arrays do not represent an entire PV system. We also need structures that point them toward the sun, and components that take the direct-current electricity produced by modules and "condition" that electricity, usually by converting it to alternate-current electricity. We might also want to store some electricity, usually in batteries or to electrical typical network, for later use. All these items are referred to as the "balance of system" (BOS) components. Combining modules with the BOS components creates an entire PV system.

2.2.1 Inorganic photovoltaic cell (IPVc).

In its simplest form, the PVc [34] consists of a junction formed between n-type and p-type semiconductors, either of the same material (homojunction) or different materials (heterojunction) (*Fig 2.5*).

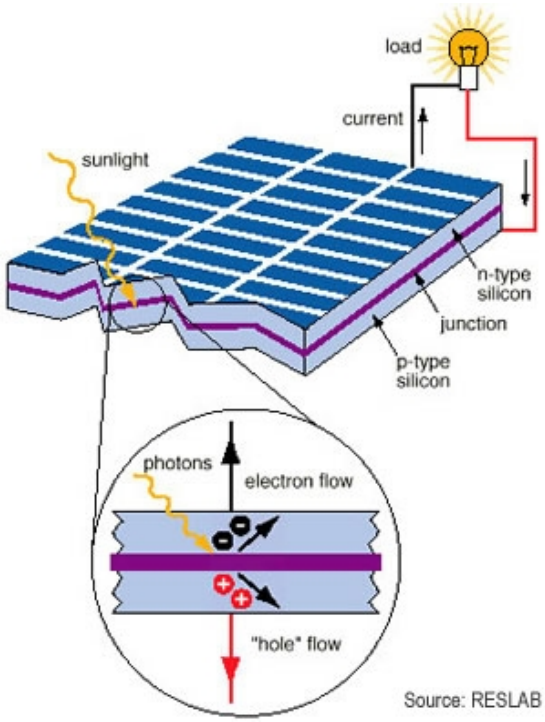

Fig.2.5 *Sun light effect on silicon(p-n) photovoltaic cell: the incident light produce a charge separation and a direct current.*

The unique possible free electrons motion is regulated by the inner electric field generates when n- and p- type semiconductor were assembled together. In fact when the two joined semiconductors have different work functions (*Fig 2.6 a,b*), electrons are driven off from the highest work function electrode that became the positive pole and, passing throw the device, they are collected at the interface near to the lowest work function electrode that became the negative pole [35]. In other words the two semiconductors reach the same Fermi level value.

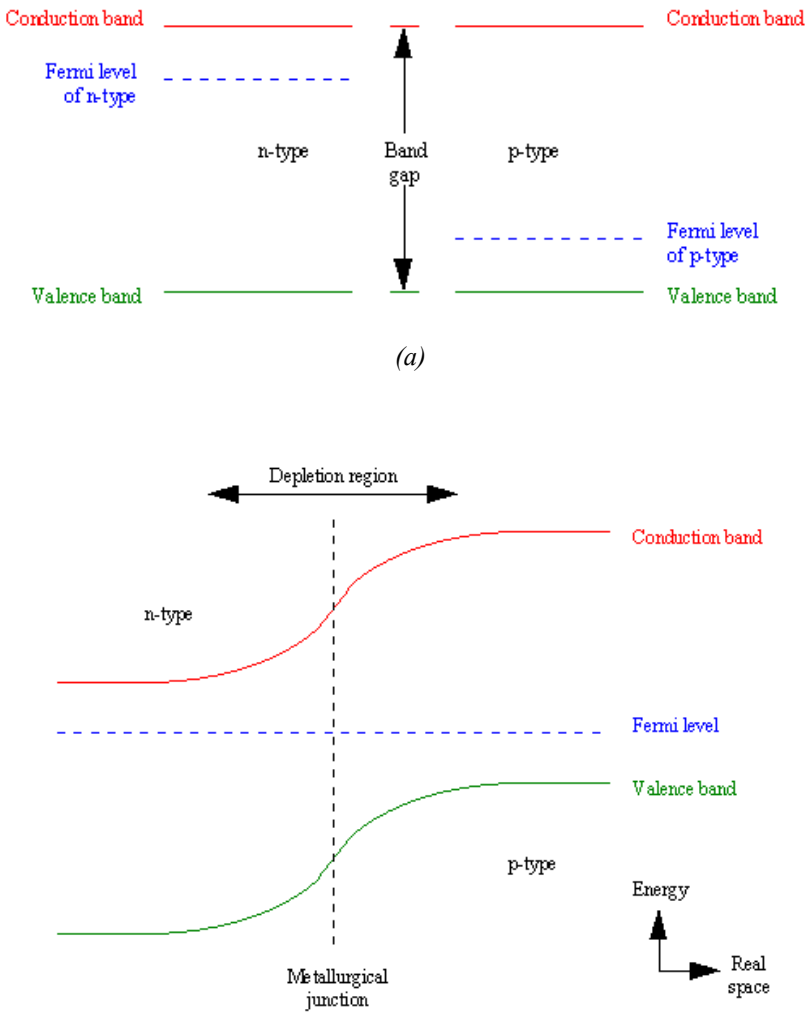

Fig.2.6 *Energetic representation of p-n semiconductors bandgap (a) in isolate p and n type, (b) when junction occurs and Fermi level achieved..*

However an inner electric field at semiconductors/electrode interfaces are generated and the system is in equilibrium state. At the p-n interface, the sunlight induces a charge separation that drives free electrons into n-type semiconductor and a electrons depleting (the "holes") into p-type one. This charges, moving across the bulk according the inner electric field, produce a direct current (*Fig. 2.7*).

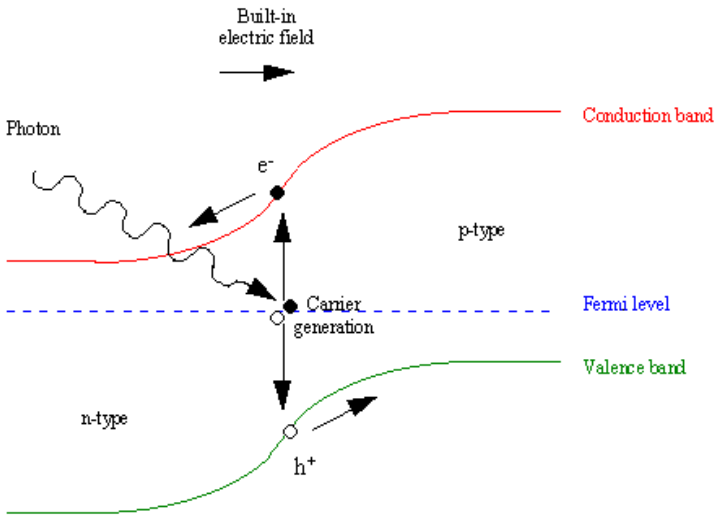

Fig.2.7 *Energetic representation of p-n semiconductors bandgap when separation charge was induced by light photons.*

If an external load is connected in series with device, a current passes through the load in order to re-establish the equilibrium condition. Obviously electron flow does not occur when no more photons irradiate the device, instead the system works in a stationary state in witch the radiation energy is converted in current.

By far the most common material for solar cells is crystalline silicon [36] and these cells can be divided into a number of categories (*Tab 2.1*): "Monocrystalline wafers" are the most efficient of the PV technologies in good light conditions. However, since they are cut from cylindrical ingots the cells are normally pseudo-square and cannot completely cover a module without a substantial waste of space. This makes them more expensive than other technologies; "Poly or multi crystalline cells**"** are made from cast ingots - large crucibles of molten silicon carefully cooled and solidified. These cells are cheaper than single crystal cells and used to be less efficient but steady developments in PV technology are now delivering comparable performance. They can easily be formed into square shapes that cover a greater percentage of a panel than monocrystalline cells; "Thin film approaches" are module-based. The entire module substrate is coated with the desired layers and a laser scribe is then used to delineate individual cells. Thin film PV is efficient in low light conditions and very sturdy; "Inorganic hybrid

cells" are a combination of monocrystalline and thin-film technologies, this has high peak output coupled with excellent performance in poor light conditions [37].

Type of Solar PV	'Thin Film'	Polycrstaline	Monocrystalline	'Hybrid'*
Cell Efficiency at STC**	8-12%	14-15%	16-17%	18-19%
Module Efficiency	5-7%	12-14%	13-15%	16-17%
Area needed per kWp* (for modules)**	**Kaneka** module: 15.5m² Unisolar module: 16m²	**Sharp** modules: 8m²	**Sharp** modules: 7m²	**Sanyo** modules: 6 - 6.5m²
Area needed per kWp (for BIPV)	Solar metal roofing: 23.5m² Glass-Glass laminate: 25m²	Glass-Glass laminate: 10m² - 30m² (dependent on cell spacing)	**C21e** tile: 7.8m² **Sunslate**: 10m² Glass-Glass laminate: 8m² - 30m² (dependent on cell spacing)	n/a
Annual energy generated per kWp (in UK) (for south facing system at 30°)	800 kWp/kWp	810 kWp/kWp	830kWp/kWp (C21e) 750kWp/kWp (generic)	865kWh/kWp
Annual energy generated per m² (for south facing modules at 30°)	50-52kWh/m²	100kWh/m²	107kWh/m²	139-150kWh/m²
Annual CO2 savings per kWp	454kg/kWp	460kg/kWp	471kg/kWp	491kg/kWp
Annual CO2 savings per m²	28kg/m²	57kg/m²	61kg/m²	79-85kg/m²

* 'Hybrid' PV combines both monocrystalline and thin-film silicon to produce cells with the best features of both technologies
** Standard Test Conditions are: 25 °C, light intensity of 1000W/m2, air mass = 1.5
*** kWp = kilowatt 'peak'. Solar PV products and arrays are rated by the power they generate at STC

Tab.2.1 *Some characteristic values of the four main different types of silicon PVc.*

However many doped semiconductor alloys could be used to built more efficiency IPVcs like gallium arsenide, gallium seleniure, copper indium diselenide or gallium indium phosphate (25% of module efficiency for monocrystalline GaAs

and 30% for GaInP/GaAs device) [38]. Whenever intrinsic costs are so high that their application are for scientific purpose like space research.

2.2.2 Organic photovoltaic cell (OPVc).

Considerably less effort and production energy is necessary if organic semiconductors are used because of simpler processing at much lower temperatures (20-200 °C) than the above mentioned inorganic cells. For example an electro-chemical solar cells using tanium dioxide in conjunction with an organic dye and a liquid electrolyte (ex. the Graetzel dye-sensitized cells) already exceeded 6% power conversion efficiencies and are about to enter the commercial market thanks to their relatively low production costs [39]. The organic photovoltaic cells could be divided into tree main groups: the organic-electrolytic dye sensitized solar cell (DSSC), the fully organic semiconductor polymers cell (POPVc) and the most recent organic/inorganic hybrid cell (HOPVc).

Dye sensitized solar cells (DSSc).

The dye sensitized solar cell (DSSc) [40] is conceptually the nearest nature-like photovoltaic device (considering for example the leafs) and is composed of one metal cathode and one transparent conductor (mostly a conducting oxide on glass), onto one of which a few μm thick film of wide band gap semiconductor has been deposited in the form of a self-connected network of 3nm-sized particles, with a network of similarly (or large sized self-connected pores) between the particles. Energy conversion in a DSSC (*Fig. 2.8*) is based on the injection of an electron from a photoexcited state of the sensitizer dye (typically a bipyridine metal complex) into the conduction band of the nanocrystalline semiconductor (TiO2 is by far the most employed oxide semiconductor). These cells also employ a liquid electrolyte usually an iodide/triiodide redox-active couple dissolved in an organic solvent to reduce the dye cation and to regenerate the ground state of the dye. Regeneration of iodide ions, which are oxidized in this reaction to triiodide, is achieved at a platinized counter electrode (S: represents the dye sensitizer):

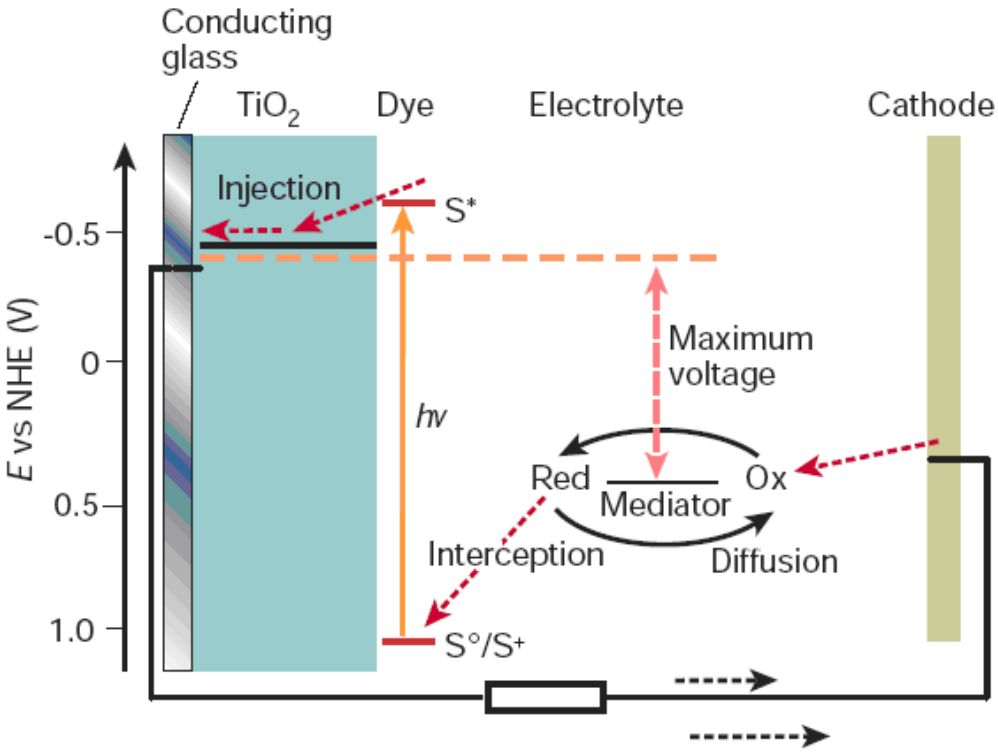

Fig.2.8 *Energetic representation of dye sensitized solar cell.*

At conducting glass (ex. ITO) electrode:

$TiO_2|S + h\nu \rightarrow TiO_2|S^*$

$TiO_2|S^* \rightarrow TiO_2|S^+ + e^-$

At chatode (ex. Aluminum or gold electrode):

$1/2\ I_3^- + e^- \rightarrow 3/2\ I^-$

$TiO_2|S^+ + 3/2\ I^- \rightarrow TiO_2|S + 1/2\ I_3^-$

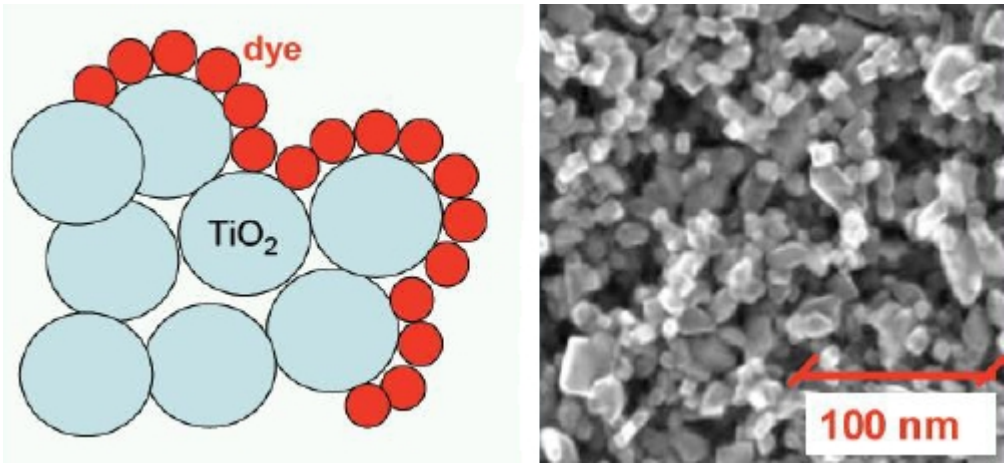

Fig.2.9 *Nanometric TiO_2 dye absorption increases dye active surface.*

The TiO_2 nanoparticles was used also to increase the dye surface and to improve the photon absorption efficiency (*Fig 2.9)*, thus as the depletion surface results larger than single layer device one as well the electron transfer probability between electrolyte molecules and dye was increased.

Organic semiconductor polymers cell (POPVc).

An interesting alternative respect the inorganic cells is given by the semiconductor polymers [41], which combine the optoelectronic properties of conventional semiconductors with the excellent mechanical and processing properties of polymeric "plastic" materials. These can be processed from solution at room-temperature onto flexible substrates using simple and therefore cheaper deposition methods like spin or blade coating. Since the discovery of electro-luminescence in conjugated polymers, this class of materials has been used to build efficient light emitting diodes, field effect transistors, optically-pumped LASERs and photovoltaic diodes.

The advantage of POPVcs when compared to electro-chemical cells is predominantly the absence of a liquid electrolyte, which generates problems with sealing against air, but also the prospect of even cheaper production using large area devices and the use of flexible substrates.

To date several approaches to organic photovoltaic active composites have been investigated. These include strategies based on photo-induced charge transfer between layers of low molecular weight organic molecules (LMW), within halogen-doped organic single crystals, within single component molecular dyes, between conjugated polymers and polymer blends, and within a single-layer blend of a conjugated polymer and an LMW molecule.

Compared with research efforts devoted to small-molecules organic materials, the polymeric photovoltaic materials (and especially donor/apceptor "bulk heterojunction composite") represent a relatively recent approach to exploiting photoinduced charge transfer phenomena for solar energy conversion considering both the small molecules and the conjugate polymer as classical semiconductors.

Interest in conducting and photovoltaic properties of conjugated polymers like polyacetylene, various derivates of polythiophenes (PT) and poly(phenylenevinylenes) (PPV) developed. Instead using of inorganic semiconductor in which electron mobility occurs rapidly after photoinduced charge transfer, the idea of using photoinduced charged state in organic semiconductor class, in conjunction with a molecular electron acceptor to achieve charge separation, is based on the stability of photoinduced exitations such "positive polarons, negative polarons or polarons-excitons" on the conjugated polymer backbone. Motivating results were found in a cell composed by mixtures or bilayers of **conjugated polymers with fullerenes** (C_{60}) [42]. This devices show in solid organic films an ultrafast (subpicosecond) and reversible photoinduced electron transfer from conjugate polymers onto C_{60} (*Fig. 2.10*).

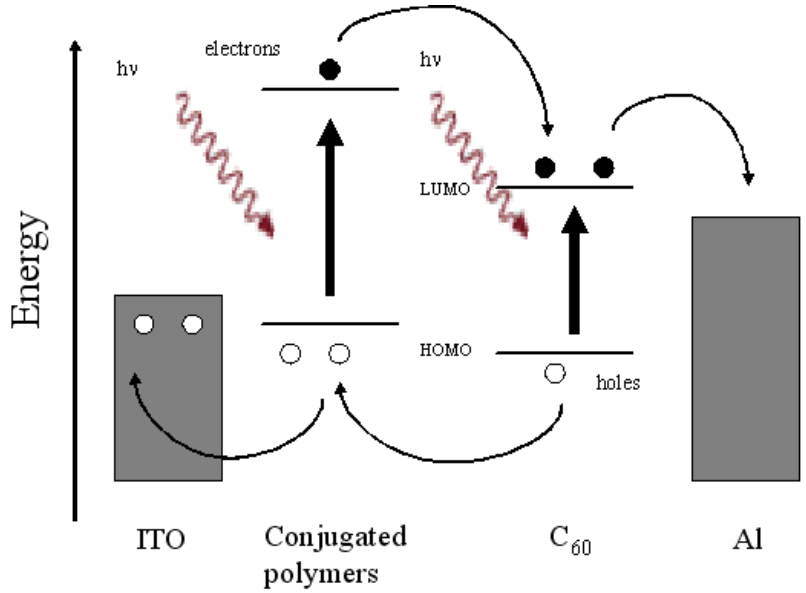

Fig.2.10 *Energetic scheme of C_{60}-conjugated polymer system during photonic exitation*

.

The first photovoltaic devices based on this photoinduced electron transfer were diodes consisting of bilayers from conjugated polymers and fullerene, showing low photovoltaic power conversion efficencies due to the small charge generating interface. However functionalized fullerenes were synthesized in order to increase the C60 group solubility and to produce highly fullerene-loaded composite films. Power conversion efficency made from poly[2-methoxy-5-(2'-ethyl-hexyloxy)-1,4-phenylenevinylene] (MEH-PPV)/fullerene composite was subsequently increased by two order of magnitude and many conjugated polymers were investigated [43]: transpolyacetilene, polythiophene (PT), polycarbazole (PCBZ), polyisothianaphtalene, polyaniline (PAN) etc.

To date exist four different architectures for OPVc: **single layer cells, blend cells, double layer cells, laminated devices**.

Single layer structures consist of only one semiconductor material and are often referred to as ***Schottky*** type devices or ***Schottky diodes*** since charge separation occurs at the rectifying (Schottky) junction with *one* electrode. The other electrode interface is supposed to be of ohmic nature. The structure is simple but absorption covering the entire visible range is rare using a single type of molecule.

The photoactive region is often very thin and since both positive and negative photoexcited charges travel through the same material recombination losses are generally high.

The Schottky barrier [44] is usually defined the energetic barrier when heterojunction occurs. The Schottky barrier is present to silicon inorganic photovoltaic cells but more relevant effect were noticed when organic compounds are put in contact with metal electrodes. Also it is possible to define when an organic material produce a ohmnic or not ohmnic contact considering the HOMO-LUMO organic semiconductor levels, metal electrodes work function and energy Fermi level after heterojunction occurs (*Fig. 2.11 a, b, c, d or also Fig.1.4 and Fig. 1.5*).

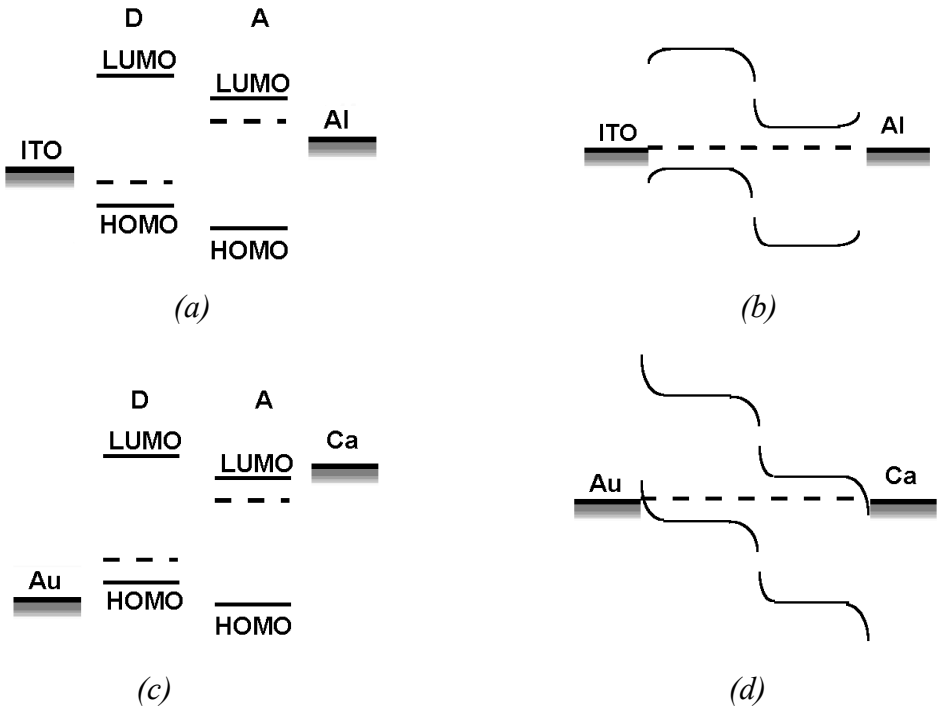

Fig.2.11 *Energy band diagrams of donor D and acceptor A materials devices. a),b) the situation before contact; c),d) after contact the Fermi levels (dashed lines) and work function equalize and band bending occurs. (b) The formation of a blocking contact for holes (ITO/D) and electrons (A/Al). (d) The formation of a non-blocking (ohmnic) contact for holes (Au/D) and electrons (A/Ca).*

The strong point of **blend cell** [45] typology is the large interface area if the molecular mixing occurs on a scale that allows good contact between alike molecules (charge percolation) and most excitons to reach the donor/acceptor interface. This can usually only be partly achieved so the defects of the network structure, particularly the connectivity with the correct electrode, represents a technological challenge.

The double layer cells [46] benefit from the separated charge transport layers that ensure connectivity with the correct electrode and give the separated charge carriers only little chance to recombine with its counterpart. The drawback is the small interface that allows only excitons of a thin layer to reach it and get dissociated.

Laminated devices [47] represent the successful attempt to unify the advantages of the two structures above. Charge separation occurs in the blend layer in the middle that is obtained after laminating the two separate layers together and charge transport can only occur via the correct transport layer. This structure also features the useful options to treat each layer separately (ex. doping, physical/chemical conversion) before form ing the blend layer and instant encapsulation between the two substrates. The drawback is that certain mechanical properties of the organic semiconductors are required (low glass transition temperature) to form the intermixed layer. Since a donor can act as an acceptor for an even stronger donor because these two terms can not really be used separately, there are certain functionalities that are likely to make a material an electron acceptor with respect to most other materials. Examples for functionalities that favour electron acceptor properties are: -CN, -CF_3, -*F*, = *O* (keto-groups) or diimides (all perylenederivatives in this thesis are perylene diimides). These groups are known as electron withdrawing groups if they are attached to an unsaturated (conjugated) system. Note that their ability to enhance the electron affinity of the entire molecule is not purely connected to the electron withdrawing properties of these functionalities. It is essentially a result of both the inductive and the mesomeric effect. The average of possible π electron locations can be regarded as the overall mesomeric effect of a specific molecular structure. Examples for organic electron acceptors are CN-PPV, CF_3 substituted PPV and

perylene diimides. Most organic semiconductors behave more like electron donors, for example PPV, PT, PPP and phthalocyanines. Examples for large π systems are phthalocyanines, naphthalocyanines and perylenes.

The bandgap can also be small if a molecule consists of a donor and an electron acceptor that are connected via a conjugated structure to create a "push/pull system" as in poly-methines. Such structures can accomplish charge transfer sometimes in the ground state (ex. **charge transfer salt**) or only little extra (light) energy is required to complete it. Examples for charge transfer salts are PVK-TNF [48] , merocyanines and 4,4' bipyrimidinium (viologens) salts [49].

Solubility is good if the planar parts of the conjugated π systems of the molecules can not get too close to each other. Otherwise they would stick together, driven by their π– π interaction, to form aggregates for example larger clusters particles which do not contain solvent. Flexible and bulky side chains or atoms that stick out of the molecular plane can prevent molecules from getting to close.

In most organic device only a small portion of the incident light is absorbed for several reasons. One of these is that semiconductor bandgap is too high: a bandgap of 1.1eV (1100nm) is required to absorb 77% of the solar radiation on earth whereas the majority of semiconductor polymers have bandgaps higher than 2.0eV (600nm) limiting the possible absorption to about 30% [50]. Further the typically low charge carrier and exciton mobilities require layer thickness in the order of 100nm. Fortunately the absorption co efficient of organic materials is generally much higher than in silicon so that only about 100nm are necessary to absorb between 60 and 90% if a reflective back contact is used. In addiction reflection losses are probably significant but little investigated in these materials and anti-reflection coatings as used in inorganic devices may then prove useful once other losses such as recombination become less dominant. But the strong points are the **exciton diffusion, the charge separation and charge transport in organic semiconductors** [51]. Ideally, all photoexcited excitons should reach a dissociation site. Since such a site may be at the other end of the semiconductor, their diffusion length should be at least equal the required layer thickness for sufficient absorption, otherwise they recombine and photons were wasted. Exciton diffusion ranges in polymers and pigments are typically around 10nm. However,

some pigments like perylenes are believed to have exciton diffusion lengths of several 100nm. Charge separation is known to occur at organic semiconductor/metal interfaces, impurities (ex. oxygen) or between materials with sufficiently different electron affinities (EA) and ionisation potentials (PI). Than one material can act as electron acceptor A while the other keeps the positive charge and is referred to as electron donor D since it did actually *donate* the electron to A. If the difference in IA and EA is not sufficient, the exciton may just hop onto the material with the lower bandgap without splitting up its charges. Eventually it will recombine without contributing charges to the photocurrent.

The transport of charges is affected by recombination during the journey to the electrodes, particularly if the same material, serves as transport medium for both electrons and holes. Also, interaction with atoms or other charges may slow down the travel speed and thereby limit the current. In order to enter an electrode material with a relatively low absolute values of work function (ex. Al, Ca) the charges often have to overcome the potential barrier of a thin oxide layer. In addition, the metal may have formed a blocking contact with the semiconductor so that they can not immediately reach the metal.

For organic semiconductor (as well as in metallic as inorganic semiconductor materials) the molecular order influence absolutely the transport of electrons (and holes) [52]. Thus to keep an high conduction in organic material thin organic solid films or polymeric ordered structure were usually investigated (*Fig. 2.12*). However some conjugate polymer shows conductivity similar to silicon semiconductor material.

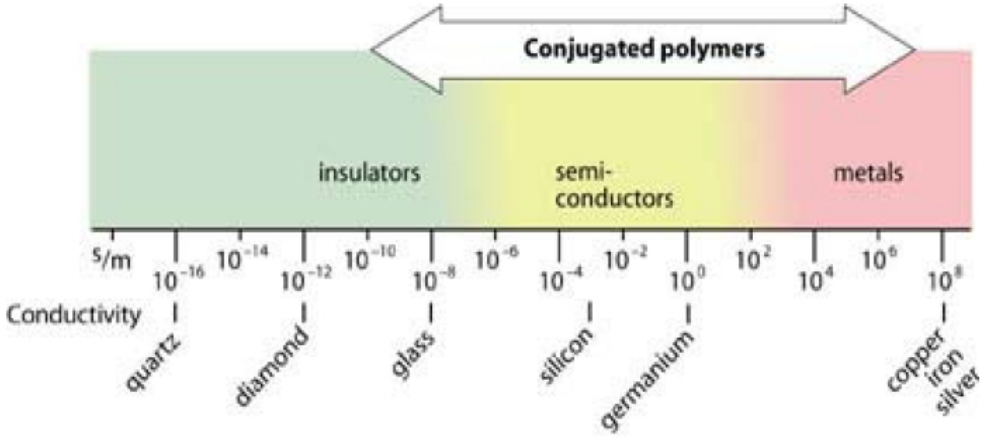

Fig.2.12 *Electrical conductivity of conjugated polymers related to insulator, semiconductor an metal materials.*

Organic/inorganic hybrid cell (HOPVc).

Recent results have demonstrated that HOPVcs based on a blend of **inorganic nanocrystals** [50] (n-type semiconductor) and polymers (p-type semiconductor) possess significant potential for low-cost, scalable solar power conversion acquiring ordered structures and increasing the PVc charge transport and efficiency. **Colloidal semiconductor nanocrystals** [53], dispersed in polymers, are solution processable and chemically synthesized, but possess the advantageous properties of inorganic semiconductors such as a broad spectral absorption range and high carrier mobilities. Significant advances in hybrid solar cells have followed the development of elongated nanocrystal rods and **branched nanocrystals** [54], which enable more effective charge transport. The incorporation of these larger nanostructures into polymers has required optimization of blend morphology using solvent mixtures. Future advances will rely on new nanocrystals, such as cadmium telluride tetrapods, that have the potential to enhance light absorption and further improve charge transport. Gains can also be made by incorporating application-specific organic components, including electroactive surfactants which control the physical and electronic interactions between nanocrystals and polymer. Although experimental printed

PVcs are far less efficient than the solid-state variety. The best results were obtained using tiny rods of **cadmium selenide** (7 nm in diameter and 60 nm long) solid semiconductor and poly-3-hexylthiophene (**P3HT**) organic polymer [55]. The technique is still highly experimental, but the hybrid cells produced worked well under low light converting the 6.9% of the sunlight energy (only the 1.6% considering the simulated full solar spectra experiments). Main problem is that the polymer and solid are in such close contact that electrons "and holes" can reach the wrong conductor, nullifying the electrical current. A suggestion could be to add some blocking layers to the cells or using different length or orientation of the rods to capture more light, but it rises production costs, such as in more sophisticated and expensive cells, like the ones just bolted onto the Hubble Space Telescope, use more than one light-absorbing semiconductors, and thus can grab light more efficiently. A suitable alternative at CdSe nanorods/polythiophene cell could be the **ZnO** crystalline nanoparticles and coniugate polymer like poly[2-methoxy-5-(3',7'-dimethyloctyloxy)-1,4-phenylene vinylene] (**MDMO-PPV**) [55] (*Fig 2.13*).

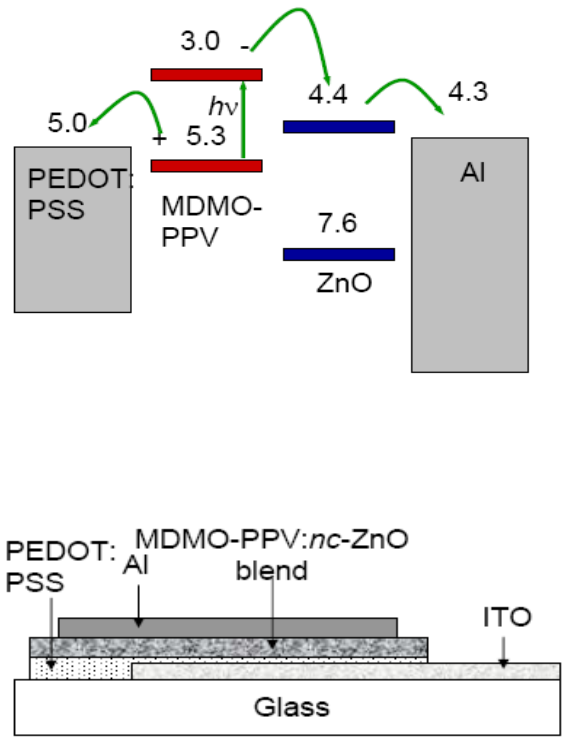

Fig.2.13 *MDMO-PPV ZnO crystalline nanoparticles device.*

This device typology could uses nanoparticles instead the **nanostructure** (like nanorods) reducing production costs without no important efficiency decrease, considering that better results were obtained using ZnO nanorods made via wet chemical procedure and aligned perpendicular to electrode surface [56] (*Fig 2.14*).

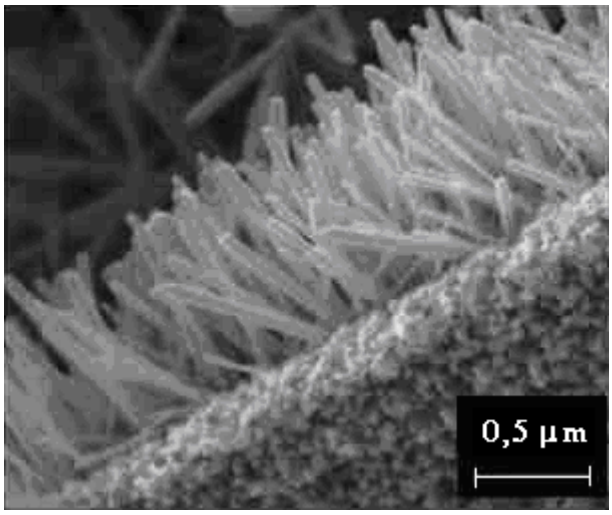

Fig.2.14 *ZnO nanorods perpendicular to electrode surface.*

Novel strategy to design nanowire functionalized electrodes are studying with much larger areas available for dye adsorption. It is worth noting that the advantages of the nanowire geometry are even more convincing for other types of PVc, such as inorganic-polymer hybrid devices in which an oriented continuous and crystalline inorganic phase could greatly improve charge collection.

2.3 Costs and limitations of PVc.

While in most organic device only a small portion of the incident light is absorbed for the explained reason in previous paragraph, several researchers believe that organic devices represent the future. In fact whenever just a little region of solar spectra is used in light conversion (*Fig. 2.15*) low production cost of devices and their wide-range use, according their mechanical properties, make the OPVc a full interest devices.

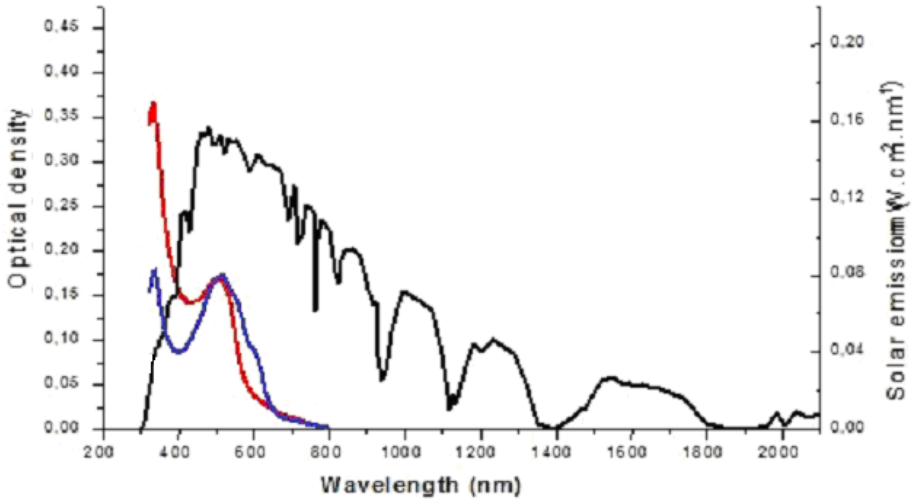

Fig.2.15 *Sea level solar spectra (black line) compared with two OPVcs: P3HT-PCBM film blu line; MDMO-PPV-PCMB film red line* **.**

Thus while the perspectives are to see low cost and high efficiency organic cell into several years, to date (*Fig. 2.16*) the largest used photovoltaic material, balancing costs and efficiencies, result the Silicon [57].

However Silicon PV technologies has an high cost due to intrinsic raw material costs and high temperature production processes: considering a four members family living in the south of Italy to have a suitable PV system (about 3 KWatt) about 23000 euros and 30 m^2 of free surface need. Than, it is possible to have an idea of the 1 MWatt power plant installation costs. However PVcs do not produce energy during the night and the power plant or family installations should be connected in a general network suitable to supply at the energy vacancies by conventional methodologies (ex. fossil fuels) or some other renewable sources (ex. wind). Obviously, considering this kind of devices and infrastructure, the PV systems could not replace the use of conventional energy sources, but just should reduce their utilizations.

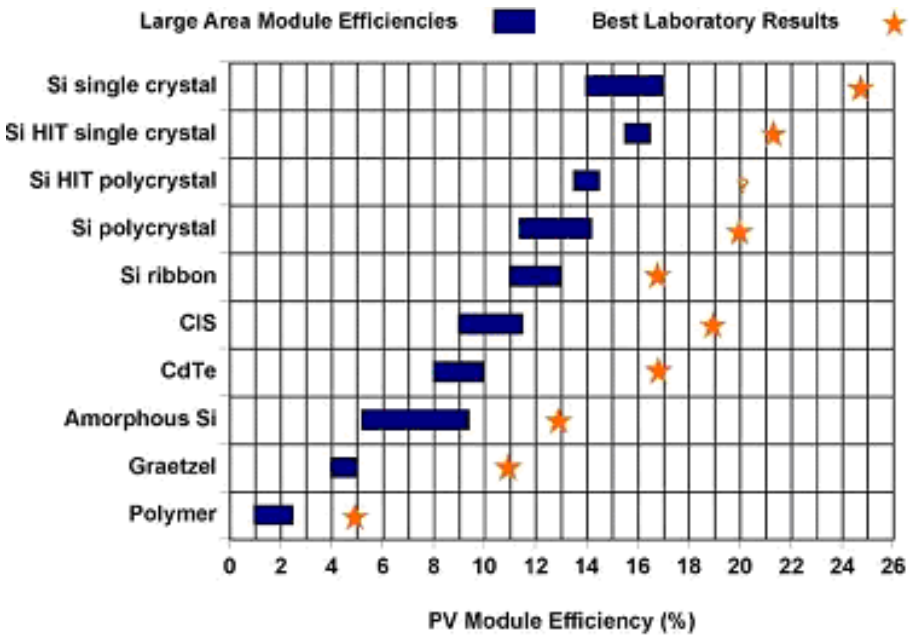

Fig.2.16 *Commercial PV module efficiencies were compared with PV best laboratory result* **.**

The unique (and ahead of its time) idea to supply at fossil fuels combustion should be to create a "global photovoltaic network" (as network existing to date for petroleum or fossil gas) to connect solar power plant in different world regions: the exceeded power supply in daylight regions could be used to night time regions during the day and vice versa during the night. Alternatively accumulators, batteries or fuel cells costs should be added to power plant cost.

2.4 State of art of solar thermal energy conversion (TPV, TI, TE).

Moreover a brief distinction between the "solar heating systems (SHS)", "concentrating solar power systems (CSP)" described in the apposite section above and the thermophotovoltaic (TPV) [58]", "thermionic (TI) [59]" and "thermoelectric (TE)" energy conversion systems mentioned in this section and in next chapter 3 need. Basically the SHS and CSP apply the sun heat to warm up fluids that could be used to produce electrical energy, while TVP, TI or TE materials convert the sun radiation directly in current. Moreover it is possible to

link up the CSP system (concentrating the sun power) with TVP,TI or TE materials.
In the following three section a brief overview of state of the art of TI, TPV and TE devices is designed, subsequently in the next chapter 3 theoretical aspects, deductions and applications will be pointed out .

Thermionic devices (TI).

In a thermionic converter [59], heat energy is converted to electrical energy by thermionic emission, whereby electrons are emitted from the surface of certain metals when the metals are sufficiently heated. The three major components of a basic thermionic energy converter are the thermionic emitter, the collector, and the working fluid, which may be vacuum or an electron gas or a partially ionized plasma (*Fig.2.17*). The input heat, Q_{in}, heats the emitter, and electrons are emitted. The cold collector receives some of these electrons at an output heat, Q_{out}. The difference (Q_{in} -Q_{out}) is the energy that drives the electrons through the external circuit, and appears as electrical energy. The collector is cooled to remove the output heat. Electrons in metal have a temperature dependent energy distribution. If the temperature of Metal 1 (the emitter) is increased, eventually some electrons can have sufficient energy to overcome the surface potential barrier called the work function Φ_1, which ordinarily prevents electrons from leaving the surface. In this process, shown by solid lines on the energy diagram, electrons accumulate a potential $\Delta\Phi= \Phi_2 - \Phi_1$, which can be used to drive electric current through the external load R, when the circuit is closed. There also is a reverse or back current of electrons shown by dashed arrows on the energy diagram, which competes with forward current. Typically this current is minimized by the larger work function of the Metal 2, Φ_2, and its lower temperature that produces fewer energetic electrons. The minimum known work function is about 1.1 electron-Volts (eV).
Vacuum converters, which have electron gas as their operating fluid, operate in the range 1200°K to 1400°K. They typically produce 1 W/cm^2 at an efficiency of 5 percent. Low-pressure converters produce 10 W/cm^2 at an efficiency of 10 percent, operating at emitter temperatures up to 2300°K. High-pressure converters

deliver 40 W/cm 2 at an efficiency of 20 percent, operating at emitter temperatures up to 2200°K. In laboratory conditions, efficiencies as high as 40% are reported.

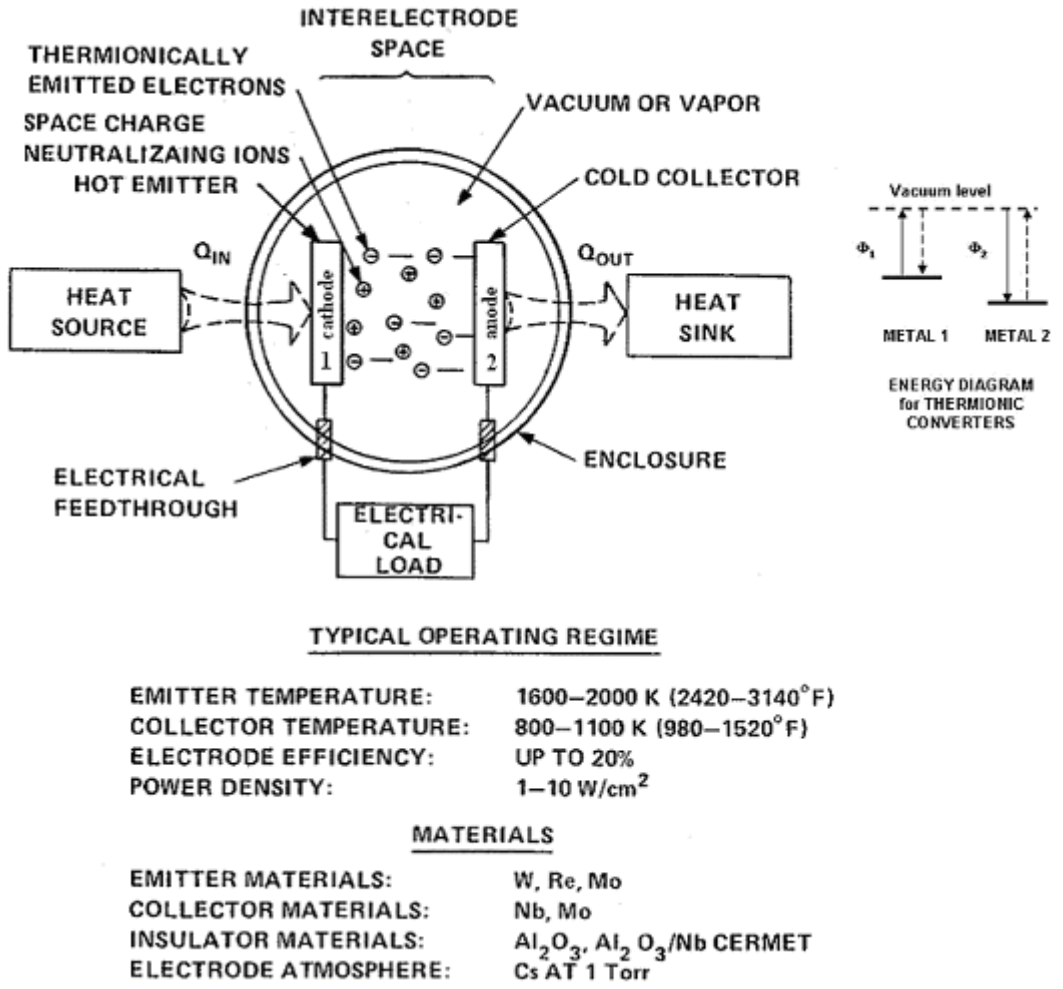

Fig.2.17 *Thermionic vacuum converter simplify scheme and energy diagram of the two metal work functions Φ_1 (the emitter) and Φ_2 (the collector).*

Obviously the principal applications of TI energy converters are in regions not easily accessible such as the outer space (using sun energy) or the undersea areas (using fuel combustion) or the polar regions (using appropriate solar collector system or fuel combustion). But The two important heat sources for TI device persist in the sun and nuclear reactors.

Direct thermal to electrical energy conversion systems that could operate at relatively lower temperatures (300-650°C) with high efficiencies (>15-20%) provide an attractive compact alternative to internal combustion engines for many applications in the W-MW range.

Materials design for these purpose is focused on increasing the efficiency of heterostructure TI power generators using embedded **quantum dot (QD)** structures and **metal/semiconductor superlattices** [60]: thermal diodes have the same functional components as TI converters but with a semiconductor wafer substituted for the vacuum gap (*Fig 2.18*).

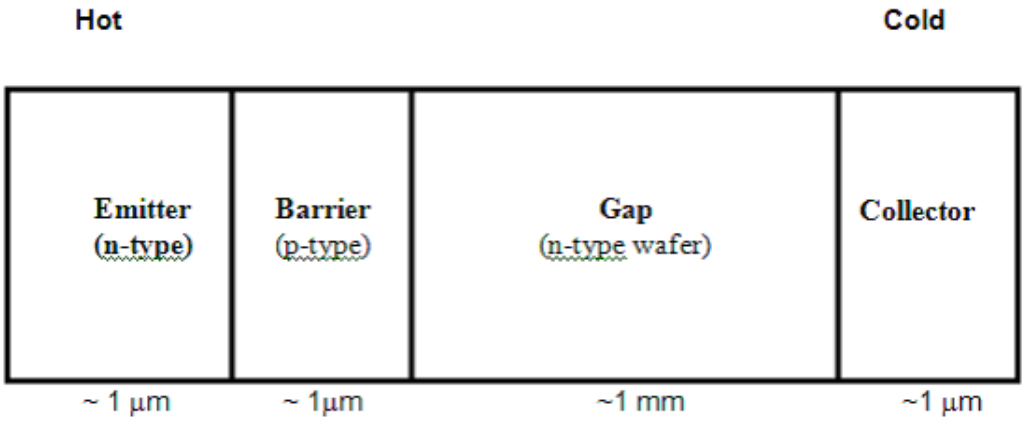

Fig.2.18 *Thermal semiconductor wafer diodes scheme.*

Manufacturing a thermal diode starts with a thermoelectric semiconductor wafer (gap) on which a thin barrier layer is deposited. The barrier layer is made of the same semiconductor, but doped differently. The deposited emitter layer is a heavily doped layer of the same semiconductor or a metal. The collector structure is basically the same two layers as on the hot side. Potential barriers at the interfaces between emitter and barrier layers and barrier layer and gap serve the same purpose as the work function in a TI converter (*Fig. 2.17*).

For relatively low voltages, there are more high-energy electrons on the hot side of the barrier, and power is generated by a net electron flow from the hot to the cold reservoirs. If the voltage is increased, the number of high-energy electrons on the cold side of the barrier increases.

By changing dopant concentration these potential barriers can be adjusted and optimized for any temperature. The first barrier on the emitter layer side sorts electrons by energy and the second barrier on the gap side prevents back flow of electrons from the gap into the emitter layer. Without potential barriers, the output of this device will be defined by the thermoelectric properties of the gap material (see the TE section below). Barrier action leads to accumulation of electric charge behind the barrier, leading to increased operating voltage. The electric resistance of the device is dominated by the macroscopic gap with very little change from its thermoelectric value, leading to current increase due to increased voltage compared with the thermoelectric performance of the semiconductor gap. The highest experimentally observed internal efficiency of a thermal diode is 88% of Carnot Efficiency, which is competitive with any existing energy converter.

However to convert sun power using the TI device sun power concentrator CSP and a efficient heat reservoir or cooling system need to warm up the emitter material and cooling the collector.

Thermophotovoltaic devices (TPV).

A generic TPV system [61] consists of a source of heat (a flame, radiative isotope, the sun, etc), a radiator, a semiconductor converter, a means of recirculating the sub-bandgap photons to conserve system energy, and a power conditioning system (*Fig. 2.19*).

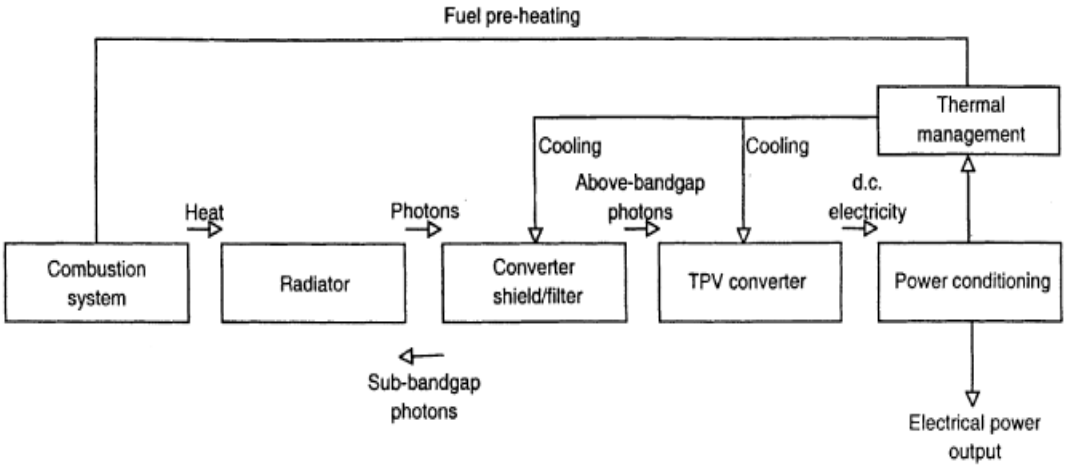

Fig.2.19 *A Generic TPV system simplified scheme.*

Early work on TPV converters focused mainly on silicon and germanium converters (*Fig, 2.20*). However, the quality of these elemental semiconductors was poor. It is the impressive progress in novel devices that has led to the high performance of modern TPV devices and the consequent interest in this field.
Most, but not all, recent device work has concerned the semiconductors GaInAs and GaInAsSb grown by organo-metallic vapor-phase epitaxy (OMVPE), or molecular beam epitaxy (MBE).

Fig.2.20 *A silicon TPV generator with 20KW methane burner that achieved a maximum output of 164 W*.

The radiator may be either broad or narrow band. If the former is used, then the spectral emittance must be as close to unity as possible and the material most commonly used has been silicon carbide. This has an emittance of about 0,9 emettance units, and it will withstand temperatures up to approximately 1900 K [62]. Optimization of the bandgap depends, as expected, on the radiator temperature and there is inevitably a large proportion of the incident photons that have of too low energy to be absorbed. For the overall system to have an acceptably high efficiency, these must be returned to the radiator to be re-absorbed using the filters. Narrow-band radiators considered to date include ytterbia, erbia, holmia and neodymia. These radiate at energies of approximately 1.1, 0.7, 0.6 and 0.5 eV respectively. Modelling of TPV systems, using broad-band radiators and design experience, suggests that energy conversion efficiencies of 15% may be achievable in the short-term but a longer-term effort would be required to reach 20%.

In solar thermophotovoltaic (STPV) systems, that represent the real renewable energy source utilization of TPV, thermal radiation resulted from the emitter (radiator) material heated up to high temperature by the concentrated sunlight is converted into the electric power by means of photocells sensitive to the IR part of spectrum. The forbidden gap and the structure of a STPV cell can be correlated for conversion of a particular radiation spectrum at definite temperature. In a STPV system, differently from conventional solar cells, application of selective filters is practicable, which reflects the radiation unused by a photocell back to the emitter. This allows to rise the emitter temperature and offers promise for increasing the total efficiency of a solar thermophotovoltaic system.

The use of the **concentrated sunlight as a heat source to a TPV** [63] system instead of a burning fuel is promising for increasing the TPV conversion efficiency with retaining all advantages of the sunlight converters.

Owing to that at the TPV conversion a radiation source can be located very close to a photocell, and also due to creation of high-effective photoconverters and emitters matched with them by spectrum the achievement of electrical power of 2-10 W/cm^2 is made possible. Thus, the actually achievable specific power output from the photoconverters in a STPV generator lies in the range of 20-100

kW hour/cm^2 per year (*Fig 2.21*), which exceeds in several hundreds times the average specific power output from the terrestrial solar arrays. It should be noted that the specific amount of electric power generated by the photoconverter unit area of a TPV generator in 100-200 times higher than in solar arrays.

A significant economical effect, but not ecological one, due to higher efficiency and life expectancy, will be ensured by application of TPV generators instead of electromechanical ones (based on the internal-combustion engine).

Supplying of a high sunlight concentration, changing the radiation spectrum of an emitter of photons, filtering the radiation to return unused photons and to reduce the heat action on photocells and assembling photocells into tandems allowing to increase the emitter radiation photovoltaic conversion efficiency, represent the problems could be arise to optimize STPV generators.

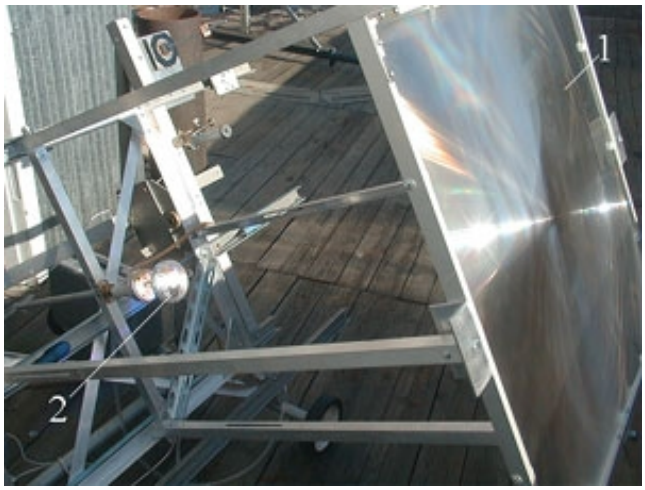

Fig.2.21 *Dual concentrator of the sunlight CSP applied on TPV device. It consists of a Fresnel lens(PMMA made) and a secondary lens of a quartz glass. 90% of the concentrated beam energy is focused in a 10 mm spot. This concentration system ensures the concentration ratio of 3600x. A special benefit of the system is its low cost.*

Two TPV modules are under development: cylindrical and conical. In general case, a photon emitter made of a refractory metal is placed in a quartz chamber

filled with a rare gas (Ar or Xe) to prevent oxidation. In the conical system, the thermal radiation is reflected by a conical shape mirror covered with gold, and photocells are mounted on a plane base. In the cylindrical type module, photocells are mounted on the internal side of the cylindrical base being cooled and surround the emitter of a cylinder form (*Fig. 1.22*).

(a) *(b)*

Fig.2.22 *A tantalum emitter (a) installed in a STPV module of cylindrical type(b).*

Both modules were tested in outdoor conditions at the direct solar radiation. At measured direct sunlight power of 800-850 W/m^2 the emitter temperature in cylindrical module was obtained in the range of 1400-1900K, depending on the emitter size and material. In a conical module, at the emitter temperature of near 2000K, the photocurrent density of 4.5 A/cm2 and the voltage of 0.49V were measured for a GaSb photocell [63].

Thermoelectric devices (TE).

In 1822-23, around the same time that Sadi Carnot was studying the limiting efficiency of the steam engine, Thomas Seebeck described in the Journal of the Prussian Academy of Sciences a discovery he called "*the magnetic polarisation of metals and ores produced by a temperature difference*". Seebeck was interested in this phenomena as supposed evidence in support of his belief that the existence of the earths magnetic field could be explained in terms of the temperature difference between the equator and the polar ice cap. However it is clear that what Seebeck

actually discovered was the existence of an electrical current in a closed circuit made up of different conductors in which the junctions of the materials are held at different temperatures. Theoretical aspect will be specially illustrated in the next chapter 3.

The real significance of the discovery was in the potential to generate power from low-grade heat. Had Seebeck developed a device to produce electricity using the best materials he found (ZnSb and PbS), he might have made a heat engine with an efficiency of ≈ 3%, equal to the best steam engines of his time.

In contrast to the thermoelectric devices (TE), in thermionic devices (TI) electron transport is ballistic: the distance electrons must travel between the hot and cold reservoirs is less than the mean-free path between. A discrete TI system (*Fig 2.23a*) consisting of two electron reservoirs with different temperatures and electrochemical potentials [59]. A continuous TE system (*Fig 2.23b*) consisting of a conductor in which electrons are subject to an opposing electrochemical potential and temperature gradient [64].

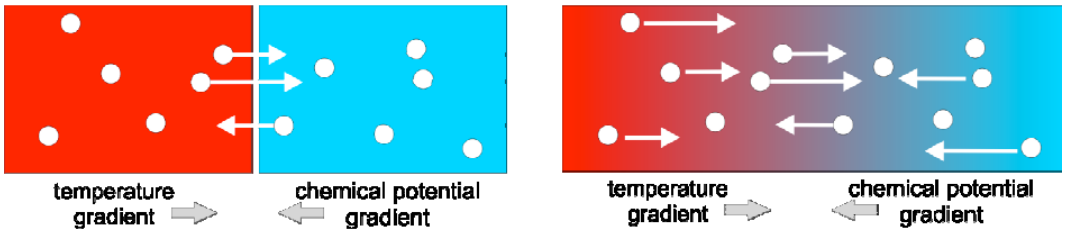

(a) *(b)*

Fig.2.23 *A discrete TI system (a). A continuous TE system (b).*

TE devices are also generally made by creating two junctions of n- and p-type semiconductor materials where a thermal gradient is imposed [64,65] (*Fig.2.24*) and the TE modules (like PV ones) are composed by several TE cells having really small size (from several μm^2 to several cm^2 surface) (*Fig. 2.25*).

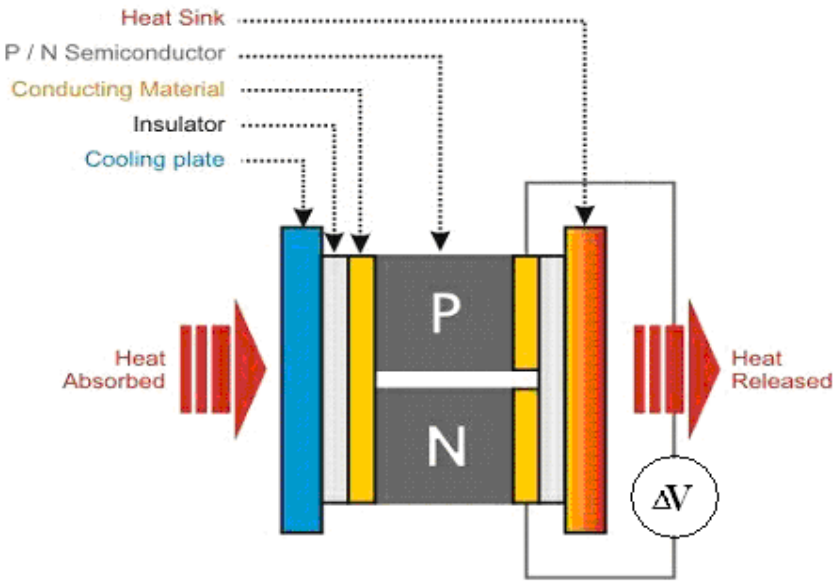

Fig.2.24 *Scheme of TE device a thermal gradient was imposed to both p and n semiconductors. Two semiconductors are joined to a conducting material (in yellow) at hot source and to an external load at cold sources. To avoid electrical influence of hot and cold plate (usually metals alloys) an electric insulator material (having high thermal conductivity) were used (in grey).*

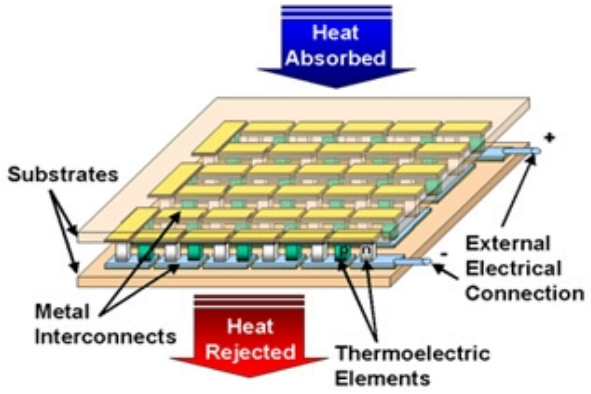

Fig.2.25 *A TE module composed by several TE cells.*

Efficiency of thermoelectric materials is characterized by the figure of merit Z [67]. Z has been believed to be a peculiar material constant and was proposed as a character which represents an efficiency of thermoelectric materials and was fundamentally determined in the condition of a finite temperature difference T_h-T_c between the high temperature side and the low temperature one in the material.

Assuming the temperature dependences of the resistivity ρ, the Seebeck coefficient α (see next chapter 3) and the thermal conductivity k to be negligible on the temperature range of Th-Tc or to be replaced by the average of the values at the heating and the cooling ends of the material, Z is usually represented by

$$Z = \frac{\alpha^{2}}{\rho k}\left(K^{-1}\right)$$

Z has been conventionally believed to be a sample size independent material constant. This means that Z and the temperature gradient, which is induced by the dc current, are constant in a sample. Three physical properties of α, r and k are measured to estimate Z, while T. C. Harman proposed another method in which the only resistance measurements by dc methods are required. The dimensionless figure of merit ZT is written by

$$ZT = \left(\frac{\alpha}{\rho_{j}}\right)\left(\frac{\Delta T}{L_{i}}\right)$$

where ρ_j is the current density and ΔT and L_i are the induced temperature difference and the length between the voltage terminals, respectively.

Perhaps the simplest example is a gas of charged particles. If a gas is placed in a box within a temperature gradient, where one side is cold and the other is hot, the gas molecules at the hot end will move faster than those at the cold end. The faster hot molecules will diffuse further than the cold molecules and so there will be a net build up of molecules (higher density) at the cold end. The density gradient will cause the molecules to diffuse back to the hot end. In the steady state, the effect of the density gradient will exactly counteract the effect of the temperature gradient so there is no net flow of molecules. If the molecules are charged, the build up of charge at the cold end will also produce a repulsive electrostatic force (and therefore electric potential) to push the charges back to the hot end. The electric potential produced by a temperature difference the Seebeck effect just explained in theoretical terms above. If the free charges are considered in the solid semiconductor material n-type, negative free charge will produce a negative

potential at the cold end. Similarly, "positive free charges" in p-type material will produce a negative potential at the cold end [64-69] (*Fig. 2.26*).

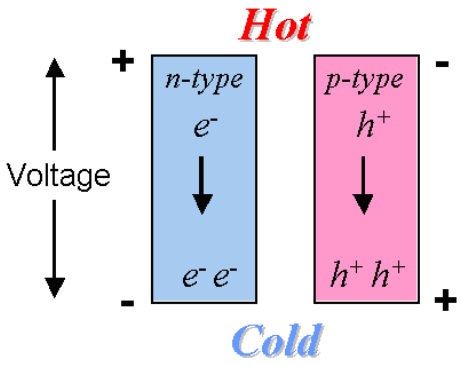

Fig.2.26 *Seebeck effect in p and n type semiconductors: imposing a thermal gradient a different charge separation occurs in the two semiconductors.*

A statistical treatment of phenomena regarding the higher electron density of n-type material (free electron) than lower electron density in p-type material (holes) could be done. The voltage produced by the Seebeck effect will cause current to flow through the load, generating electrical power [64-66] (*Fig.2.27*).

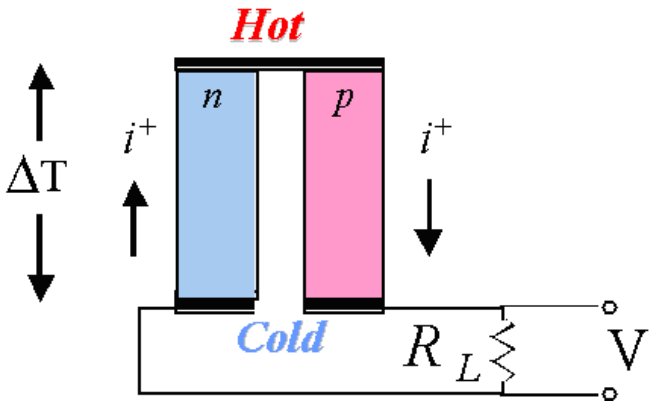

Fig.2.27 *A thermal gradient applied on p and n type semiconductors joined together: the charge separation occurs in the two semiconductors induces a ordered flow of electron.*

A material with a large thermoelectric power factor $\alpha^2\sigma$ (σ is the electrical conductivity) and consequently *z*, needs to have a large Seebeck coefficient (found in low carrier concentration semiconductors or insulators) and a large electrical conductivity (found in high carrier concentration metals). The thermoelectric power factor maximizes somewhere between a metal and semiconductors. Good thermoelectric materials are typically heavily doped semiconductors or semimetals with carrier concentration of 10^{19} to 10^{21} carriers/cm^3. To ensure that the net Seebeck effect is large, there should only be a single type of carrier. Mixed n-type and p-type conduction will lead to opposing Seebeck effect and low thermo-power (defined here as absolute value of Seebeck coefficient). But to have a large enough band gap, n-type and p-type carriers can be separated, and doping will produce only a single carrier type. Thus good thermoelectric materials have band gaps large enough to have only a single carrier type, but small enough to have sufficiently high doping and high mobility (which leads to high electrical conductivity) as shown in *Fig.2.28*.

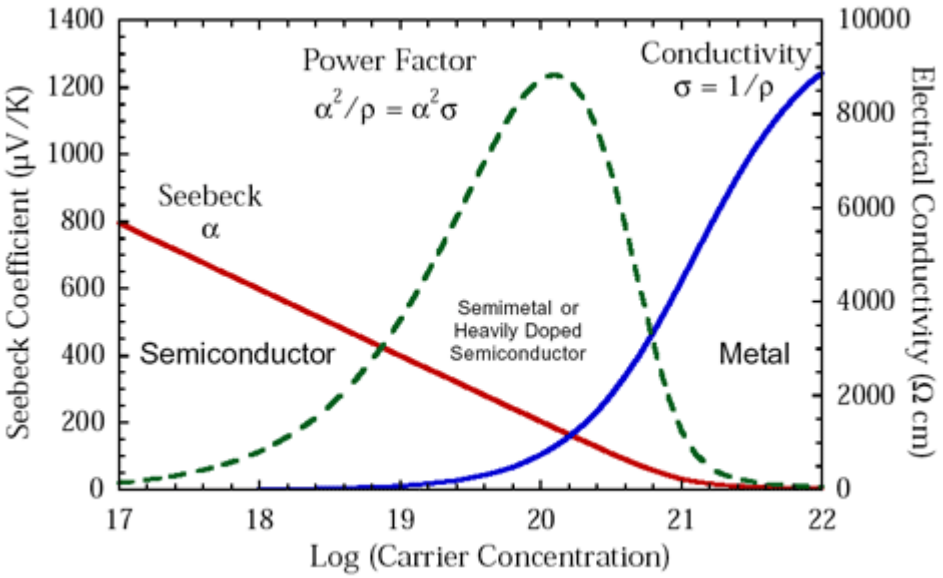

Fig.2.28 *Seebeck coefficient (in red), electrical conductivity of materials (in blue) and power factor (in green) graph in function of carrier concentration into insulators, semiconductors and metals.*

Except in a few niche applications, these solid-state heat pumps have proven too inefficient to be practical. Since the 1960s, NASA has used this effect to generate electricity for spacecraft too far away from the sun for solar cells to operate. And one Japanese company is even selling thermoelectric wristwatches powered by the wearers body heat. Although the TE materials have so far been used to considerable energy production because to make the process efficient: good electricity conductor materials are need, but that do not excel at conducting heat (*Fig. 2.29*), so the temperature difference remains. **In other words materials that blocking the heat flow while enhancing the electrical flow are needed** [64,65].

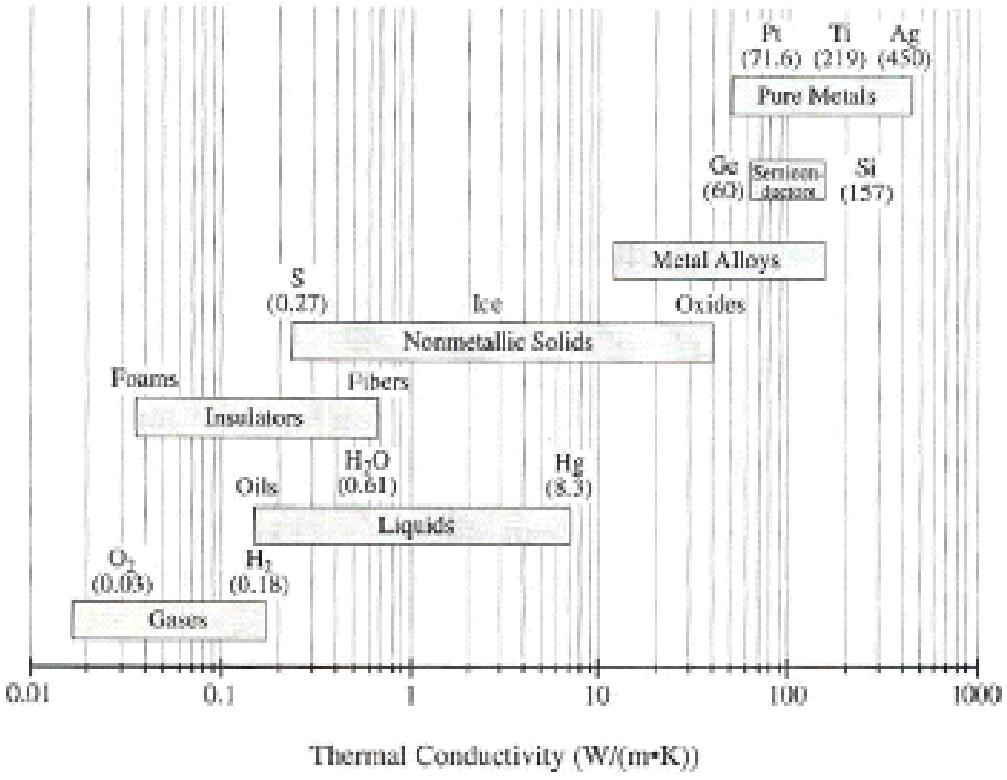

Fig.2.29 *Thermal conductivity of several materials.*

Several materials [67,68] have an upper temperature limit of operation, above which the material is unstable. Thus no single material is best for all temperature ranges, so different materials should be selected for different applications based on the temperature of operation. This leads to the use of a segmented thermoelectric generator.

A classification according ZT figure of merit could be made [67] in *Fig. 2.30 a,b*.

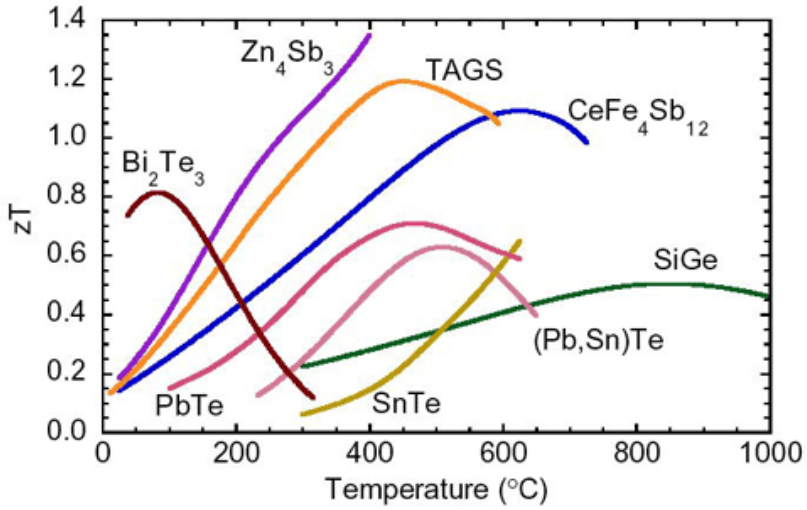

(a)

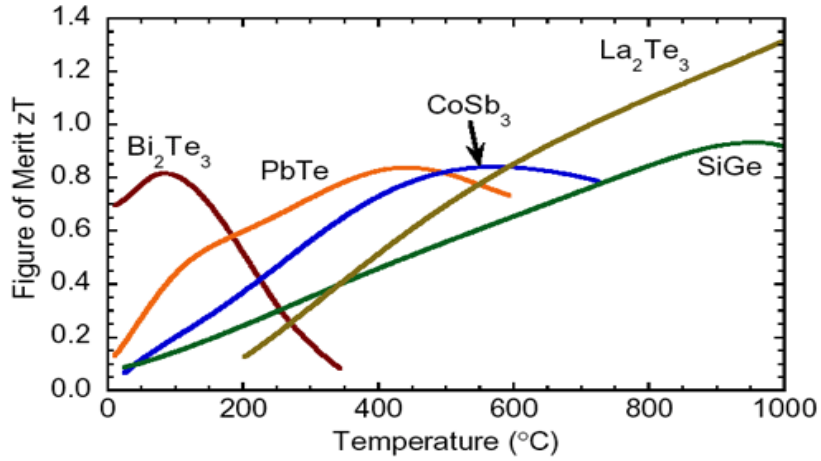

(b)

Fig.2.30 *ZT of p-type thermoelectric materials (a) and n-type thermoelectric material (b) in function of temperature.*

To achieve high efficiency, both large temperature differences and high figure of merit materials are desired. Since the material thermoelectric properties (α, ρ, k) vary with temperature it is not desirable or even possible to use the same material throughout an entire, large temperature drop. Ideally, different materials can be segmented together such that a material with high efficiency at high temperature is segmented with a different material with high efficiency at low temperature. In

this way both materials are operating only in their most efficient temperature range [65,67-69] (*Fig 2.31*).

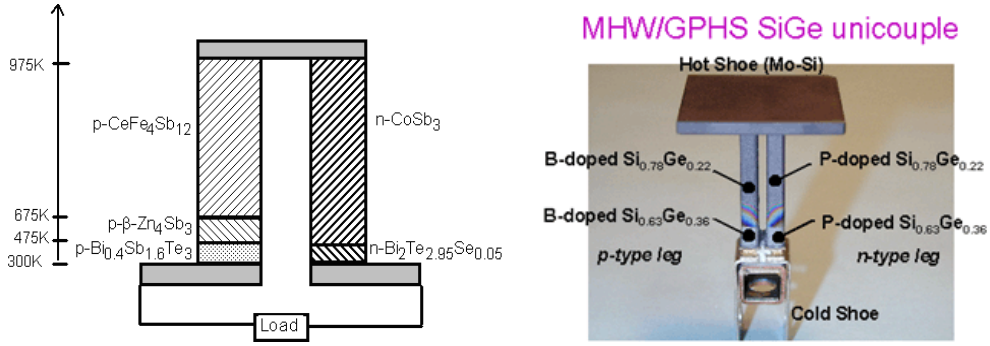

Fig.2.31 *Mixed semiconductor materials devices act according the temperature range of imposed thermal gradient (designs for NASA Mars Rover RTGs) [69].*

However it is better use materials with the ZT higher than possible, but having a ZT>>1 represent a important technologic challenge, recently ZT > 2 has been observed in thin film **superlattices** or **"quantum well"** materials with feature sizes of tens of nanometers [66] (*Tab 2.2*).

Modern thermoelectric energy conversion devices achieve only a small fraction of Carnot efficiency. The fundamental problem is that the transport properties of available materials are insufficient. Experimentally, there are several rather different thermoelectric materials available which achieve about the same efficiency over different temperature ranges: BiSb alloys (100 K), Bi_2Te_3-based alloys (300-400 K), PbTe-based alloys (600 K-700 K), and SiGe alloys (1100-1200 K). The best thermoelectric materials each achieve peak efficiency values up to about 17%-30% of Carnot efficiency.

Thermoelectric Module Material	Temperature Difference °C	Voltage at Maximum Power	Maximum Efficiency %	Maximum Power W
N & P-type bulk Bi_2Te_3	200	1.6	5.8	14
	Hi-Z's Commercial Alloys			
N type Si/SiC & P-type B_4C/B_9C Quantum Well Kapton substrate 25 µm thick	200	10.0	17	60
	250	12.4	20.9	72
	Under Development			
N type Si/SiC and P-type B_4C/B_9C Quantum Well SiGe Substrate ~5µm thick (too hot for Kapton)	450	22.6	32.5	338
	Under Development			

Tab.2.2 *Novel TE material: used gradient of temperatures and maximum power achieved for a 6.3 x 6.3 x 1.0 cm module sized [65].*

A QD can be made from a semiconductor nanostructure that confines the motion of conduction band electrons, holes, or excitons. The confinement can be due to an electrostatic potentials generated by doping, impurities or external field. A QD has a discrete quantized energy spectrum. The corresponding wave functions are spatially localized within the QD, but extend over many periods of the crystal lattice. QD contains a small finite number (of the order of 1-100) of conduction band electrons, valence band holes, or excitons, i.e., a finite number of elementary electric charges. It can be contrasted to other semiconductor nanostructures: the quantum wires, which confine the motion of electrons or holes in two spatial directions and allow free propagation in the third; and the quantum wells, which confine the motion of electrons or holes in one direction and allow free propagation in two directions. QD having quasi-zero dimensional, shows a sharper density of states than higher-dimensional structures. As a result, they have superior transport and optical properties. Quantum well raw materials cost less than current materials reaching the at about 0.1 euro per Watt versus the Bi_2Te_3 device with about 1 euro per Watt, offering the possibility to have high efficient devices (*Fig. 2.32 a,b*).

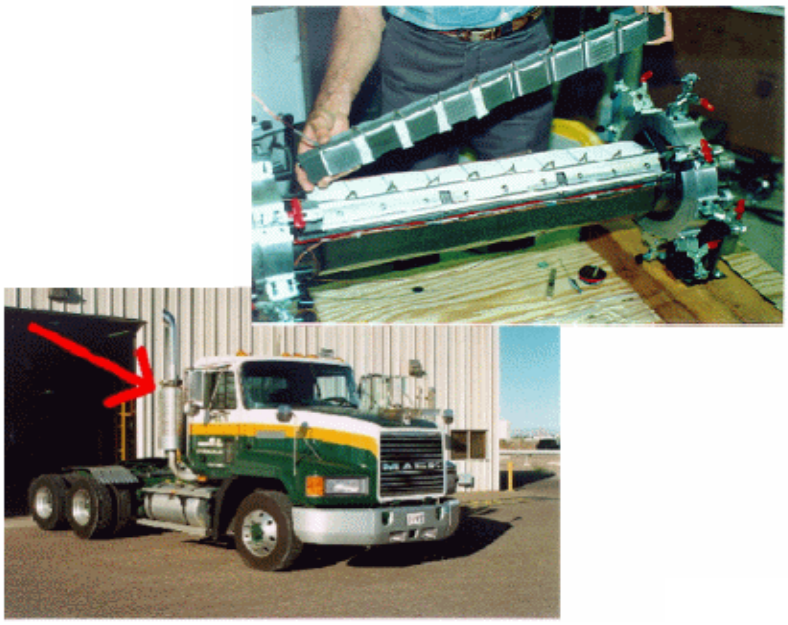

(a)

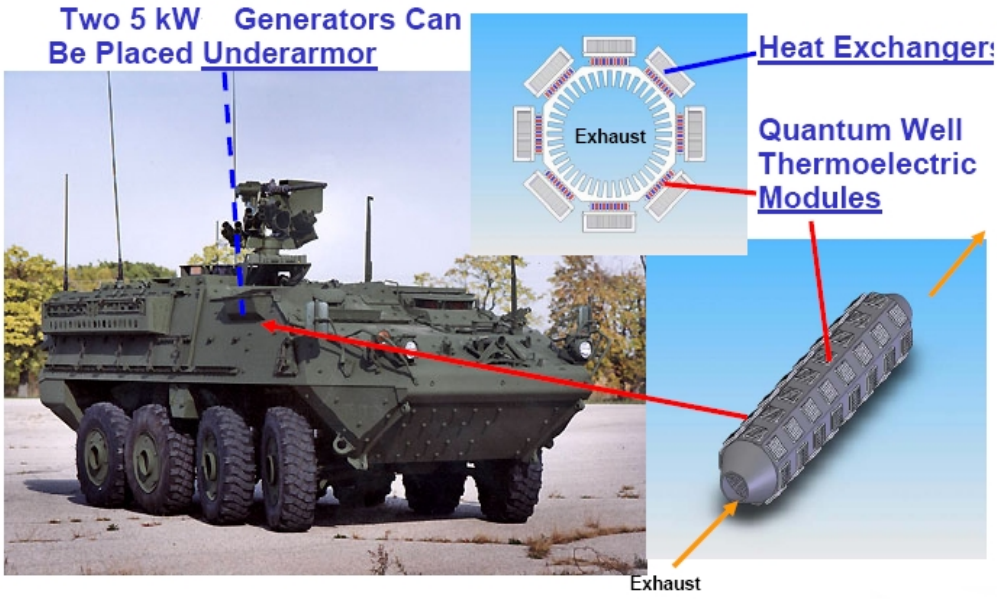

(b)

Fig.2.32 *Two QD TE generators applications: (a) in a truck silencer, (b) under a military light tank to supply electrical current from exhaust.*

Beside QD a great impulse at this technology is given by nanotechnology and furthermore organic nanotechnology. **Tiny superlattice** structures appear to be

more than twice as efficient as previous thermoelectric materials. The nano films consist of several alternating layers, each less than five nanometers thick. These layers block the travel of atomic vibrations that produce heat flow but still let the electrons flow as current. First application could be a device for "siphoning off" electrical power from the heat in automobile exhaust. Nanotechnology was employed in inorganic **semiconductor nanowires** [66,68] device blended with organic polymers, for example parylene®/Bi_2Te_3 device (*Fig. 2.33 a,b,c*) that is composed from bundles of 1000 legs/cm^2 of p and n doped Bi_2Te_3 semiconductors, blended with the high melting temperature organic polymer parylene®.

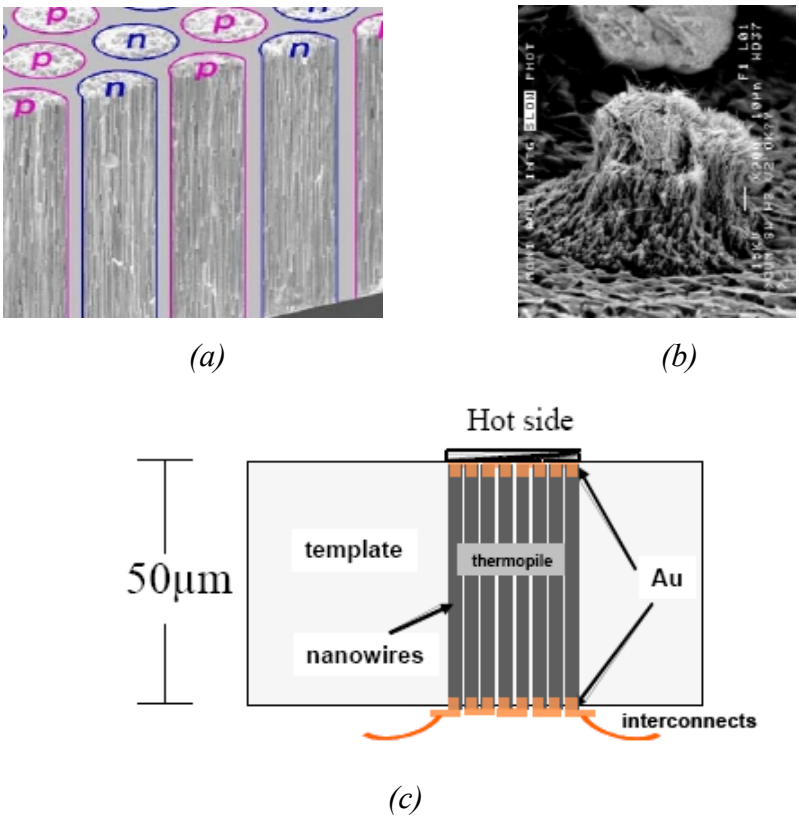

Fig.2.33 *(a) Bundles of 1000 legs/cm^2 of p and n doped Bi_2Te_3 semiconductors blended with the high melting temperature organic polymer parylene®; (b) free-standing nanowire bundle; (c) TE cell scheme.*

The goal could be to find a material with a large ZT. However, if an analogy is drawn between thermoelectric technology and gas-cycle engines then selecting

different materials for the thermo-elements is analogous to selecting a different working gas for the mechanical engine. And an attempt to improve ZT is analogous to an attempt to improve certain thermodynamic properties of the working-gas. An alternative approach is to focus on the thermoelectric process itself (rather than on ZT), which is analogous to considering alternate cycles, rather than ‘merely’ considering alternative ‘gases’. Focusing on the process is a radically different approach compared to previous studies focusing on ZT. The aspects of the thermoelectric thermodynamic and an alternative approach to efficient thermoelectric conversion in organic materials, thermovoltaic devices, are discussed in this thesis work into the next chapters.

Chapter 3

Scientific background.

"*We live in a world that is not in thermodynamic equilibrium. The thermal radiation that fills the universe is not in thermal equilibrium with the matter in the galaxies. On a smaller scale, the earth, its atmosphere, biosphere and the oceans are all in a nonequilibrium state due to the constant influx of energy from the sun. In the laboratory, most of the time we encounter phenomena exhibited by system not in thermodynamic equilibrium, while equilibrium systems are the exception*", Ilya Prigogine.

3.1 Some fundamental thermodynamic concept.

The aim of this work is to obtain an innovative organic thermovoltaic device where a thermal gradient, driving an heat flow in a composite device, would generate an electric current flow. The properties of this device cannot be interpreted in terms of the equilibrium thermodynamic but must be interpreted in the framework of the Thermodynamic of the irreversible processes, in similar way as well known effects, such us Seebeck or Peltier effect have been interpreted. One fundamental point, concerning the kind of system we wonted to build up, was that concerning the real possibility to keep a device made by to metal layers and a plastic film interposed between them (actually the plastic film from our point of view should have been a kind of glue able to sold together the two external metal layers) in a stationary state where a constant heat flux, generated by a constant thermal gradient, would maintain a constant current in an electric external circuit. It is quite probable that the operative state of the thermovoltaic device which is the object of this thesis must be considered as a stationary state not far from the

thermodynamic equilibrium. If so the entropy produced by the system defined according to the equation (1) [70,72] :

$$\sigma = J_q \cdot \nabla \frac{1}{T} - \sum_k J_k \cdot \nabla \left(\frac{\mu_k}{T} \right) + \frac{I \cdot (-\nabla \Psi)}{T} + \sum_j \frac{A_j v_j}{T} \qquad (1)$$

is maintained at the minimum (principle of the minimum entropy production in the linear regime) allowed by the imposed boundary condition (external heat flow). $\boldsymbol{J}_q$ rapresents the heat flow, T the temperature, μ the chemical potential, I the electric current, Ψ the electric potential, A_j the chemical affinity of the chemical reaction occurring in the system. According to the well known formalism of the irreversible process thermodynamics, the entropy production can be expressed in the form

$$\sigma = \sum_i F_i J_i \qquad (2)$$

that shows the entropy production as forces F_i and flows J_i bilinear combination[61]. Since equation 1 and 2 are equivalent the forces and fluxes in equation 2 must be defined according to the following *Tab. 3.1:*

	Force F_i	Flow J_i
Heat conduction	$\nabla \frac{1}{T}$	J_q or J_u energy flow
Diffusion	$-\nabla \frac{\mu_k}{T}$	J_k diffusion
Electrical conduction	$-\frac{\nabla \phi}{T} = \frac{E}{T}$	I_k current density
chemical reactions	$\frac{Ai}{T}$	v_i reaction velocity

Tab.3.1 *Table of related thermodynamic forces and flows.*

Having in mind the type of thermovoltaic device conceptually illustrated in *Fig 1.4* and *Fig 1.5* which represents the object of this thesis work, we can immediately reduce the number of the terms required in equation 1 to model its thermodynamic behaviour. Since no gas or liquid phases are present we can cut the molecular diffusion term in equation 1 so that the entropy production reduces to:

$$\sigma = Jq \cdot \nabla \frac{1}{T} + \frac{I \cdot (-\nabla \Psi)}{T} + \sum_j \frac{A_j v_j}{T} \qquad (3)$$

So only three different effects comes to play a role in our hypothesized device: the thermal gradient, the electric conduction through the system, and the chemical reactions taking place at the interfaces between the to different metal layers and the charge carrier molecules contained in the central plastic film. Another consideration can bring a further simplification. We can build up the thermovoltaic cells by molecules which (hopefully) do not give any other chemical reaction but the electron charge transfers at the electrode interfaces. So the unique role of these electrodes redox processes will be that to regulate the electronic current flowing into the device. The stationary value of this current will be determined by the slowest charge transfer process occurring into the system. This could be the charge transfer across the plastic film and not the charge transfer at the interfaces, but in any case the slowest process will lead the others. So chemical reaction occurring at the electrodes interfaces are not independent from the electric current flowing into the device. Since equation 1 must in principle contain only independent terms we can reduce the entropy production terms to a couple of force and related fluxes.

$$\sigma = J_q \cdot \nabla \frac{1}{T} + \frac{I \cdot (-\nabla \Psi)}{T} \qquad (4)$$

This last equation is the same which has been used in past to study the thermodynamics of Seebeck and Peltier effects which in this thesis work remain the reference effects for the study of our proposed new thermovoltaic cells.

Admitting that the system will work not much far away from the equilibrium state we can make a further step forward by using the Onsager linear relations [73] between thermodynamic forces and fluxes. According to Onsager (5) when the system is maintained in a stationary state not very far from equilibrium the flows can be expected to be liner functions of the forces, that is to say:

$$J_k = \sum_j L_{kj} F_j \qquad (5)$$

underlining that even if J_k and F_j are flows and forces related to different Physical phenomena, they are any way linearly correlated by the L_{kj} coefficients, which are called **phenomenoogical coefficients**. Thus **cross effects** between different physical phenomena become possible. Phenomenological coefficients imply not only that a force drive the respective flows but also that any force can drive flows not necessarily directly linked to it. For instance a force like the thermal gradient (1/T) can cause not only an heat flow, but also an electrical current and vice versa (ex. *Seebeck* and *Peltier* effects); a gradient in concentration of one compound can drive diffusion current of an other one. Cross effects were known long before irreversible process thermodynamic formulation. In order to describe thermoelectrical cross-coupling two equation became relevant

$$J_q = L_{qq} \cdot \nabla\left(\frac{1}{T}\right) + L_{qe}\frac{E}{T} \qquad (6)$$

$$I_e = L_{ee}\frac{E}{T} + L_{eq}\nabla\left(\frac{1}{T}\right) \qquad (7)$$

in wich the flow of heat J_q is related to thermal gradient and electrical conduction and also the current I_e is relate to electrical conduction and thermal gradient by the linear phenomenological coefficients (Lqq, Lqe, Leq, Lee).
However phenomenological coefficients creates a phenomenological matrix in which the Lqe and Leq coefficients follow the **Onsager reciprocal relation**, according to which Lij = Lji. Although the following aspect will not be argued exhaustively, the symmetry principle provides to constrain the possible coupling between several forces and flows: not all cross coupling are allowed because "irreversible process of different tensorial character (scalar, vectors and higher-order tensors) do not couple each other".

3.2 Thermoelectric phenomena.

The above *(6)* and *(7)* equations could be rewritten in one dimensional form [70-72]:

$$J_q = -\frac{1}{T^2} L_{qq} \frac{\partial T}{\partial x} + L_{qe} \frac{E}{T} \qquad (8)$$

$$I_e = L_{ee} \frac{E}{T} - L_{eq} \frac{1}{T^2} \frac{\partial T}{\partial x} \qquad (9)$$

To relate the Lij and Lii coefficients to the heat conductivity k and resistance R some limit conditions should be considered: the Fourier's heat conduction law, when the electric field is equal to zero (E = 0, first limit condition) results to be

$$J_q = -k \nabla T_{(x)} \qquad (10)$$

In which heat conductivity k is related to Jq and $T_{(x)}$ is a function of position only in the approximation that change in T from one end to the system to another is small compared to the average T value ($T^2 \sim T^2_{average}$). Using the Fourie's equation in equation (*8)* and consider E = 0, one can write

$$Lqq = k \cdot T^2 \qquad (11)$$

Considering in *(9)* the integration from 0 to *l*, where, at costant temperature (second limit condition) Ie is independent from x values the following two equations are obtained

$$\int_0^l I_e dx = \frac{L_{ee}}{T} \int_0^l E dx \qquad (11)$$

$$L_{ee} = \frac{T}{(r/l)} = \frac{T}{\rho} \qquad (13)$$

which *r* is the electrical resistance and ρ is specific resistance.
Reorganized the phenomenological coefficients to physical quantity, seebeck and Peltier effects could be introduced.

Seebeck effect.

Seebeck effect (SE) [70-72] occurs for example when two dissimilar metal wires are joined and the junction are maintained at different temperature, as result a thermal gradient drive an electromotive force (EFM) at the metals' ends (*Fig. 3.1*).

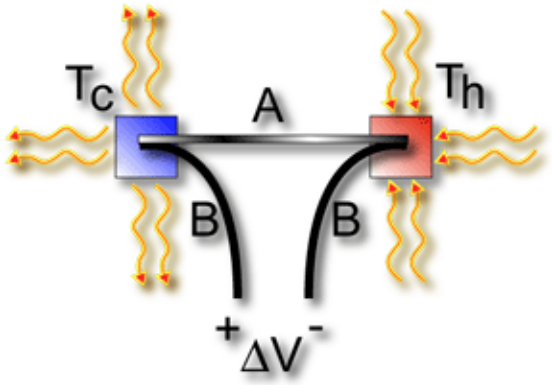

Fig.3.1 *Seebeck effect between two metallic wire (A and B) heterojunction, imposing a thermal gradient an external voltage could be measured .*

The EFM is measured at zero current, so setting Ie = 0 in equation *(9)* we obtain

$$\int LeeET = \int Leq \frac{\partial T}{\partial x} dx$$

$$- \frac{Leq}{TLee} = \left(\frac{\Delta V}{\Delta T} \right)_{I=0} = \alpha$$

α is the thermoelectric power, experimentally measured in several materials as shown in the second chapter, paragraph 2.4.

Peltier effect.

Iinitial condition studying the Peltier phenomena is that the two junctions are maintained at same temperature (T costant); according this initial condition equations *(8)* and *(9)* become [70-72]:

$$J_q = L_{qe} \frac{E}{T}$$

$$I_e = L_{ee}\frac{E}{T}$$

Thus, Jq/Ie ratio was obtained as

$$\frac{Lqe}{Lee} = \Pi \Rightarrow Lqe = \Pi \frac{T}{r}$$

with Π defines the Peltier heat.

Onsager relations [73] (Lqe = Leq) show clearly that Seebeck and Peltier effect are one referable to each other:

$$\Pi Lee = Lqe = Leq = -TLee\left(\frac{\Delta V}{\Delta T}\right)_{I=0}$$

$$\alpha = \left(\frac{\Delta V}{\Delta T}\right)_{I=0} = -\frac{\Pi}{T}. \qquad (14)$$

3.3 The electrochemistry point of view.

An effort to consider the thermovoltaic device object studied in this work, by using the language of the equilibrium chemistry thermodynamics has been done, in order to higligth the thermodynamic factors from which the efficiency of the thermovoltaic system might be dependent. The system can be considered as two coupled redox reactions as illustrate in the next *Fig. 3.2*. Let us consider the cell made by the two supporting metal layers having two different work functions, glued together by a plastic film containing a charge transport molecule which can exist in two oxidation states (OX and Red). Let us connect the two metal layers by an external circuit containing an appropriate electrical load. Let as assume that:

a. Metal 1 has a higher surface electronic charge density with respect to metal 2;
b. An endothermic reduction reaction of the Ox specie, absorbing the heat Q1, goes on at the electrode 1 (metal 1) . The reduced Red specie is than formed in the inner film at the border with the metal1;
c. An exothermic oxidation reaction of the Red specie, releasing the heat Q_2 (lower in absolute value with respect to Q_1) takes place at electrode 2 (metal 2) The oxidized Ox specie is than formed in the inner film at the border with the metal 2;
d. A charge transport process, due to electron jumps between neighbouring Red/Ox species, takes place;
e. The charge transported through a,b,c,d processes from metal 1 to metal 2 flows back to metal 1 through the external load;
f. The processes from a to e can occur in a stable stationary state.

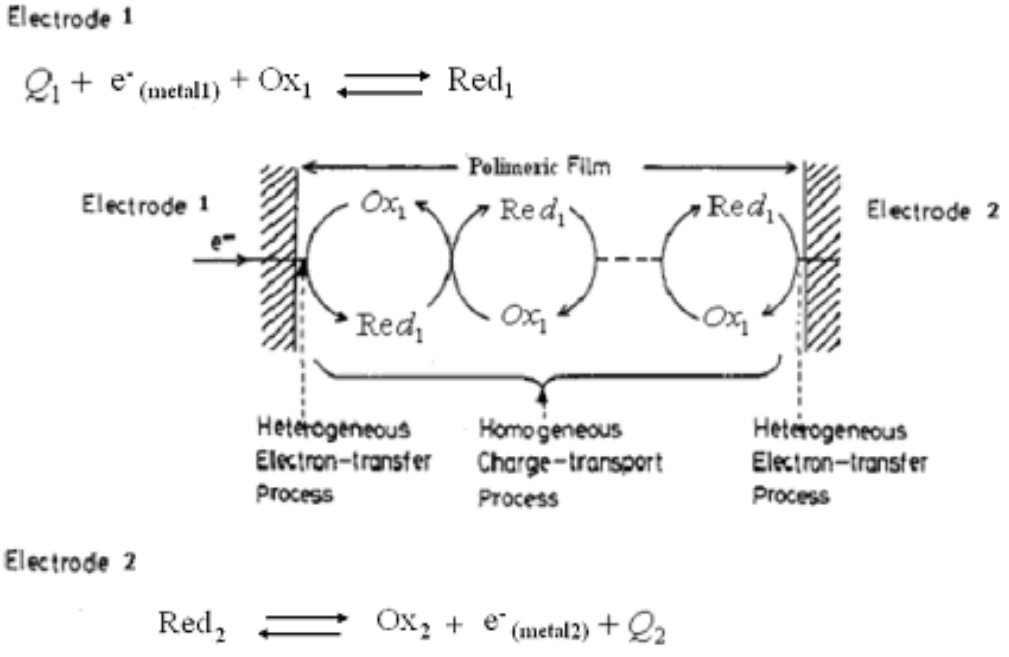

Fig.3.2 *Coupled redox reactions occur at electrodes surfaces and into film [74]*.

The above hypothesized process are all possible provided that the metals have the right electronic work functions and that the Ox/Red species have a matching Redox potential, or, to say it in different words, the Ox specie possesses an adequate LUMO level, where the transferred electron can be guest, which energy is not too far away from the metals work functions. From a general thermodynamic point of view we remind what has been said above: the system does not go to an equilibrium dead state since a flux of heat is furnished to it from an external sources. Of course the difference between the absorbed heat Q_1 and the released heat Q_2 is used to promote the charge circulation: the electric machine is done. In other terms the device works like a generator of dc current where thermal flow is converted in electric one.

The reactions taking place at the two electrodes interfaces, kept at different temperature value (T1 at electrode and T2 at electrode 2, with T1 > T2), are:

Electrode 1 Electrode 2

$$e^-_{(metal1)} + Ox_1 \rightleftharpoons Red_1 \qquad Red_2 \rightleftharpoons Ox_2 + e^-_{(metal2)}$$

where the index 1 and 2 define the species at the two different electrodes.

The corresponding free energy equations are:

$$\Delta G_{Metal_1} = \overline{\mu}_{(\mathrm{Re}d_1)} - \overline{\mu}_{(Ox_1)} - \overline{\mu}_{(e^- Metal_1)} \qquad (15)$$

$$\Delta G_{Metal_2} = \overline{\mu}_{(Ox_2)} + \overline{\mu}_{(e^- Metal_2)} - \overline{\mu}_{(\mathrm{Re}d_2)} \qquad (16)$$

Here $\overline{\mu}$ terms are the electrochemical potentials which can be further expressed as $\overline{\mu} = \mu + zF\phi$ where μ is the chemical potential, zF is the charge and ϕ is the electric potential. In our practical application (see chapter 4) the Ox specie is a divalent cation (z = 2) and consequently Red is a monovalent cation (z = 1), so these will be the z value taken into account in the following. The total free

energy variation, due to the simultaneous occurring of the above two processes (ΔG_{tot}), is, of course, the sum of ΔG_1 and ΔG_2 , and after separating the electrochemical potential in their chemical and electric part:

$$\Delta G_{tot} = (\mu_{e^-_{Metal\,2}} - F\phi_{2m}) + (\mu_{(Ox2)} + 2F\phi_{2f}) - (\mu_{(\mathrm{Red}2)} + F\phi_{2f}) - (\mu_{(Ox1)} + 2F\phi_{1f}) - (\mu_{e^-_{Metal\,1}} - F\phi_{1m}) + (\mu_{(\mathrm{Red}1)} + F\phi_{1f}) \quad (17)$$

where the indices "*im*" define the potentials in the metals 1 and 2, while the indices *"if"* define the potential in the central film next to the metal 1 and 2. Due to interface polarization the potential in the metals and in the plastic film next to the metal surfaces are not generally the same (see *Fig.1.4* and *Fig.1.5* in chapter 1). Terms in equation *(17)* can be collected in the following way:

$$\Delta G_{tot} = \Delta G_1^* - \Delta G_2^* + \Delta G\phi_{\mathrm{int}erfaces} \quad (18)$$

being :

$$\Delta G_1^* = \mu_{(\mathrm{Red}1)} - \mu_{(em1)} - \mu_{(Ox1)} \quad (19)$$

$$\Delta G_2^* = \mu_{(\mathrm{Red}2)} - \mu_{(em2)} - \mu_{(Ox2)} \quad (20)$$

$$\Delta G\phi_{\mathrm{int}erfaces} = F[(\phi_{1m} - \phi_{1f}) - (\phi_{2m} - \phi_{2f})] \quad (21)$$

where $(\phi_{1m} - \phi_{1f})$ and $(\phi_{2m} - \phi_{2f})$ are the electrical potential differences at the interfaces 1 and 2 respectively.

Equation *(18)* can rewritten by highlighting the enthalpic and entropic contribution to the free energies:

$$\Delta G_{tot} = \Delta H_1^* - \Delta H_2^* + (T_2 \Delta S_2^* - T_1 S_1^*) \quad (22)$$

The entropic terms in this particular case must be expected much lower than the enthalpic one, since chemical reactions occur between molecules embedded in solid state phases , where the entropies are generally small, and the temperatures T1 and T2 are never different more than 100 degrees, in the applications taken into consideration in this thesis work.
In first approximation we can than write:

$$\Delta G_{tot} \cong \Delta H_1^* - \Delta H_2^* + \Delta G\phi_{\text{int}erfaces} \quad (23)$$

On the other hand:

$$\Delta H_i^* = Hred_i(T_i) - Hox_i(T_i) - Hem_i(T_i) \quad \text{for i = 1,2} \quad (24)$$

and

$$H_k(T_1) = H_k(T_2) - Cp_k(T_2 - T_1) \quad (25)$$

Where Cp are considered independent from temperature.

After easy calculations one gets:

$$\Delta G_{tot} \cong \Delta Cp_r \Delta T + \Delta H_e(T_2) + \Delta G\phi_{\text{int}erfaces} \quad (26)$$

where:

$$\Delta H_e(T_2) = Hem_2(T_2) - Hem_1(T_2) \quad (27)$$

is the difference of the electronic hentalpy exiting between the metal 2 and metal 1, and

$$\Delta Cp_r = (Cp_{red} - Cp_{Ox}) - Cp_{em1} \qquad (28)$$

A further consideration concerning the relative weight of the terms contained in equation (28) can be made. Since the Red specie differs from the Ox species only for one electron contained in the LUMO level, and since in discrete molecule KT is not able to promote variation of the electronic state population in discrete molecules where the electronic levels are separated more then one electronvolts, Cp_{red} and Cp_{Ox} must be almost equal, so equation (26) can be written, more synthetically:

$$\Delta G_{tot} \cong -Cp_{em1}\Delta T + \Delta H_e(T_2) + \Delta G\phi_{interfaces} \qquad (29)$$

This last equation gives some simple physical insight to our problem. The hypothesized process generating the Thermovoltaic active mechanism can only occur if $\Delta G_{tot} < 0$. The term ΔH_e (T2) is surely positive, since metal2 work funcion is bigger than that of metal1. It is quite difficult to make prevision with respect to the interface polarization term $\Delta G\phi_{interfaces}$. This should quite small if the electron conduction into the central film is enough big. The only well established helping term is the term $Cp_{em1}\Delta T$ which is intrinsically positive but gives a negative contribution to the free energy since of the minus sign. It appears that in order to get the correct thermodynamic conditions, to fulfil the hypothesized process the separation between the to metal work functions must be not very different, otherwise ΔH_e , which is expected to be positive will reduce the thermodynamic pressure. On the other hand we cannot use the same metal on both the device sides, since in this case the yield of the process will be reduced to zero or next to zero (in a stationary state where electrons are pumped on metal 2 the work function would be any way different, even for equal metals, because of the

different accumulated charge). The simple thermodynamic consideration made above just tells as that is possible to have a thermodynamic pump when ΔT is big enough. Of course one should plane the devices in such away that the energy jump between the LUMO level of the film should be very next to metal 2 work function. In this case the heat absorbed by the electron once transferred from metal1 to the film would be kept and used into the external circuit. In conclusion, in order to have an efficient thermovoltaic system the following conditions should be fulfilled:

1. The energy difference between the LUMO level in the film and the metal1 worfunction should not be bigger than 0.1-0.2 eV;
2. The LUMO level in the film should be very next to the metal2 worfunction;
3. In the stationary state the configuration of the electron levels should be similar to that shown in the following scheme:
4. 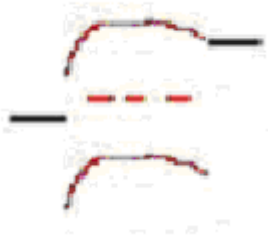

   in order to have no blocking contacts;
4. The electronic conduction in the central semiconductor film should be of the same order of magnitude with respect to that of the external circuit.

Chapter 4

Experimental work, results and discussion

4.1 introduction

The aim of the work was to develop and study a novel thermovoltaic device to produce electric current by the application of a thermal gradient between to metal layers, having different electron work functions, and separated by a plastic layer containing molecules with appropriate LUMO levels (*Fig. 4.1*). In order to reach this goal several different films made by blends of organic polymer matrices with several kind of active molecules (the term active molecule it will indicate in the following a molecule with a suitable LUMO) , such as organic and organo-metal molecules as well as charge-transfer complexes.

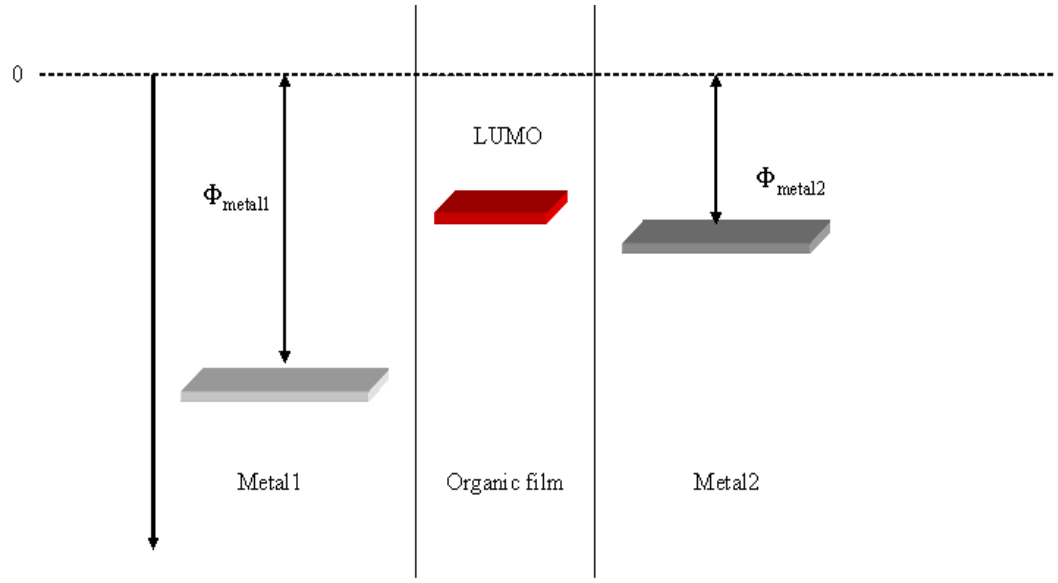

Fig.4.1 *Scheme of novel thermovoltaic device considering the metals work functions before that junctions occur.*

He thermoelectric behaviour of these devices it was needed to develop an experimental apparatus not commercially available, which could perform the following operation:

- impose given programmed thermal gradients between the metal layers of the devices;
- Measure the voltage developed ad metal terminal in closed and open circuit configurations;
- Take records of the data by acquiring them in in an interfaced computer.

The set up of the experimental apparatus, the methods of thermovoltaic devices preparation, the measurement made, and the obtained results will be given in the following paragraphs.

4.2 Instrumentation.

Experiments were done with an home made thermoelectric device voltmeter (TDV) which is shown in *Fig.4.2 a,b*. This apparatus allowed to place samples between a Peltier's element and an electric heater. The imposed temperature gradients could be electronically regulated by computer. In closed circuit configuration voltage was measured, with high resolution voltmeter, at the ends of an external impedance serial connected with the sample's electrodes. The voltage could be measured as function of the time at different imposed temperature gradients. The instrument could supply controlled power by a 40Watt power supply for general uses, and four independent, digitally controlled, 40Watt power supplies, devoted to the control of t two Peltier elements and two heaters (*Fig. 4.3a*). This configuration allowed the contemporaneous investigation of two thermovoltaic elements. The measurements were made using two couples of high precision solid-state switches, to select the hot-cold plates combinations and seven high precision solid-state switches: six switches

related to different serial impedances (10MΩ, 1MΩ, 100KΩ, 10KΩ, 1KΩ, 100Ω) circuits and one to a free-slot circuit to use several load (*Fig. 4.2 b)*. This instrument reached a 10 bit analogical/digital conversion precision which allowed voltage measurement with errors less than 0,5 ‰ .

Also Wheatston bridge h/p Hewlett Packard 4284a (20 Hz- 1 MHz) LCR, ISO-Tech IDM 91 tester and METEX-3800 digital multimetr were used to measure the devices internal impedance.

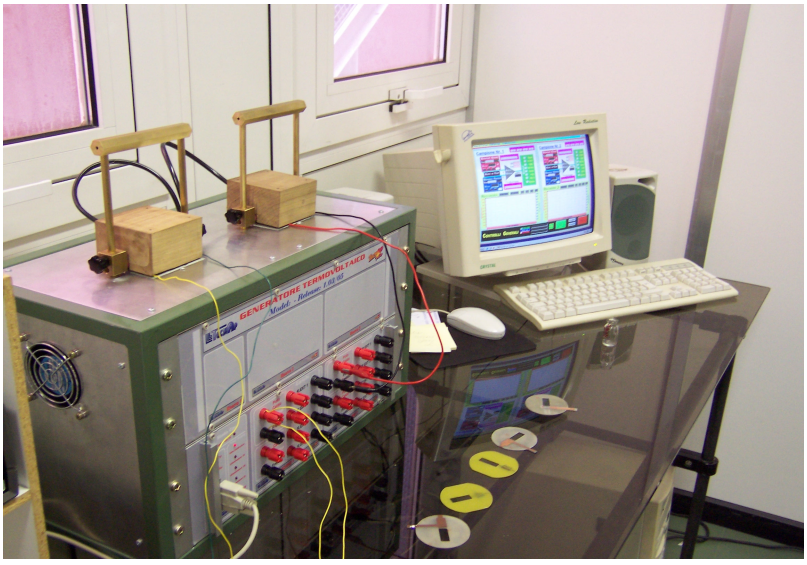

(a)

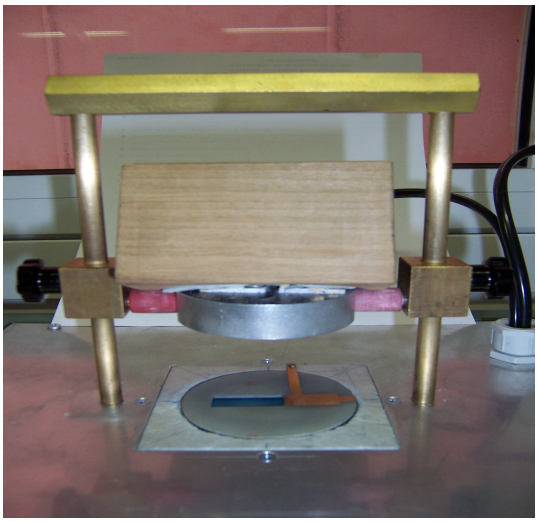

(b)

Fig.4.1 *TDV instrument (a) and measure core (b): Peltier cell stays at the bottom of the instrument and electrical heater stays at the top of the instrument.*

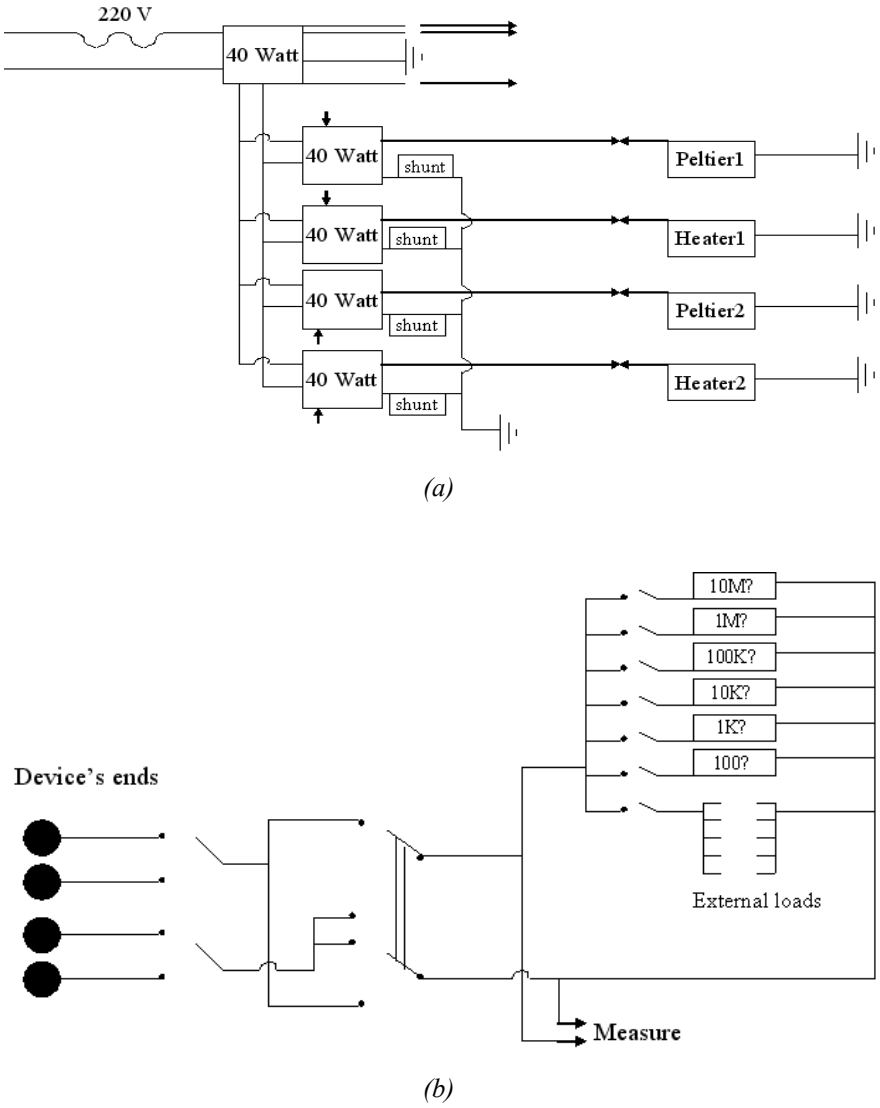

Fig.4.2 *TDV instrument temperature control (a) and voltage measure (b) circuits.*

4.3 Procedures for sample preparation.

The following procedures have been used to prepare the thermovoltaic elements.

In situ Polymerization.

In some case the device was prepared starting from a solution of the active redox molecules in a fluid monomer. This solution was always prepared by mixing the components at a temperature of 60-80°C, by a magnet stirrer. An appropriate thick

layer of this fluid mixture has been sandwiched between two metal layers and has been subsequently hardened by polymerizing the monomer component.
Thickness of samples was controlled using silicon internal spacer particles until 200 microns thickness, external spacers above 200 microns and home made PVC or metal stamps for thickness above 500 microns. Surface was set at 1 cm^2 for all samples.
In most of the case bisphenolAglycerolate(1-glycerol/phenol)diacrylate (BAGD) has been used as an acrylate polymerizing monomer. The UV polymerization technique has been used when at least one of the metal layer was supported on a transparent glass substrate (this was the case when one of the external layer was constituted by Indium Tin Oxide (ITO). One of the active molecule most frequently used was the1-(11-(acryloyloxy)undecyl)-4,4'-bipyridin-1-ium bromide (Vacr). When the metal extern support were both opaque Uv polymerization could not be applied. In those cases the sample has been hardened by thermal polymerization in a temperature interval generally comprised between 100 and 150 °C.

Mixing of the active components in thermoplastic polymer.

Polymeric raw material like poly(vinyl butyral-co-vinyl alcohol-co-vinyl acetate) (PVB) or poly(vinyl formal) (PVFM) were mixed with solutions in propylene carbonate (PC) of the active molecules by stirring for 4-6 hours at 120-180°C. the active molecules were previously dissolved in propylene carbonate by stirring the mixtures at 80-100°C for 1-2 hours. Films of the plastic blends obtained as described above were laminated at temperature of about 80-100 °C between two metal support.

Samples with nanoparticle.

In some of the samples conductive nanoparticle have been added to the mixtures in order to improve the electron conductivity. When the film was prepared by the in situ polymerization method, nanoparticle were previously dispersed in the monomer solution by ultrasound vibrations in the presence of a surfactant agent.

They were instead dispersed in the PC solution in the case of film s prepared by mixing in thermoplastic polymers.

4.4 First evidence of a stationary state in a Single Organic Film Thermovoltaic (SOFT) cell.

Starting from the theoretical consideration illustrated in chapter 3 several cells made by a single organic film sandwiched between two different work-function metals have been prepared and investigated. For brevity these cell will be defined by the acronym SOFT (Single Organic Film Thermovoltaic) in the following.
Our choice for a promising active molecule was oriented from the first beginning on the 1,1'-diethyl-4,4'-bipyridine-1,1'-diium diperchlorate (ethyl viologen diperchlorate (Vet))

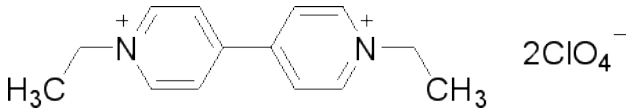

since the electron transport properties of organic films containing this molecule (actually a divalent organic cation salt well known in literature as ethyl viologen) have been previously studied in our laboratory, where Vet was used in the as a dopant of self supported plastic film for electrochromic and electrooptical devices [75-77]. From these studies there was evidence that the presence of viologen molecules in a plastic film could allow the transport of electron by intermolecular electron jump across the doped film. Another reason to devolve attention to this molecule came by the inspection of the metal work function values. Values of the work function for several metal [78] are reported in the following *Fig. 4.3*.

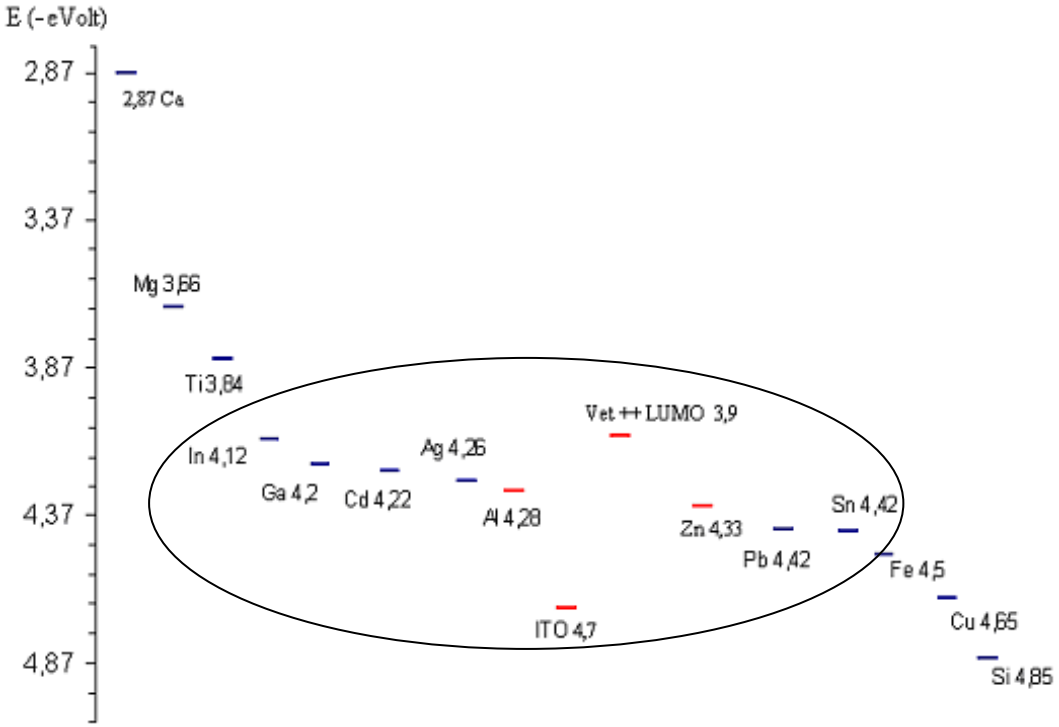

Fig.4.3. Values of the work function for several metal and Vet^{++} LUMO level [78,79].

In the same *Fig. 4.3* The LUMO level of the Vet molecule has been also reported. As it is possible to see in the above *Fig 4.3* many metals (see the encircled ones) have work functions not much far away from the Vet LUMO. These factors made the Vet molecule a unique reference point for our investigation.

Of course in our first experiment two metal layers easy available were chosen: ITO and aluminum. ITO is not a metal but a n doped semiconductor composed by a mixture of indium(III) oxide (In_2O_3) and tin(IV) oxide (SnO_2), typically 90% of In_2O_3, 10% of SnO_2 by weight [80,81].The first investigated devices were made by a solid plastic films, containing Vet, laminated between an ITO and an aluminum electrodes. The plastic films were mixtures of poly(vinyl butyral-co-vinyl alcohol-co-vinyl acetate) (PVB), a commercial available low cost polymer, and a solution of Vet in propylene carbonate (PC), that need to dissolve the bipyridinium salts in order to achieve a uniform dispersion in the polymer matrices.

A first thermovoltaic experiment made on ITO/Viologen-PVB-PC/Al SOFT cells, where the percentile composition of the Viologen film was 32% in weight of viologen, 35% of PC solvent and 33% of PVB, is shown in the next *Fig. 4.4*, where the averaged thermovoltaic response of 5 SOFT cells, having the same composition indicated above, was measured as a function of the time after the application of 60°C thermal gradient (red line). The voltage has been measured in a closed circuit configuration at the heads of a 100 Kohm serial resistor. The dimension of the cells was 1cm^2 per 100 microns thickness.

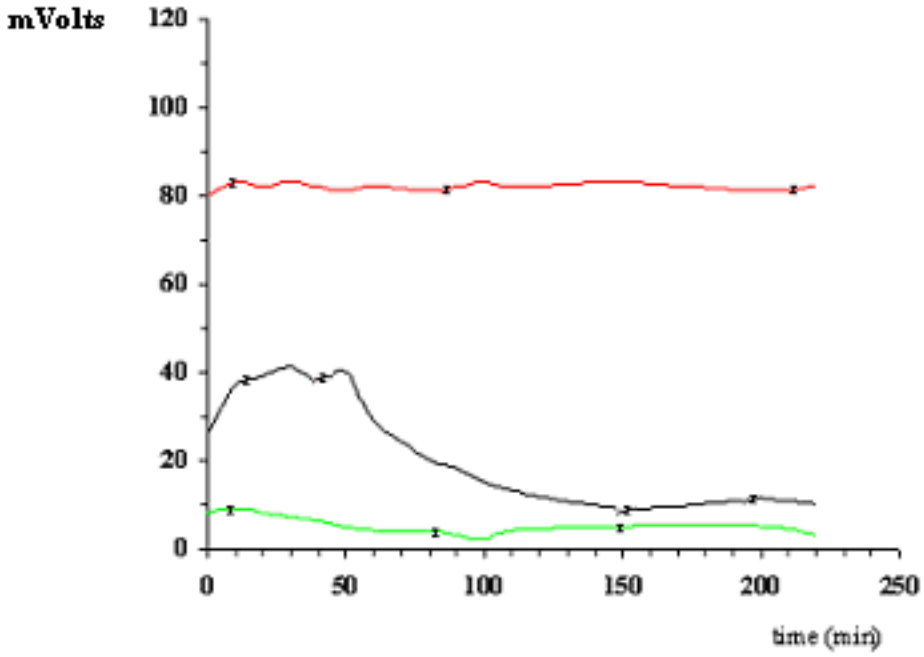

Fig.4.4 *Average voltage values of five sample measured at the end of 100 KΩ serial impedance as function of time, imposing a thermal gradient of 60 °C (20°C Tc 80°C Th); black line shows average voltage values of three devices at uniform temperature T=80°C; green line: average voltage of three devices at room temperature.*

In the same *Fig.4.4* two other experiment are reported: that is to say the voltaic response when the temperature gradient is kept equal to zero at room temperature (green curve) and for a temperatre of 80°C (black curve). Above experiments are not relevant from a practical technologic point of view, since the system shoved a stationary state (In the presence of thermal gradient) where the elctric current

furnished to the closed circuit was only 8mA/m^2, but this first set of experiments confirmed the correctness of the main hypothesis made with respect to the objectives of this PhD Thesis. Giving a look to the three different curves of *Fig.4.4* it is possible to drive the following conclusion. The SOFT cell is not in equilibrium once prepared. So an electric current should be furnished for a certain time to the circuit, due to the occurrence of the hypothesized chemical processes at the two electrodes. There is not evidence of this "battery like" mechanism at room temperature. But at 80 °C this effect comes up in evidence. The black curve shows that the cell furnishes a current of 4mA/m^2 to the circuit for about 1 hour, before discharging gradually in about a couple of hours, when the systems reaches its stable thermodynamic equilibrium. At room temperature the activation energy for charge transfer processes prevents, very likely, any charge circulation. In the presence of a thermal gradient two facts occur. The negative term $Cp_{em}\,\Delta T$, in the equation (29) in chapter 3, starts to play a role increasing the free energy released by the system, and the coupling of the heat flux with the electric flux, driving the system in a stationary out of equilibrium state.

There might be several reasons for the low efficiency of the system, but first of all we have to mention that the internal electric impedance of the SOFT cell was about 1000KΩ·cm. We still do not know (Impedance Spectroscopy analysis was out of the aim of this thesis work) the ionic and electron contribute to the cell conductivity, but in the case of the discussed cells the electronic inner conduction was for sure very low, thus strongly preventing charge circulation. It must be also underlined that the ITO work function is in the isolated materials separated from the Vet LUMO level of about 0.8 eV. We do not know how the level adjust in stationary state, but is very likely that this level separation, remains to high to efficiently overcome by the KT activation.

The number of the Vet charge carrier molecules regulates the efficiency of the system. The influence of Vet concentration on the cell stationary voltage is shown in the Fig. 4.5. A linear positive trend of the voltage is observed up 29% of Vet. Then the voltage keeps a substantially constant value in the range of 29%- 34%. Nevertheless, in this range of the concentration, it is possible to appreciate achievement of a maximum value, 83,2 mV, corresponding to a Vet

percentage of 32%, which represents the limit of Vet solubility inside PC. For values greater than 32% the film becomes very opaque and optical microscopy shows that above 32% the Vet salt starts to precipitate as crystal in the film, so the number of the charge carriers do not increases any more inside the SOFT film. For concentration of Vet above 34%, as Fig. 4.5 shows, the voltage gradually drops.

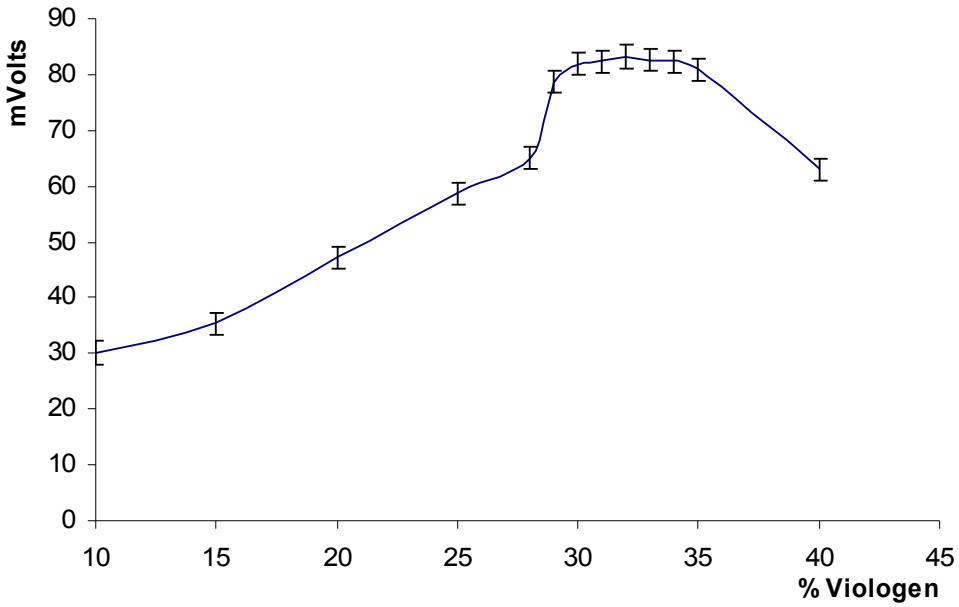

Fig.4.5 *Stationary thermoelctric voltage measured in closed circui configurationt for at least 5 hours with a 60 °C thermal gradient (20, 80 °C) in ITO/Vet/) as a function of the Vet weight ratio. Eeach voltage value reported was the average of three samples voltage values measured at the ends of 100KΩ external serial impedance. The Vet 32% and PC 35% ratio were constant.*

On the other hand for such an high Vet concentration the plastic structure of the film starts to degrade to state of a very viscous fluid.

4.5 A trial to improve the performance of the PVB/Vet film trough the formation of Vet charge transfer complexes.

Considering that it is impossible to increase the number of Vet molecules in the film beyond the critical value of about 34%, a trial was made to improve its effectiveness as charge carrier by allowing it to form Charge Transfer Complexes (CTC) with some donor molecules, having the proper LUMO energy level.

As it is reported in literature [82], the conduction of an organic film can be increased by the introduction of some CT complexes.

Driven by considerations about solubility and stability with the PVB polymer matrix, we chose Hydroquinone and Ferrocene as donors molecules and investigated the voltage behavior of SOFT films containing Vet/Hydroquinone or Vet/Ferrocene charge transfer complexes [79-82].

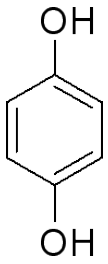

Hydroquinone

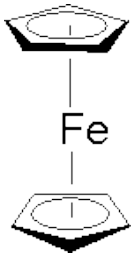

Ferrocene

Following the literature suggestions concerning the CTC complexes obtained from thiophenic oligomers such as 3',4'-bis-(2-metossi-etil)-[2,2';5',2'']tertiophene and 3',4'-Bis[(Metossicarbonil)-metil]-[2,2';5',2"]tertiophene (TERs) or other molecules as rose Bengal, tetraphenilporfirine and Ethidium bromid, we prepared some films based on other CTC donor partner in Vet-Pc-PVB blends, but significant voltage improvements are observed only using hydroquinone and Ferrocene.

Following ITO/PVB-PC-Vet-Dopant/Al devices voltage are measured in function of its components weight percentage, in order to study the effect of dopants on the device efficiency.

The *Fig. 4.6* shows the stationary voltage that was measured in SOFT films keeping the Vet concentration 32% and PC 35% concentrations not varied, and increasing gradually the donor dopant percentages (Hydroquinone ,black line or Ferrocene, green line) at expense of the polymer matrix. Two different behaviors can be observed depending on the type of dopant. In fact, samples containing Hydroquinone molecules exhibited a bigger value of the voltage measured in the stationary state with respect to the samples containing Ferrocene.

This result can be interpreted by taking into account the CTC formation-dissociation equilibrium reaction. The dissociation constant measured for Vet/Ferrocene CTC in polar solutions, was greater than the Vet/Hydroquinone one [83], so the effective number of CTC molecules is surely bigger in the case of the Vet/Hydroquinone CTC at the same analytical concentration the dopant molecules.

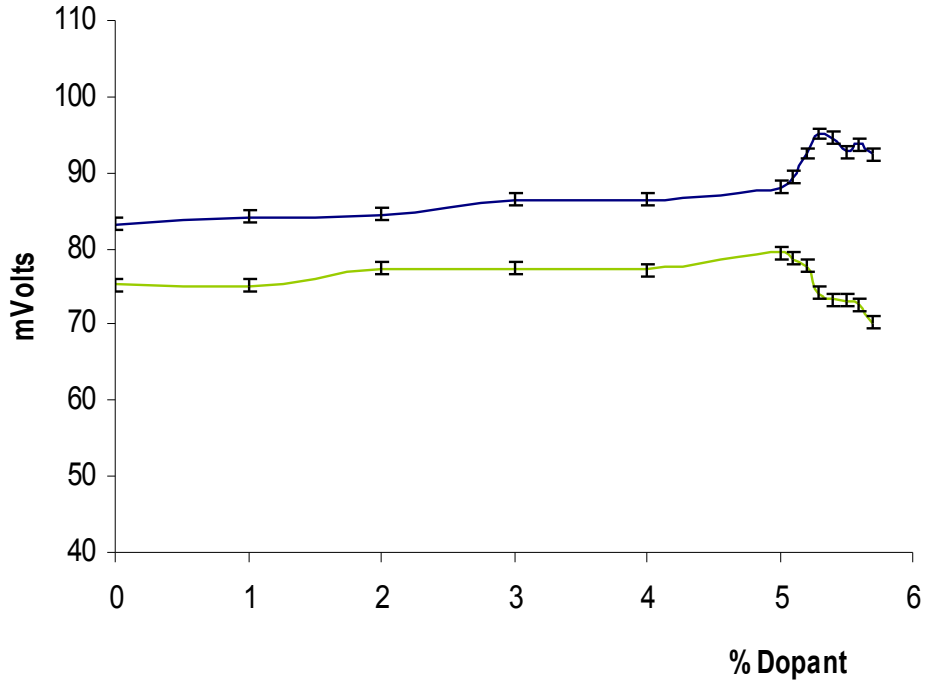

Fig.4.6 ***S****tationary thermoelctric voltage measured in closed circuit configuration for at least 5 hours/point with a 60 °C thermal gradient (20, 80 °C) in ITO/Vet-Hydroquinone/ Al (black line) and ITO/Vet-Ferrocene / Al (green line, as a function of the) weight ratio of the dopants. Eeach voltage value reported was the average of three samples voltage values measured at the ends of 100KΩ external serial impedance. The Vet 32% and PC 35% ratio were constant.*

Moreover *Fig. 4.6* shows that the maximum voltage value in the case of Vet/Hydroquinone CTC is 95,1 mV and was obtained for a Hydroquinone percentage of 5,3%, while in the case of Vet/Ferrocene CTC the 79,4 mV maximum value was measured, corresponding to a 5.0% Ferrocene concentration.
From this first set of experiments it was impossible to reach a conclusion on the real effect of the dopant concentration on the device performance, and to give a meaning to the maxima observed in fig. 4.6. This was due to the fact that while increasing the dopant concentration ; keeping constant the Vet concentration, the film stated to ruin loosing the solid stability and going in a viscous jelly phase transition. Of course this was due to the fact that the PVB concentration had to be lower at the expenses of dopant concentration.
The physical degradation of the film, when the PVB matrix concentration is lowered below 27%, didn't allow us to further increase the dopant in order to reach at least a 1:1 Vet/dopante molar ratio, which would be obtained for weight ratios of 3.757 for Vet/Hydroquinone and of 2,265 in the case of Vet:Ferrocene.
The maximum effect due to the presence of donor dopantas, when taking into consideration formation of charge transfer complexes with the Vet, should occur for a Vet/dopant molar ratio equal 1.1.
Further experiments have been performed in observe the effect of the dopants for wider ranges of Vet/dopant concentration ratios. The results are shown in *Fig. 4.7*.
In this case, in order to prevent films phase transition, the percentages of PVB and PC have been kept constant to 32,7% and 35% respectively, for Hydroquinone , and to 33% and 35%, for ferrocene dopant, while the Vet and dopant concentration have been both changed.

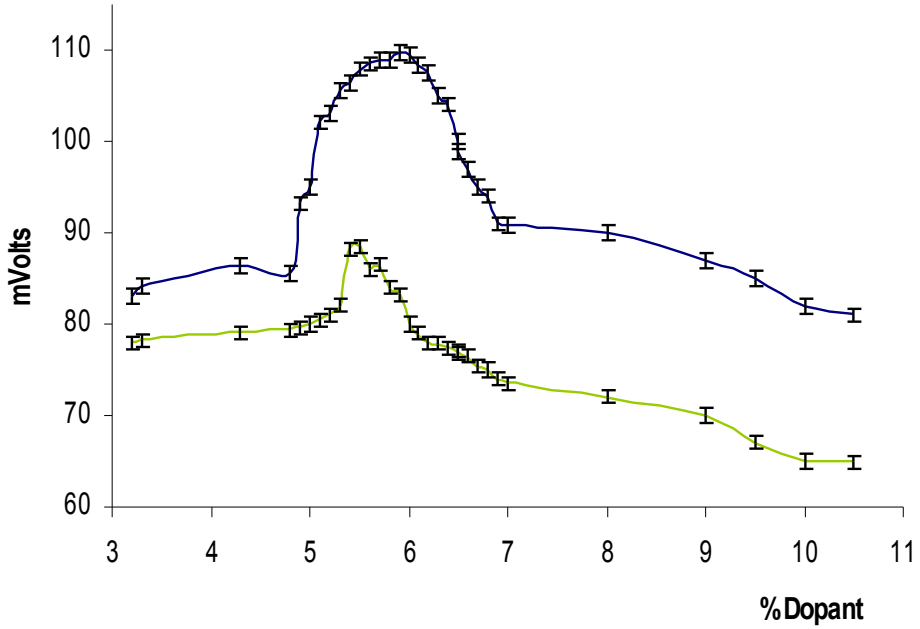

Fig.4.7. *Stationary thermoelctric voltage measured in closed circuit configuration for at least 5 hours/point with a 60 °C thermal gradient (20, 80 °C) in ITO/Vet-PBV-PC-Hydroquinone/Al (black line) and ITO/Vet-PVB-PC-Ferrocene/Al (green line), as a function of the weight % of the dopants. Each voltage value reported was the average of three samples voltage values measured at the ends of 100KΩ external serial impedance. In this experiment PC and PVB were kept constant at values of 35 % and 32.7 % for Hydroquinone, and 35 %and 33 % for Ferrocene respectively.*

In this case the structure of the film remained solid in the full range of investigated concentrations, but the results given by the experiment is similar to that obtained in the previous one. The maximum of the device response was observed at the almost the same weight ratio of the two dopants that is to say and precisely at 5.9% for Hydroquinone and 5.5% for Ferrocene.

The maxima did not occur at vet/dodant molar ratios equal to 1:1, but in correspondence of the following compositions:

Vet · $2ClO_4^-$	26.4 %
Hydroquinone	5,9 %
PVB	32,7 %
PC	35,00 %

and

Vet · $2ClO_4^-$	26,5 %
Ferrocene	5.5 %
PVB	33,00 %
PC	35,00 %

Another set of experiments has been made by fixing the dopant concentration to the value of 5,3% for Hydroquinone and 5% for Ferrocene and PC at 35% (values where the maxima were observed in the experiments described in *Fig. 4.6*), but varying the Vet concentration between 23 and 33%: in this condition PVB wt% remains always higher than 26.7% (*Fig. 4.8*). *In Fig. 4.8* is shown that in this case the film response remains almost constant in the full range of compositions, but two small maxima are observed around a Vet wt% of 27%. So we have to conclude that donor dopants have an important effect on the devices bua this effect is not linked to the formation of charge transfer complexes, since the maxima observed for two different dopants having different comnplessation constant fall at the same wt%. Even in the case where the vet/dopant molar ratio is varied in a wide range the response of the film remain next to the maxima response obtainable in this experimented devices (around 105 mVolts for Hydroquinone and 87 mVolts for Ferrocene) provided that the percentage of the dopants (no matter which of the two) remains around 5%. So the response do not seems linked to the stochiometry of transfer charge complexes.

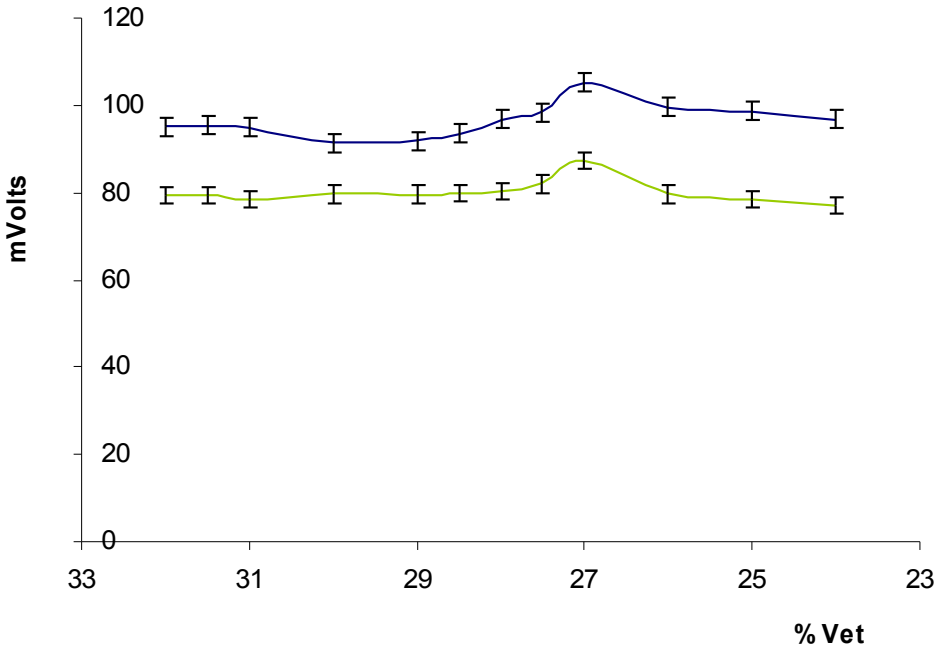

Fig.4.8 *Stationary thermoelctric voltage measured in closed circuit configuration for at least 5 hours/point with a 60 °C thermal gradient (20, 80 °C) in ITO/Vet-Hydroquinone-PC-PVB/ Al (black line) and ITO/Vet-Ferrocene-PC-PVB/Al (green line), as a function of the weight % of the dopants. Each voltage value reported was the average of three samples voltage values measured at the ends of 100KΩ external serial impedance. In this experiment PC, Hydroquinone and Ferrocene were kept constant at values of 35% , 5.3%and 5% respectively.*

In Fig.4.9, the stationary behaviour of the best thermovaltaic elements obtained in ITO/PVB-PC-Vet/Al systems and corresponding Hydroquinone and Ferrocene doped systems , is shown

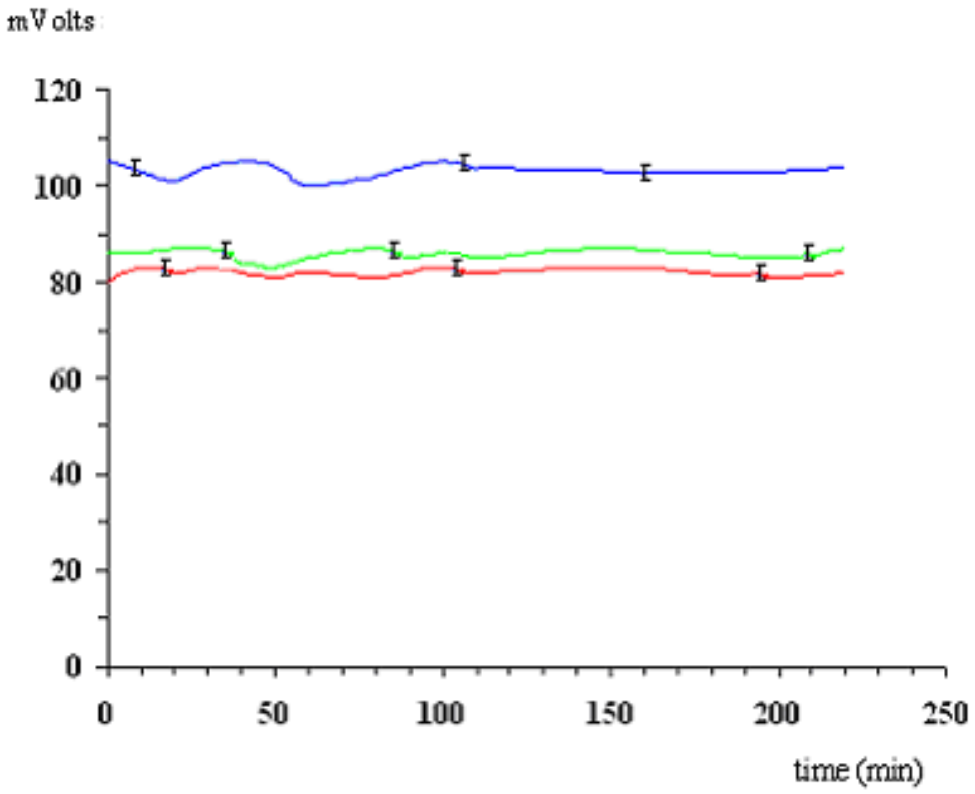

Fig.4.9 V*oltages measured at the ends of 100 KΩ serial impedance in function of time, imposing a thermal gradient of 60 °C (20°C Tc 80°C Th). (a) Average values for 5 samples prepared with a ITO/PVB-PC-Vet/Al devices (red line); (b) Average values for three ITO/PVB-PC-Vet-Ferrocene/Al devices (green line); (c) average values of to three ITO/PVB-PC-Vet-Hydroquinone/Al samples (blue line).*

Remains to explain what could be the role plaid by the dopants. In order to find an explanation we have investigated the electrical impedance of the same devices which thervoltaic response has been reported in *Fig. 4.7*. Before going into discussion of these data, a preliminary discussion of the observed electric behaviour of the devices when the D.C. impedance was measured, by using a simple multimeter instruments, is required. As expected, due two the asymmetry of the system, the multimeter response was not symmetric when exchanging the meter connection point to the cell (while measuring the system was at equilibrium: the thermal gradient was zero). When the multimeter red tip (+) was placed on the ITO electrode (work function -4,7eV) and the black tip (-) was placed on the Aluminium electrode (work function -4,28eV), as in *Fig. 4.10a,* the

measured impedance was out of scale. In the opposite configuration, shown in *Fig. 4.5b,* a finite impedance could be measured.

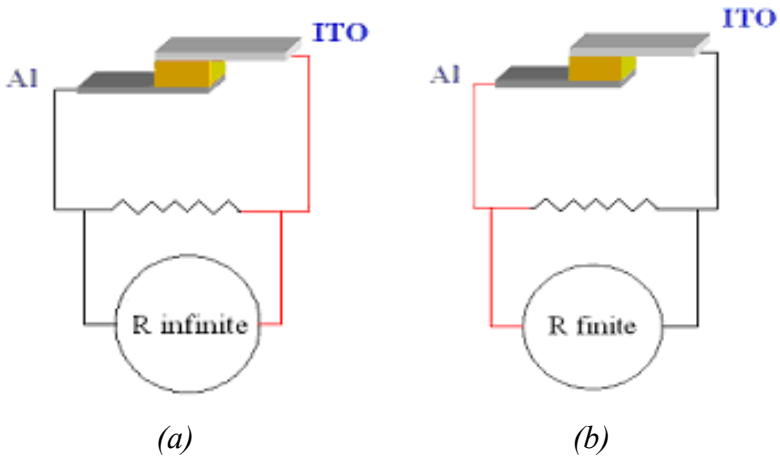

Fig.4.10 *Configurations for impedance measurement.*

The device shows a behaviour similar to that of diode [84]. The impedance measurement made in the configuration (b) of *Fig. 4.10.* are illustrated in the Fig. 4.11, where the thermovoltaic stationary response has been also reported to show the strict correlations between this and the impedance of the devices.

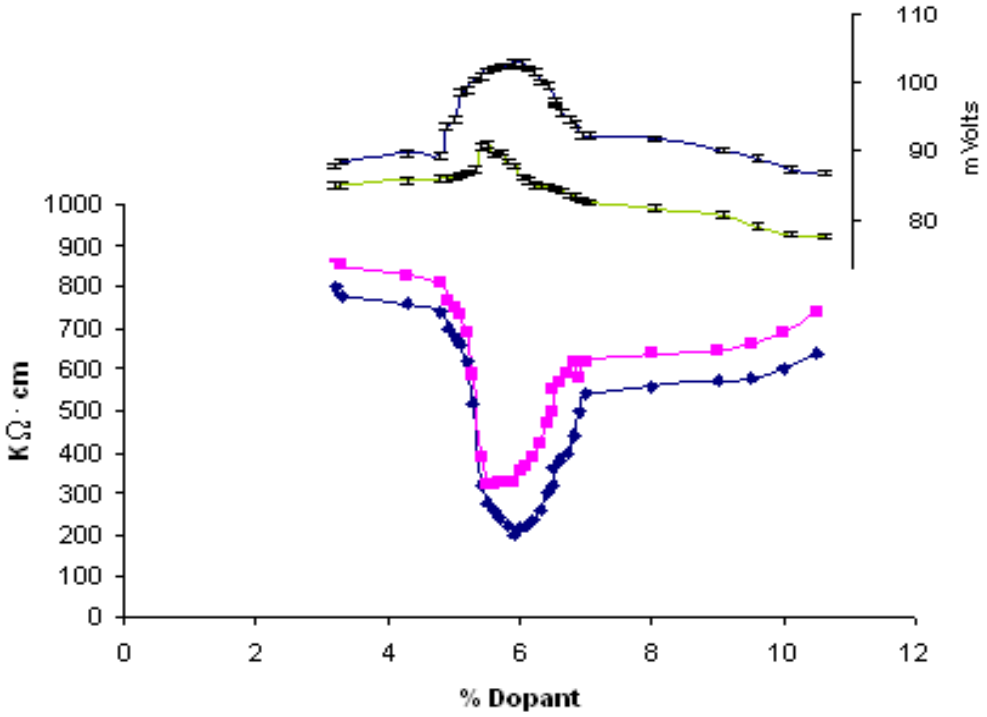

Fig. 4.11. *Electric impedance of ITO/Vet-Hydroquinone-PC-PVB/ Al (black line) and ITO/Vet-Ferrocene-PC-PBV/ Al (green line, as a function of the) weight % of the dopants. In this experiment PC and PVB were kept constant at values of 35% and 32.7% for Hydroquinone, and 35%and 33% for ferrocene respectively. On the top voltage data already reported in fig. 4.6 are shown for comparison*

The perfect correspondence of thermovoltaic data and impedance data is not , of course surprising: the current flowing into circuit is inversely proportional to the inner impedance of the generator, but it must be explained why the dopants make creates the impedance hole shown in *Fig 4.11* at a specific weight%, in dependently from their specific chemical structure. This remains one of the point open for future investigations.

Another interesting feature of the devices investigated is that when inverting the temperatures of the electrodes reversing the sign of the thermal gradient a stationary closed circuit voltage can be also measured, even if its value is lower with respect to that measured when heat is furnished at the lowest work function

electrode. This means that the isolated metel levels can be inverted under stationary state conditions.

The blue line reported in *Fig. 4.12* is the thermovoltaic response measured when the ITO is the hot electrode, while the red line represents the analogous response measured when heat is furnished at the aluminium electrode.

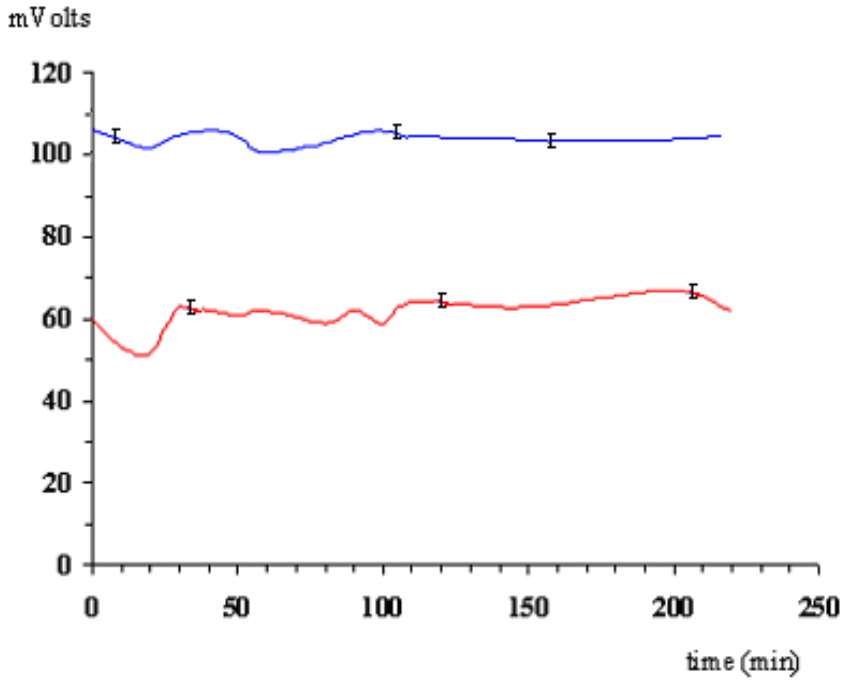

Fig.4.12 *ITO/PVB-PC-Vet-Hydroquinone/Al device voltages measured at the ends of 100 KΩ serials impedance as function of time, imposing a thermal gradient of 60 °C (20°C Tc 80°C Th). Blue line: values measured on warming the ITO electrode; red line: measurements performed on warming the Aluminum electrode.*

Just for completeness, we compare in *Fig. 4.13*, three different responses given by the same ITO/PVB-PC-Vet-Hydroquinone/Al device: (a) in absence of gradient at room temperature (green line); (b) in absence of gradient at T= 80 °C (black line); (c) with a gradient (blue line).

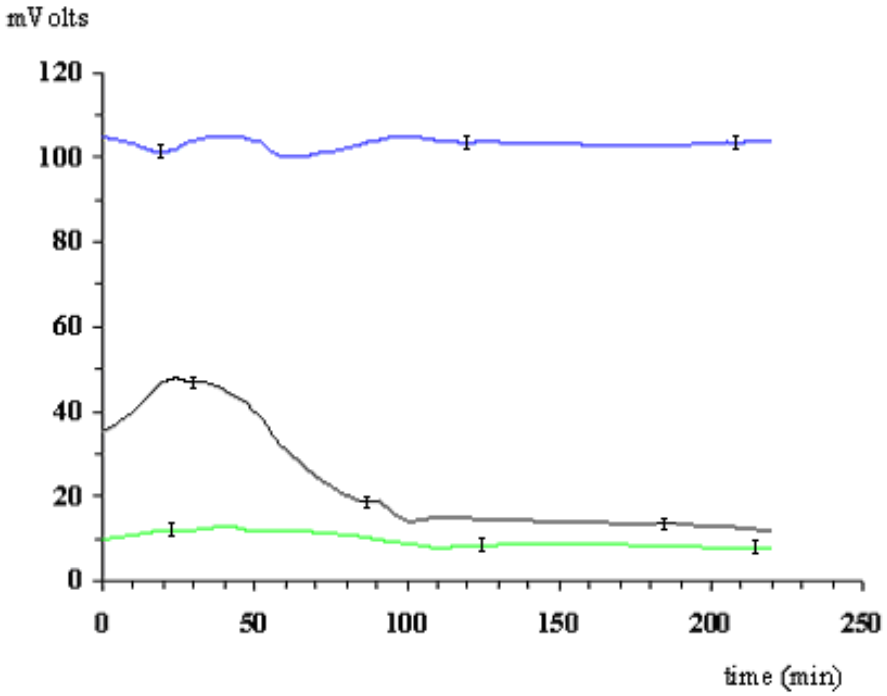

Fig.4.13 *ITO/PVB-PC-Vet-Hydroquinone/Al device voltages measured at the ends of 100 KΩ serial impedance as function of time. (a) blue line: average voltages of three devices obtained imposing a thermal gradient of 60 °C (20°C Tc 80°C Th); (b) black line: average voltages of three devices at uniform temperature T=80°C; (c) green line: average voltages of three devices kept at room temperature.*

We were driven at the same conclusions derived from *Fig.4.4* highlighting the fact that the SOFT film doped by CTCs exhibits the highest efficiency.

Many other experiments have been done changing the viologen salt counter anion. The experiments discussed above were made on ethyl viologen diperchlorate (Vet) salts. Since in literature [83] is reported that the nature of the counter anion can influence the charge transport in organic salts, experiment on ITO/PVB-PC-$Vet^{++}2X^{-}$- Hydroquinone/Al similar to those shown before have been repeated by with viologen salts where the counter anions (X^{-}) were Iodine, Bromine, and Chloride. No improvements have been observed. Their results are reported in the next *Fig. 4.14*.

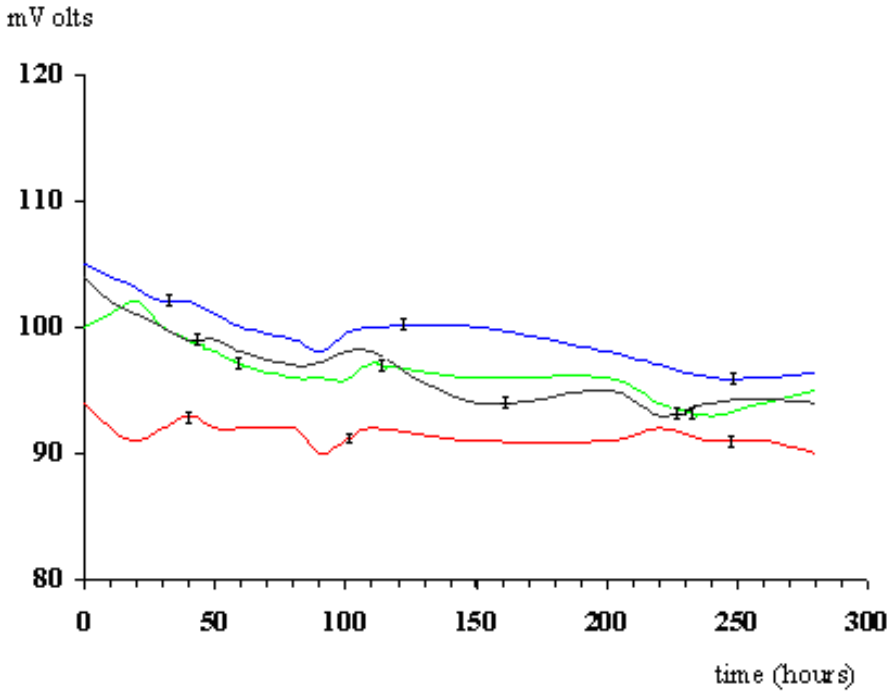

Fig.4.14 *ITO/Aluminum devices voltages measured at the ends of 100 KΩ serials impedance as function of time and imposing a thermal gradient of 60 °C (20°C Tc 80°C Th). Blue line: average voltages of three PVB-PC-Vet · $2ClO_4^-$-Hydroquinone devices; black line: average voltages of two PVB-PC-Vet · $2Cl^-$-Hydroquinone samples; green line: average voltages of three PVB-PC-Vet · $2Br^-$-Hydroquinone devices and red line: average voltages of two PVB-PC-Vet · $2I^-$-Hydroquinone devices.*

4.6 Thermovoltaic celles (TVC) made with side chain viologen acrilate polymers.

The main limitation of the TVCs illustrated in paragraph 4.4 and 4.5 is not the value of the voltage, but the furnished current. In order to keep the system in a stationary state in a closed circuit configuration the external load must not lower than 50KΩ. If one tries to get bigger current in the external circuit the voltage drops since the conduction in the inner film is very low and the electrodes are not recharged with an efficient mechanism. That is to say the activation energy to charge transfer inside the organic film becomes a limiting kinetic factor. From a

certain point of view viologens seem to have the right LUMO levels but they are not enough good electron conductors. We made an attempt to improve their electron conduction by linking them in a polymer chain as laterals side chain groups [74]. In other words synthesized poly(acrylate viologen) has been used to build up the central film of the thermovaltaic devices. We have chosen to prepare the side chain polymer starting from the the1-(11-(acryloyloxy)undecyl)-4,4'-bipyridin-1-ium bromide

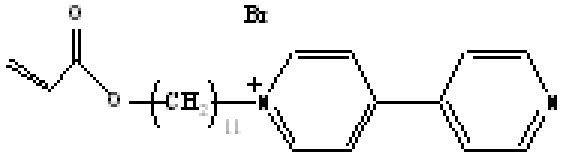

which will be defined as Vacr in the next. From Vacr as stating monomer it is possible to obtain a polymer (or co-polymer with some other acrylate or diacrylate monomer precursors) using a thermal or photonic polymerization to obtain a polymer containing side chain viologens. Unfortunately the polymer made by polymerizing the Vacr monomer is not stable during the time, especially for temperature above the 50-60°C (perhaps for its hygroscopic behaviors), so it could not be used in the thermovoltaic devices. To avoid this problem the monomer bisphenolAglycerolate(1-glycerol/phenol)diacrylate

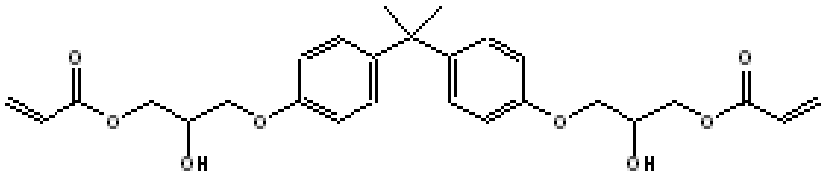

defined as BAGD was used as a copolymerising monomer of the Vacr in different concentration. These copolymers have a much higher melting point and could be used to build up thermovoltaic cells. Despite to the fact that viologen percentage in these films can be of the order of 96% no relevant reduction of the film impedance has been obtained, so no real improvement was possible, as shown in *Fig.4.15*.

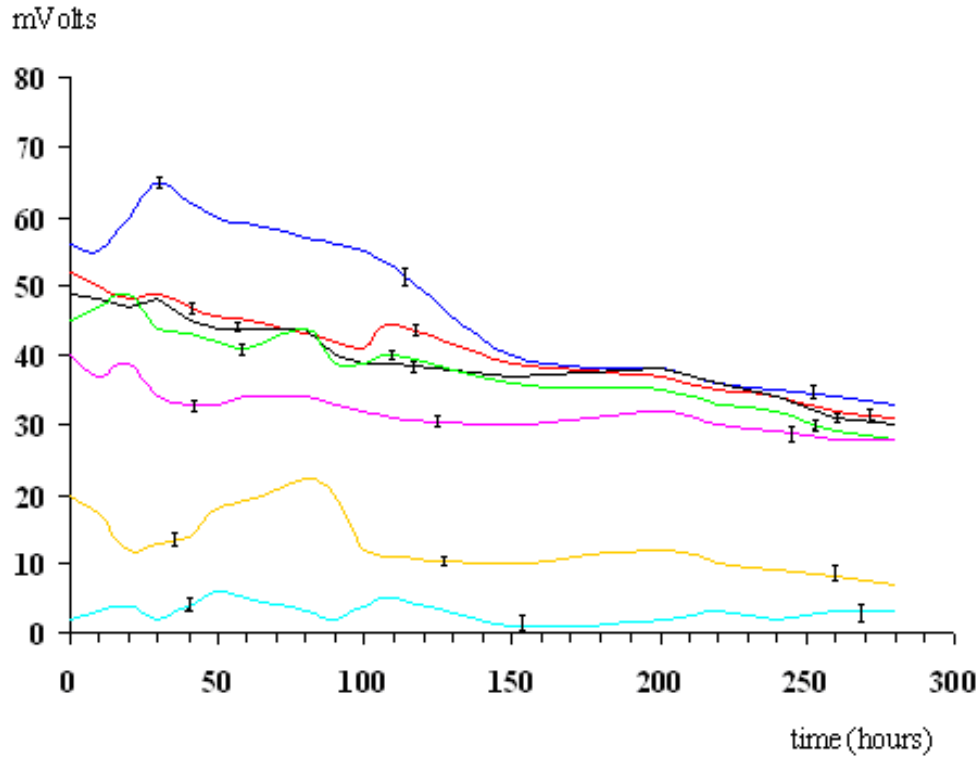

Fig.4.15 *ITO-Aluminum device voltages measured at the ends of 100 KΩ serial impedance as function of time, imposing a thermal gradient of 60 °C (20°C Tc 80°C Th); samples were made using 1% of radical iniziator. Blue line: average voltages of three Vacr 96% BAGD (3%) polymer devices; red line: Vacr 80% BAGD 19%; black line: Vacr 60% 39% BAGD; green line: 49,5% Vacr 49,5% BAGD; pink line: Vacr 40% BAGD 59%; orange line: Vacr20% BAGD 79%; light blue line: BAGD 99% . Radical initiator"irgacure"1% was used in all sample.*

4.7 TV cells made by PVFM support matrix.

In the paragraph 4.5 it has been seen that the PVB supporting matrix becomes very plastic above certain Vet concentration levels. This problem could be solved by using a similar polymer having an higher glass transition temperature. Thus experiments on cells made with Poly(vinyl formal) (PVFM), having a higher transition temperature (Tg = 108°C) [85] respect to the PVB Tg (62-72°C) [85], have been performed. In *Fig 4.16* the voltage values of ITO/PVFM-Vet-

Hydroquinone-PC/Al devices (red line) compared with ITO/PVB-Vet-Hydroquinone-PC/Al devices (blu line) are shown.

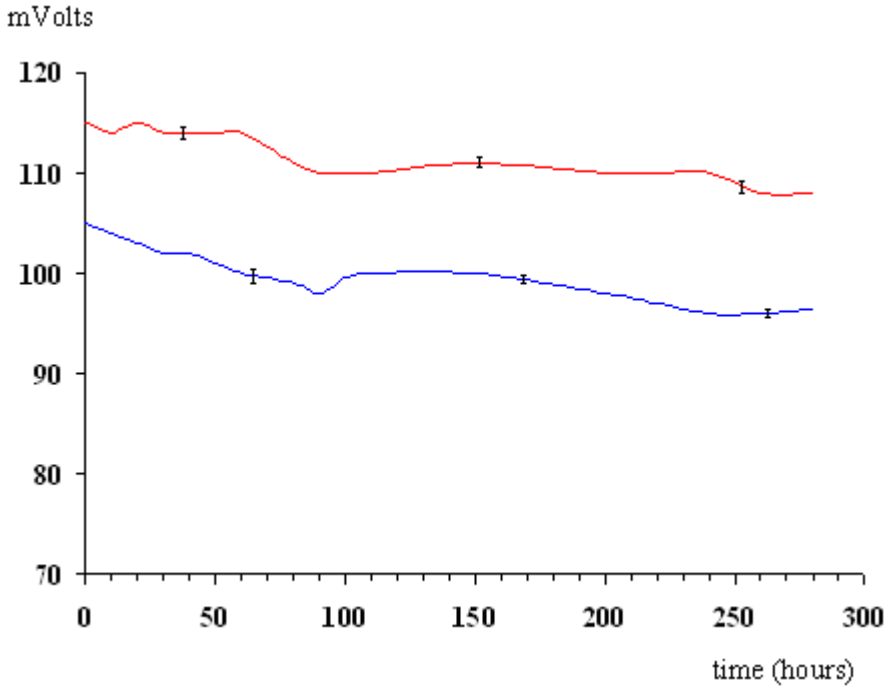

Fig.4.16 *ITO/Aluminum device voltages measured at the ends of 100 KΩ serial impedance as function of time, imposing a thermal gradient of 60 °C (20°C Tc 80°C Th). Blue line: average voltages of three PVB-PC-Vet · $2ClO_4^-$-Hydroquinone devices; red line: average voltages of three PVFM-PC-Vet · $2ClO_4^-$-Hydroquinone devices.*

The voltage values of PVFM SOFT devices are slightly higher than those of PVB SOFT devices. This last system has been used for further investigations as it will be shown in the next paragraphs.

4.8 Effect of the film thickness.

The film thickness plays a central role in the performance of the devices. From one side the thickness needs to be big enough to prevent to the conduction between the two electrodes. On the other hand the increasing of the film thickness film impedance thus limiting the electron recharging currents (here the term recharging indicates the refilling of the highest level electron by the electron coming from the lowest level electrode). In order to understand the influence of

the film thickness on the thermo-voltage of PVFM-Vet-Hydroquinone-PC films interposed between ITO and aluminum electrodes, the stationary state thermo-voltages, obtained with a gradient of 60°C, have been measured as a function of the film thickness. The results are reported in *Fig.4.17*.

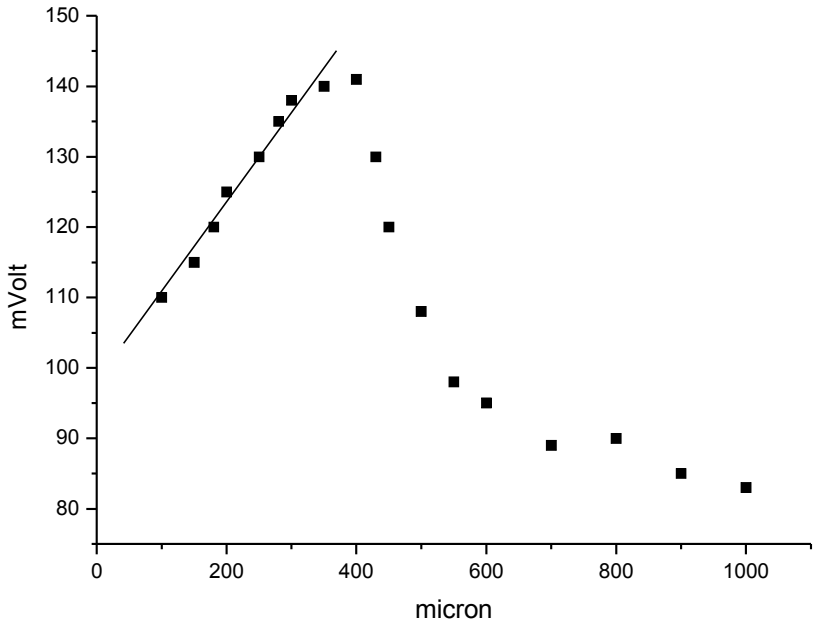

Fig.4.17 *Maximum voltages reached in the stationary state (kept almost 300 minutes) of several thickness ITO/PVFM-PC-Vet-Hydroquinone/Al samples measured at the ends of 100 KΩ serial impedance, imposing a thermal gradient of 60 °C (20°C Tc, 80°C Th). Data collected under 450 microns value were interpolated by a straight line.*

The voltage increases linearly with increasing of the SOFT film thickness for thickness below 450 microns. For ticker films the voltage decreases with an almost hyperbolic trend . On a qualitative level the above trend can be explained by the presence of the two competing factor introduced above. For low thickness the prevention of heat transfer between the electrodes, which increases the efficiency of the cells, prevails on the gradual increase of the film impedance. The second part of the curve is dominated by the impedance growth. The almost hyperbolic experimental trend agrees with the fact that an increased impedance gives a reduction on the central film electron conductivity as a function of the

thickness with a hyperbolic trend. We have seen before (*Fig. 4.11* in paragraph 4.5) that the stationary state voltage follows strictly the film conductivity.

4.9. Experiments with other metal electrodes

After having chosen the best film formulation obtained in the course of the experiments described above, and having optimized the thickness of the film obtained by this formulation, the attention has been devoted to the observation of the cells for longer time in order to asses their life cycle. New experiments were done the stationary state of the cells continuously for at least 600 hours (25 days) with no vanishing thermal gradient applied.

Long time experiments conduced in ITO/PVFM-PC-Vet-Hydroquinone/Al devices (red line in *Fig 4.18)* brought to the conclusion that a smoothly decreasing of the potential starts to appear after about 300 hours.

At the actual state of investigation is very difficult to explain this deterioration of the film performance: some chemical degradation of the electrons could occurs, due to impurities or humidity. Our apparatus did not consent us to isolate completely the film from the external environments. Some ionic long term polarization in the film could also influence the interface potential (see equation (29) in chapter 3) creating barriers to the electron fluxes in the central films (see *Fig.1.4*, *Fig.1.5* in chapter 1 and *Fig. 2.11* in chapter 2). Both the argument given above strongly suggested to study new devices where the best films obtained before could be sandwiched between other metals. In particular we wonted to change the ITO electrode which work function is very low with respect to the Vet LUMO comparing the results obtained when observing for 600 hours devices where that of film is interposed between ITO and Al (*Fig. 4.18*). Several electrodes work functions were considered (see *Fig. 4.3*) in order to diminishing the energy barrier that electrons have to overcame at the metal 1 electrode (see *Fig. 1.4*, *Fig. 1.5* in chapter 1 and *Fig. 3.2* in chapter 3). In future it could be used a polymeric material having higher thermal impedance and electrical conductivity than that exhibited by PVFM polymer.

Thus several electrodes were studied glued with 450 micron thickness PVFM-Vet-PC-Hydroquinone SOFT films (*Fig.4.18*), to the Al electrode.

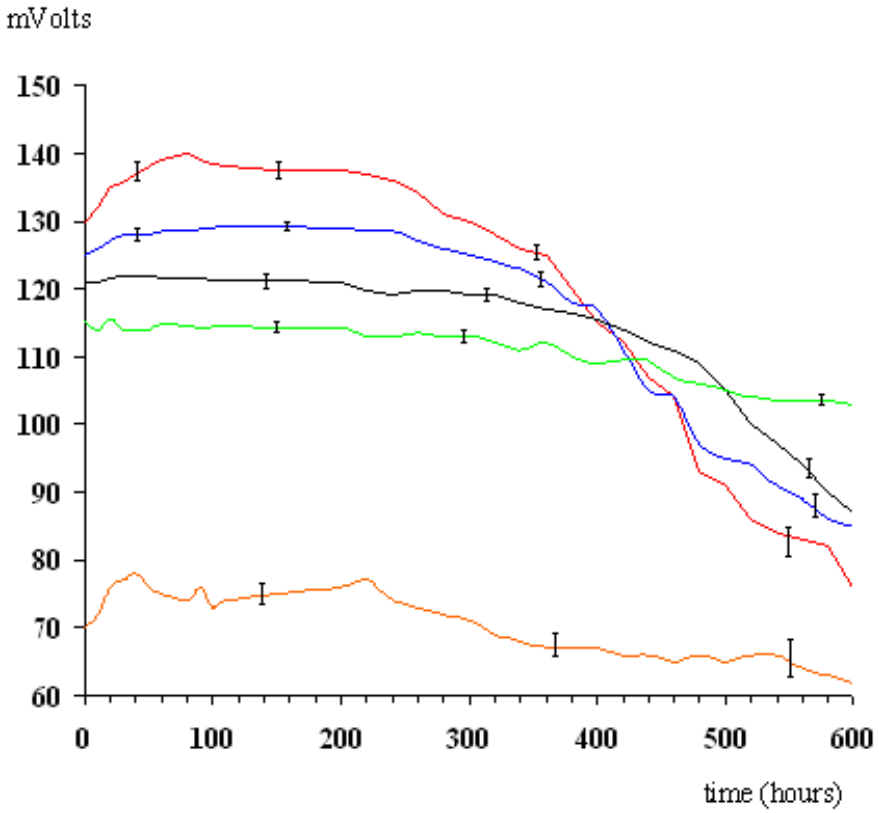

Fig.4.18 *PVFM-PC-Vet-Hydroquinone SOFT film voltages measured at the ends of 100 KΩ serial impedance as function of time, imposing a thermal gradient of 60 °C (20°C Tc 80°C Th). Red line: average data of three ITO/Al devices; blue line: average data for three Cu/Al samples; black line: average data of three Pb/Al samples; green line: average data of five Zn/Al samples; orange line : average data of three Ag/Al samples.*

The lowest energy gap between LUMO and the lowest electrode work function allowed an increased number of thermally promoted electrons to flow through the film from the lowest electrode's work function to the highest one. As a result the direct current increases.

As mentioned before for the impedance measures in *Fig. 4.10*, to measure positive voltage values, samples were measured putting black tip (-) of voltmeter (tester, multimeter or TDV instrument) on Aluminum electrodes. Otherwise measuring

Ag-Al devices black tip was paced on Ag electrode to measure a positive voltage (according to literature aluminum and silver's work function data are Ag -4,26 eV higher than Al -4,28eV [78]. Moreover the almost equal values of the two Ag and Al metals energy work functions produce the similar effect that occurs when film is glues to the same electrodes, vanishing the power supply production because electrons, recharged on the highest work function electrode, do not implement enough their energy.

In order to use an electrode having an higher work function values respect to the Al one (trying to reduce the heat lose at the lowest temperature electrode), Silver electrode was used instead of aluminum electrode with modest improvement (*Fig.4.19*), so chipper aluminum was preferred to silver in our device.

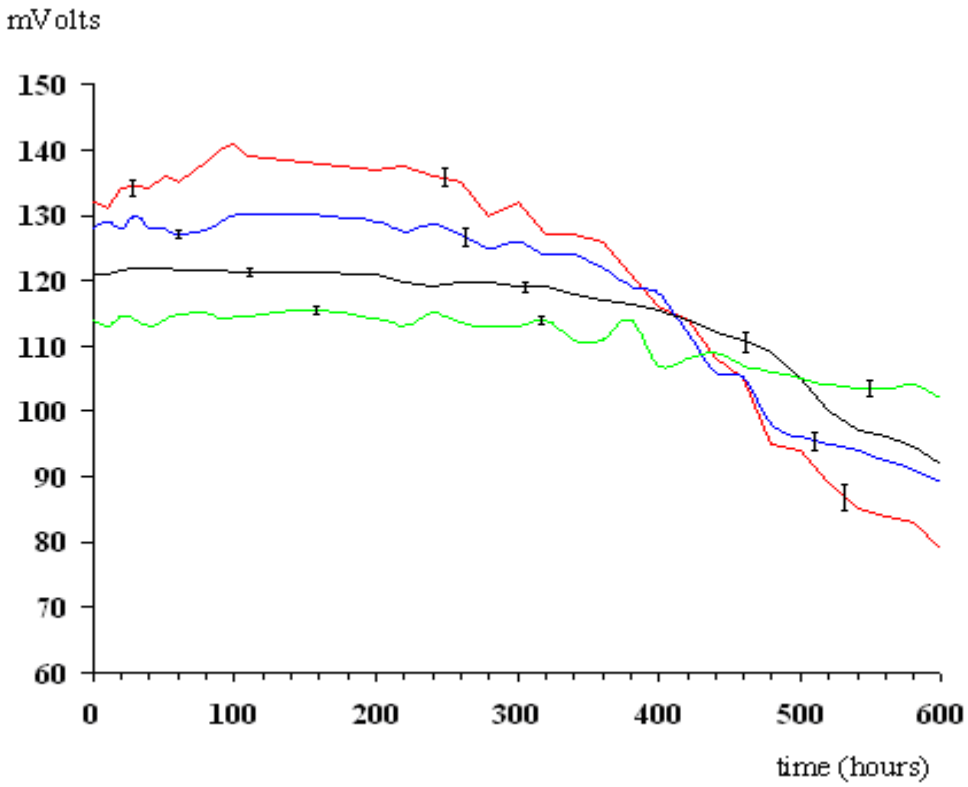

Fig.4.19 *PVFM-PC/Vet/Hydroquinone device voltages measured at the ends of 100KΩ serial impedance as function of time imposing a thermal gradient of 60 °C (20°CTc, 80°C Th): red line: the average data of three ITO-Ag devices; blue the average of three Cu-Ag samples; black the average three Pb-Ag samples; green line is referred to the average voltage value of five Ag-Zn devices.*

From *Fig.4.18* and *Fig.4.19*, we can conclude that Zn-Al devices shown interesting characteristics: maximum current reached kept in stationary state of 11,45 mÅ per square meter with no evident potential depletion (open circuit voltage is 0,27 Volts).

4.10 Devices thermoelectric power.

In the previous paragraphs the wt% composition and thickness SOFT film optimization (paragraphs from 4.4 to 4.7), the SOFT film thickness (paragraph 4.8) and the more convenient electrodes combination (paragraph 4.9) were shown, consequently in this section the thermoelectric power α is studied (see chapter 3). In order to calculate the thermoelectric power voltage behaviour respect several values of the thermal gradients imposed (from ΔT equal to 0°C to ΔT equal to 80°C) is investigated (*Fig 4.20*). Data show that thermo electrical conversion occurs even if a modest thermal gradient had been imposed and the voltage was significantly influenced by modest deviation of the thermal gradient. Furthermore it is possible to appreciate how the voltage increase linearly with the thermal gradient (*Fig.4.21*), thus the system did not reach yet the maximum conversion efficiency. It means that if we could use polymeric matrices and molecules stables at high temperatures, higher voltages than that reaches at ΔT=80°C, could be suitable for our system.

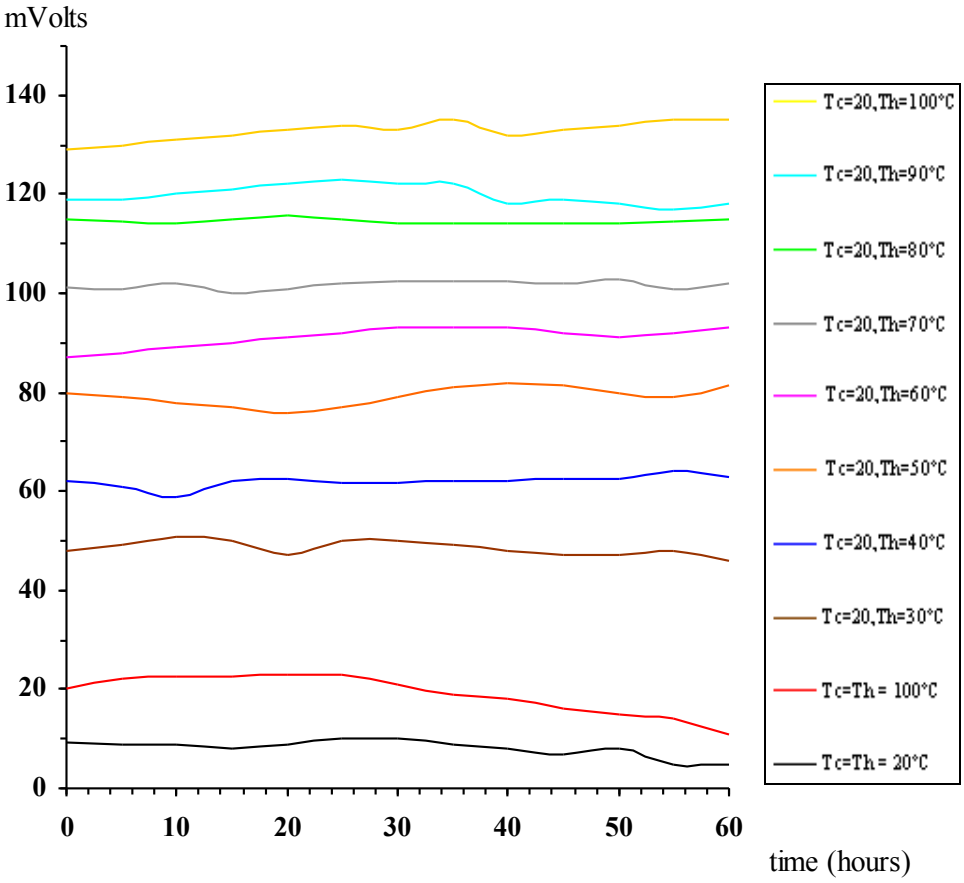

Fig.4.20 *Zn/PVFM-PC-Vet-Hydroquinone/Al device voltages measured at the ends of 100 KΩ serial impedance as function of time. Average data of two devices per each line was made.*

Thermoelectric power [70,72,86] of our novel organic thermovoltaic device is deduced from the *Fig. 4.21*, in which the thermal gradient is shown in function of voltage values . We obtained an α coefficient ($\Delta\phi$ /ΔT) almost equal to 1,2 mV/K versus the value of about 1,9 mV/K of the BDT,BBDT or BBBDT organic molecules[87] and several μV/K of the inorganic materials.

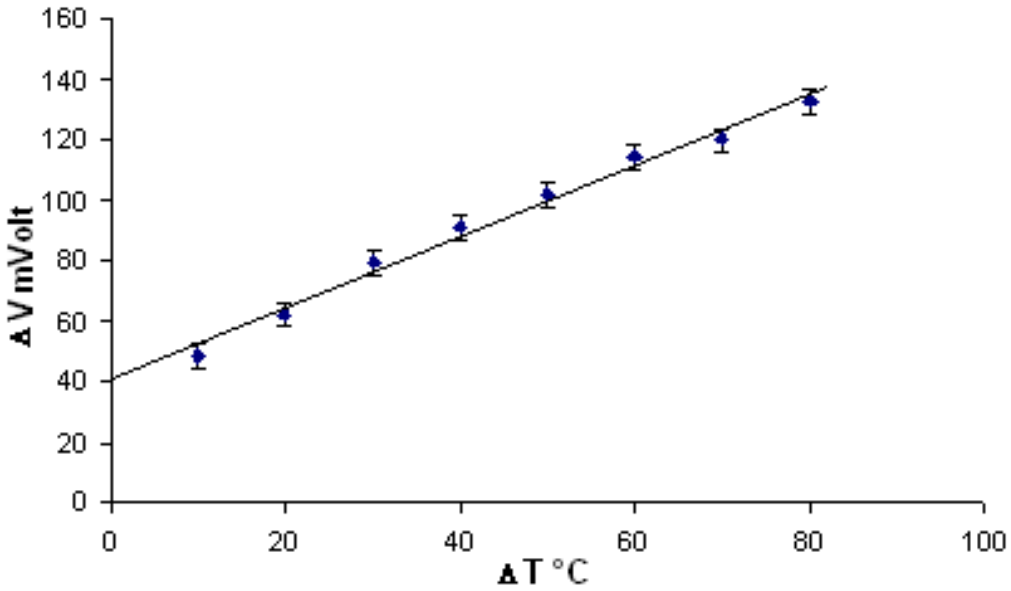

Fig.4.21 Average *voltages plotted against thermal gradient. Linear interpolation is shown.*

4.11 Experiments with 10KΩ external load.

During the experiment above illustrated, studying the device voltages, an 100KΩ external load has been always use. As mentioned above in 4.6 paragraph external load must not lower than 50KΩ, because if one tries to get bigger current in the external circuit, the voltage drops since the conduction in the inner film is very low and the electrodes are not recharged with an efficient mechanism. To understand if the SOFT devices works like power supply generator limited by current and not by voltage, some experiments were performed using an external impedance of 10KΩ. During the fist 60 hours of observation, a voltage discharge was measured (*Fig. 4.22*). Here the SOFT film inner resistivity (240-340KΩ·cm) did not allow to get an external impedance lower than its impedance inner value (Rint = 11-15KΩ). Anyway a novel stationary state was observed at lower voltage values and 20 mÅ per square meter current was measured for almost 100 hours.

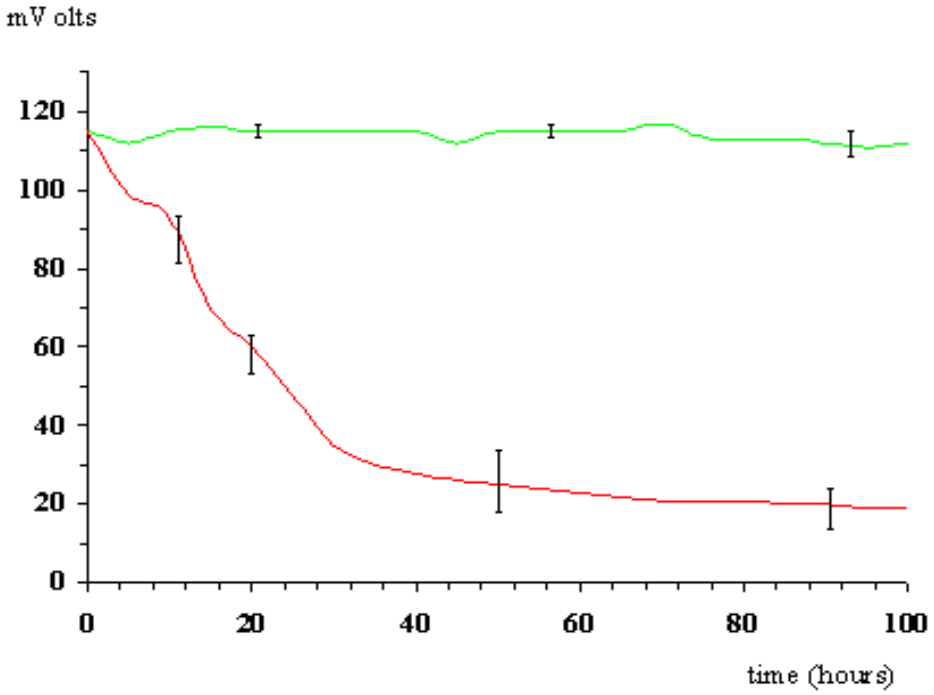

Fig.4.22 *Zn/PVFM-PC-Vet-Hydroquinone/Al device voltages measured at the ends of a serial impedance as function of time, imposing a thermal gradient of 60 °C (20°C Tc,80°C Th). Closed-circuit voltage was measured using 100KΩ (green line) and 10KΩ (red line) external impedances.*

Trying to explain if the deviation effect was due to a low thermovoltaic power generation, "switching" experiments are made using Zn/PVFM-PC-Vet-Hydroquinone/Al SOFT device, measuring the closed-circuit voltage on 100 KΩ and 10 KΩ (*Fig. 4.23*) impedances alternatively.

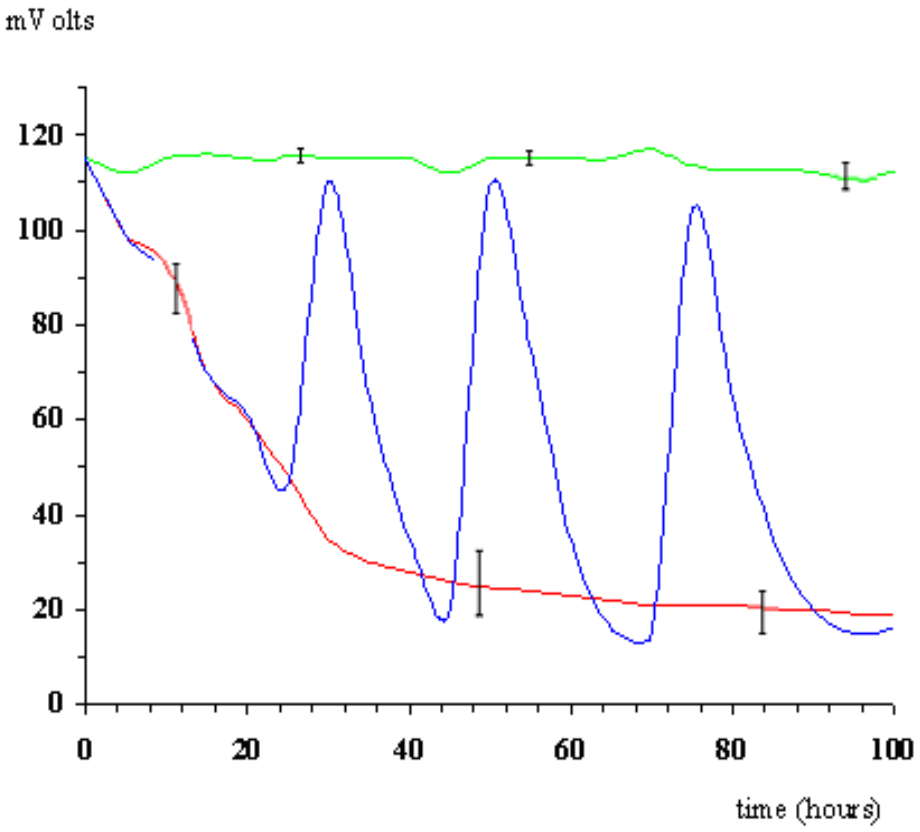

Fig.4.23 *Zn/PVFM-PC-Vet-Hydroquinone/Al device voltages measured at the ends of a serials impedance as function of time, imposing a thermal gradient of 60 °C (20°C Tc,80°C Th). Closed- circuit voltage was measured using 100KΩ (green line) and 10KΩ (red line) external impedances; blue line: the alternate use of 100KΩ and 10KΩ external loads.*

However looking at Fig.4.23 it is possible to see how the devices reach about the same voltage values anytime that the voltage is measured at the ends of 100KΩ external load. Thus is it possible to conclude that the devices shown an appreciated thermoelectric power, but the power supply decreases anytime that an external load lower than SOFT film inner impedance is used: Soft device is a power supply generator limited in current but not in voltage. Thus the limiting step in our devices is the too high films inner resistivity.

In the next paragraphs the use of metals nanodispersion inside polymeric matrices, in order to decrease the inner impedance without to create short-circuit connections inside the SOFT films has been studied.

4.12 Use of nanoparticles to decrease SOFT film inner impedance.

An interesting conclusion achieved by the last paragraph is that SOFT device power supply is strongly limited by too high SOFT film inner impedance. Thus the use of nanoparticles, as improvement to electric conductivity of the film has been take in account. Obviously the mechanism that acts to reduce the inner impedance must be not independent from the thermovoltaic active mechanism, otherwise a more conductive parallel line of electric conduction could be preferred by the electrons, creating a close-circuit system and avoiding any thermal activation. So, to accomplish at the goal must be considered nanoparticle having work functions between LUMO and the highest work function electrode work function values: nanoparticles having work function levels lower than one of the electrode work functions could induce a parallel electrons flow avoid the thermovoltaic mechanism. On other hand nanoparticles having work functions higher than LUMO level do not work in order to reduce the films impedance, because they could be not reachable by the electrons. In conclusion Silver nanoparticles (work function equal to -4.6eV [78]) have been used, considering the system energy levels settings**.**

Preliminary studies were conducted on Zn/PVFM-PC-Vet-Hydroquinone/Al SOFT film doped with silver nanoparticles (< 100 nm 99,5% pure), reducing the PVFM matrix wt% and using surfactant agents sodium dodecyl sulphate (NaDS) and UP400S Hielscher ultrasonic processor.

Fig. 4.24 shown the resistivity data as function of silver nanoparticles kept constant the surfactant agents (2%), PC(35%), Vet(26,4%) and Hydroquinone (5,9%) wt% concentration. The curve trend in *Fig. 4.24* reveals that resistivity drops sturdily around the critical value of 1,5-2% of silver nanoparticle ratio (ex. ρ = 360KΩ·cm for 1,2% of Ag nanoparticle weight concentration and ρ = 3600Ωcm for 2% of Ag nanoparticles wt %). According these information we

can conclude that silver forms aggregates bigger than its nanoparticle size when a silver weight percentage around 1,5% or higher is used.

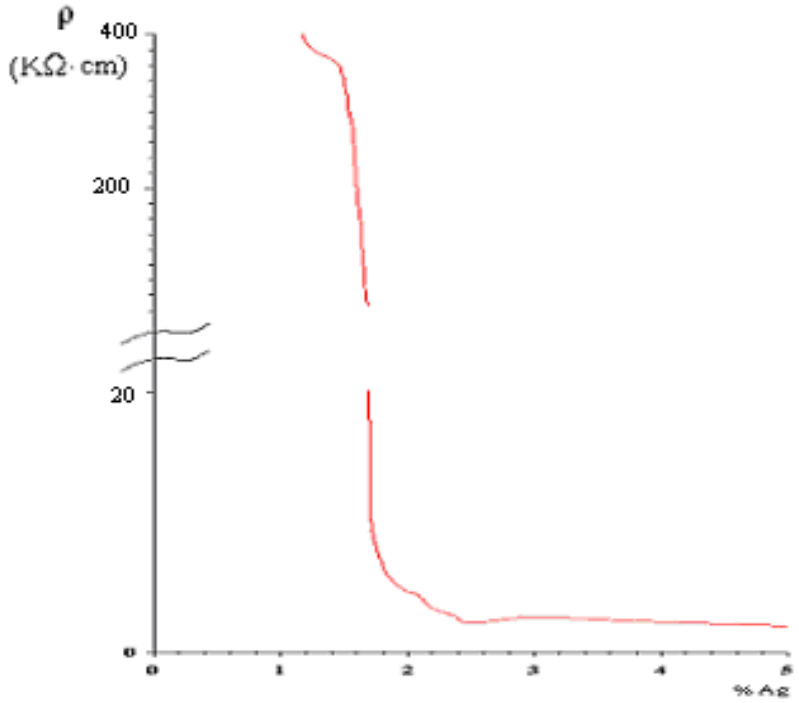

Fig.4.24 *Resistivity measured as function of Ag nanoparticles weight ratio in PVFM. PC, NaDS surfactant (2%), Vet(26,4%) and Hydroquinone (5,9%) solution was stirred by ultrasound waves per 24 hours.*

The presence of 1-100 micron aggregate was confirmed by optical microscope pictures (Fig 4.25a,b), thus films resistivity significantly drops when aggregates become like a conductive micro-loop that put in directly connection the two device's electrodes.

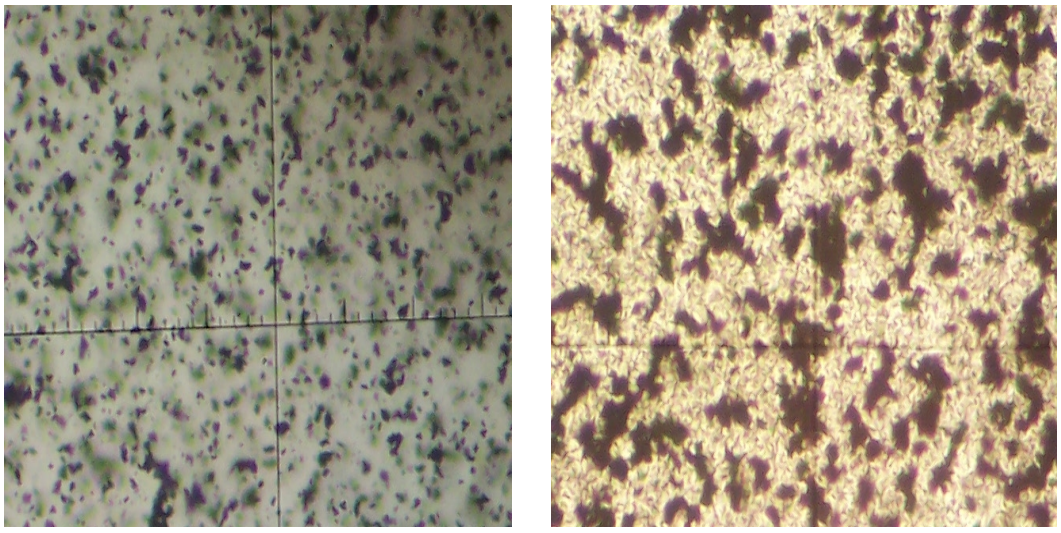

(a) *(b)*

Fig.4.25 *Optic microscope pictures of Ag nanoparticles in PVFM polymer (NaDS (1%) were used as surfactant agent): (a) 1,2% of Ag (b) 2% of Ag.*

Thus a good dispersing methods has to been investigate in order to use silver nanoparticles in SOFT devices.

4.12 Role of oxygen radicals.

As well known in literature, some radical reaction could occurs with the materials used into SOFT films [79,83]. To study the oxygen radicals effects on SOFT device, one Zn/PVFM-PC-Vet-Hydroquinone/Al sample is prepared under nitrogen atmosphere in aseptic glove-box and using anhydrous raw materials. Device was sealed with butylver® [88], that is an high oxygen and water impermeable poly(isobutene) polymer. The *Fig. 4.26* compares the voltages of the two samples in function of time: one sample was prepared under normal atmospheric condition (green line) the other sample was prepared under inert atmosphere (red line). The voltages functions are similar, excepting the for the initial voltage values that are slight higher in the samples containing no oxygen, respect the other.

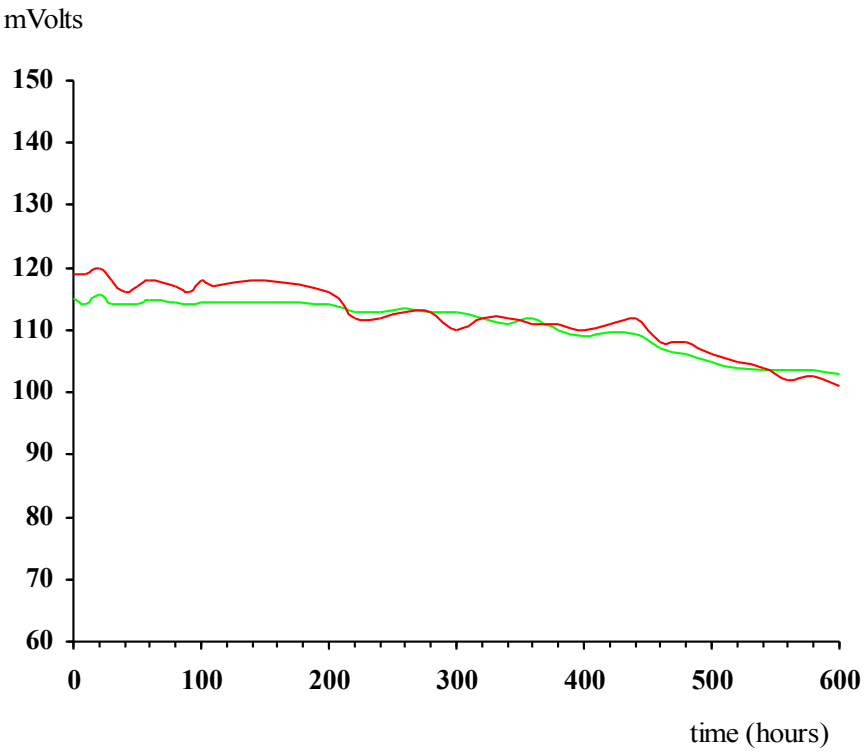

Fig.4.26 *Zn/PVFM-PC-Vet-Hydroquinone/Al device voltages measured at the ends of a 100KΩ serial impedance as function of time imposing a thermal gradient of 60 °C (20°C Tc,80°C Th). Green line: sample prepared under normal atmospheric condition. Red line: the sample prepared under inert atmosphere.*

However we do not know exactly if some reaction with oxygen could ruin the SOFT devices, because the oxygen radical collateral reaction effect could be observed even after several months. Thus a future task of this work should be to measure experiments for a time longer than 600 hours.

4.13 Reproducibility measures and life time of devices.

In order to appreciate the reproducibility of voltage measurements in function of the imposed thermal gradient, the voltage were studied for several days in a "cyclic experiment" varying the imposed thermal gradient. Five continuous cycles were measured and each cycle was monitored first increasing the thermal gradient

(keeping costant the Tc at 20°C and increasing the Th) and after decreasing it (keeping constant the Tc at 20°C and decreasing the Th), as shown in *Fig. 4.27*.

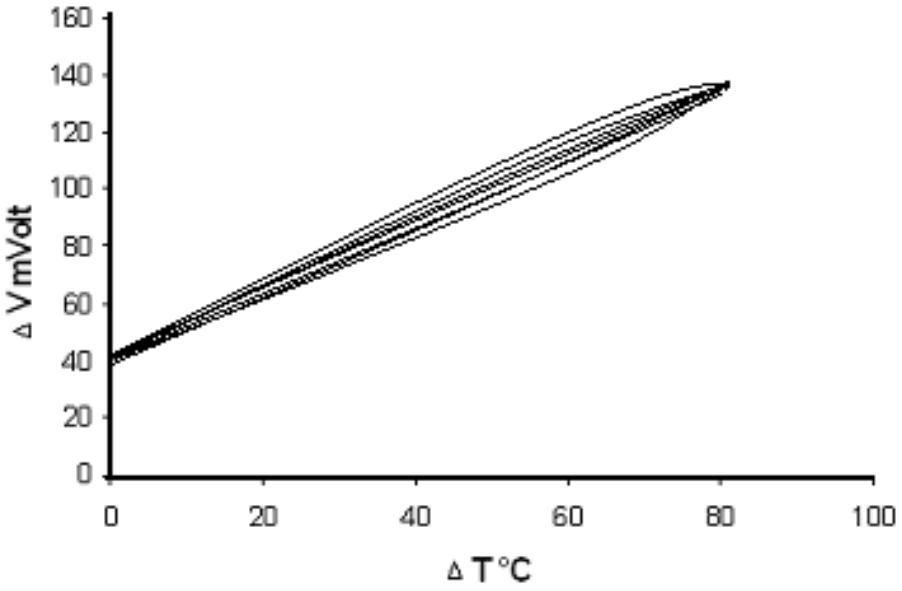

Fig.4.27 *Zn/PVFM-PC-Vet-Hydroquinone/Al voltages measured at the ends of a 100KΩ serial impedance as function of the imposed thermal gradient.*

The above graph shows that the initial gradient increasing-decreasing cycle differ slightly from the other cycles and that in any of them voltage values have being kept during the experimental measurements. The deviations are trivial and confirm a good stability and reproducibility of the novel organic thermovoltaic systems.

Conclusions.

In the course of this Ph.D. thesis attention has been devoted for the first time to the possibility to use a single plastic organic film in combination with metal electrodes to realize thermovoltaic elements, working in a thermodynamic stationary state, for direct conversion of the heat in electricity. The results show that this possibility can become real. It has been shown that blend of bipyrimidinium salts, organic solvents and supporting polymer is a first example of the hypothesized organic film. The devices shows a big seebeck coefficient equal to 1.2 mvolts/°K which is much bigger with respect to those obtained in more complex termoelectric devices made by inorganic semiconductors materials (0.5 mV/°K). The efficiency of the devices is not jet big enough to consent the technology applications of the devices since the electric current is limited by the impedance of the film. At least three order of magnitude in the current need to be gained to have application in direct heat energy conversion. But such aspect can be very much improved since organic film conductivity can be regulated by planning the active charge transport material in appropriate way. We think to the application of molecular oriented polymer with semiconductor properties. The bipyrimidium salts itself can be adapted to become semiconductor oligomers with liquid crystalline properties. A further line to better explore in the next future is to use dispersion of nanoparticles in polymer having matching Fermi levels and a tunable electric conductivity. In this way we believe that the cells here investigated can become useful energy converter tools. Another aspect which need to be emphasized is that the cells here investigated can be applied also as very stable thermal sensors.

Bibliography.

1. A. de Miguel and J. Bilbao *"Test reference year generation from meteorological and simulated solar radiation data"* Solar Energy Volume 78, Issue 6, June 2005, Pages 695-703.
2. José Goldemberg, Suani Teixeira Coelho, Plinio Mário Nastari and Oswaldo Lucon *"Ethanol learning curve-the Brazilian experience"* Biomass and Bioenergy Volume 26, Issue 3, March 2004, Pages 301-304.
3. H. S. Geller *"Ethanol Fuel from Sugar Cane in Brazil"* Annual Review of Energy
   Vol. 10: 135-164 (November 1985).
4. J. Goldemberg and O. Mielnik "*Energy balance of Brazil"* Energy for Sustainable Development Volume II No. 6 March 1996.
5. J. Twidell, A. D. Weir "Renewable Energy Resources" Taylor & Francis; 2 edition (December 16, 2005).
6. G. Boyle "Renewable Energy" Oxford University Press, USA; 2 edition (April 14, 2004).
7. A. Green "Global Energy - The Next Decade and Beyond" 2004-05 AAPG foundation distinguished lecture.
8. J. Auer "Technology to clean up coal for the post-oil era" Journal of business chemistry Vol. 4 Issue 2, 2007-11-15.
9. M.R. Raupach, G. Marland, P. Ciais, C. Le Quéré, J. G. Canadell, G. Klepper and C. B. Field *"Global and regional drivers of accelerating CO2 emissions"* PNAS June 12 2007 Vol. 104 Issue 24 Pag.10288-10293
10. J.A. Logan *"Nitrogen oxides in the troposphere: Global and regional budgets"* J. Geophys. Res. ; Vol.88 Issue C15.
11. S.J. Oltmans, E. Cuevas et all.*"Long-term changes in tropospheric ozone"* Atmospheric Environment Volume 40, Issue 17, June 2006, Pages 3156-3173.
12. T. E. Humphrey and H. Linke, Physica E **29**, 390-398 (2005).
13. R. Landauer, J. Stat. Phys. **53**, 233-248 (1988).
14. L. D. Hicks and M. S. Dresselhaus, Phys. Rev. B **47**, 12727 (1993).
15. L. D. Hicks and M. S. Dresselhaus, Phys. Rev. B **47**, 16631 (1993).
16. D. Vashaee and A. Shakouri, Phys. Rev. Lett. **92**, 106103 (2004).
17. M. F. O'Dwyer, T. E. Humphrey, C. Zhang, and R. Lewis, Phys. Rev. B **72**, 5330 (2005).
18. A. Shakouri and J. E. Bowers, Proc. 16th Annual Conference on Thermoelectrics, 636 (1997).
19. A. Shakouri and J. E. Bowers, Appl. Phys. Lett., 1234 (1997).
20. G. D. Mahan and J. O. Sofo, Proc. Nat. Acad. Sci (USA) **93**, 7436 (1996).
21. W. S. Capinski, H. J. Maris, T. Ruf, M. Cardona, K. H. Ploog, and D. S. Katzer, Phys.Rev. B **59**, 8105 (1999).
22. R. Venkatasubramanian, Phys. Rev. B **61**, 3091-3097 (2000).
23. T. Borca-Tasciuc, et al., Superlatt. and Microstruct. **28**, 199-206 (2000).
24. T. C. Harman, P. J. Taylor, M. P. Walsh, and B. E. LaForge, Science **297**, 2229 – 2232 (2002).
25. R. Venkatasubramanian, E. Siivola, T. Colpitts, and B. O'Quinn, Nature **413**,

597-602 (2001).
26. G. Chidichimo, M. DeBenedittis, J. Lanzo, B. C. Desimone, D. Imbardelli, B. Gabriele, L.Veltri, G. Salerno, "*Solid Thermoplastic laminable elctrochromic films"*, Chemistry Of Materials, 2007, Vol. 19, n. 3, pp. 353-358.
27. P.Reddy,S.Y.Jang,R.A.Segalman,A.Majumdar, Science, 2007, *315*, 1568.
28. G. Hoogers *"Fuel Cell Technology Handbook"* CRC Press September 27, 2002.
29. F. Mitlitsky, B. Myers, and A. H. Weisberg *"Regenerative Fuel Cell Systems"* Energy Fuels, 12 (1), 56 -71, 1998.
30. J.F. Manwell, J.G. McCowan and A.L. Rogers *"Wind Energy Explained: theory, design and application"* Wind Engineering, Volume 30, Number 2, March 2006 , pp. 169-170(2).
31. P. Söderholm and G. Klaassen *"Wind Power in Europe: A Simultaneous Innovation–Diffusion Model"* Environmental and Resource Economics Volume 36, Number 2 February, 2007.
32. A. Ucar and M. Inalli *"A thermo-economical optimization of a domestic solar heating plant with seasonal storage"* Applied Thermal Engineering Volume 27, Issues 2-3, February 2007, Pages 450-456.
33. *"Concentrating Solar Power: Energy from Mirrors"* U.S. Department of Energy (DOE) by the National Renewable Energy Laboratory (NREL), a DOE national laboratory March 2001.
34. R. W. Miles, G. Zoppi and Ian Forbes *"Inorganic photovoltaic cells"* Materials today Volume 10, Issue 11, November 2007, Pages 20-27.
35. W. R. L. Lambrecht and B. Segall *"Interface-bond-polarity model for semiconductor heterojunction band offsets"* Phys. Rev. B 41, 2832 - 2848 (1990).
36. R.N. Hall*"Silicon photovoltaic cells"* Solid-State Electronics, vol. 24, July 1981, p. 595-616.
37. Solar energy company *"Solarcentury"* , Waterloo, London UK.
38. B. A. Andersson and S. Jacobsson *"Monitoring and assessing technology choice: the case of solar cells"* Energy Policy Volume 28, Issue 14, November 2000, Pages 1037-1049.
39. B. A. Gregg and M. C. Hanna *"Comparing organic to inorganic photovoltaic cells: Theory, experiment,and simulation"* Journal of Applied Physics Volume 93, Number 615 March 2003.
40. B. O'Regan and M. Grätzel *"A low-cost, high-efficiency solar cell based on dye-sensitized colloidal TiO2 films"* Nature 353, 737 - 740 (1991).
41. C. J. Brabec, N. S. Sariciftci, J. C. Hummelen *"Plastic Solar Cells"* Advanced Functional Materials Volume 11, Issue 1 , Pages 15 – 26.
42. S. E. Shaheen, C. J. Brabec and N. S. Sariciftci *"2.5% efficient organic plastic solar cells"* Applied Physics LettersVolume 78, Number 6 5 February 2001.
43. G Yu, J Gao, JC Hummelen, F Wudl, AJ Heeger *"Polymer Photovoltaic Cells: Enhanced Efficiencies via a Network of Internal Donor-Acceptor Heterojunctions"* Science, Vol. 270 15 December 1995.
44. N. F. Mott *"Note on the contact between a metal and an insulator or semiconductor"* Proc.Cambr.Phil. Soc.34, 568-572 (1938).

45. J. J. Dittmer, E. A. Marseglia and R. H. Friend "Electron Trapping in Dye/Polymer Blend Photovoltaic Cells" Advanced Materials Volume 12, Issue 17 , Pages 1270 – 1274.
46. P. Peumans and S.R. Forrest *"Very-high-efficiency double-heterostructure copper phthalocyanine/C 60 photovoltaic cells"* Appl. Phys. Lett, Vol. 79-1 2 July 2001.
47. P. Peumans, S. U. and S.R. Forrest *"Efficient bulk heterojunction photovoltaic cells using small-molecular-weight organic thin films"* Nature 425, 158 - 162 (2003).
48. K. Yamashita, T. Suzuki and T. Hino *"Photovoltaic Properties of Thin Polymer (PVK-TNF) Films"* Jpn. J. Appl. Phys. Vol. 21 (1982) 1506-1508.
49. L. S. Li and A. D. Q. Li *"Probing Surface Electronic Potentials and Photovoltaic Effects of Self-Assembled Multilayers of Metal Phthalocyanine and Oligomeric Viologen on Conductive Substrates"* Phys. Chem. B, 105 (41), 10022 -10028, 2001.
50. H. Hoppe, N. S. Sariciftci *"Organic solar cells: An overview"* Journal of Materials Research, Volume 19 Issue 7 Pag.1924-1945, July 2004.
51. N. C. Greenham, X. Peng, and A. P. Alivisatos *"Charge separation and transport in conjugated-polymer/semiconductor-nanocrystal composites studied by photoluminescence quenching and photoconductivity"* Phys. Rev. B 54, 17628 - 17637 (1996).
52. S. R. Forrest *"The path to ubiquitous and low-cost organic electronic appliances on plastic"* Nature 428, 911 - 918 (2004).
53. M. Shim, C. Wang, and P. Guyot-Sionnest *"Charge-Tunable Optical Properties in Colloidal Semiconductor Nanocrystals"* J. Phys. Chem. B 2001, 105, 2369-2373.
54. D.J. Milliron, I. Gur, A.P. Alivisatos *"H ybrid Organic–Nanocrystal Solar Cells"* MRS January 2005.
55. W.J.E. Beek, L.H. Slooff, M.M. Wienk, J.M. Kroon and R.A.J. Janssen *"Hybrid Solar Cells Using a Zinc Oxide Precursor and a Conjugated Polymer"* Advanced Functional Materials Volume 15, Issue 10 , Pages 1703 – 1707.
56. W.J.E. Beek, M.M. Wienk and R.A. J. Janssen *"Hybrid polymer solar cells based on zinc oxide"* J. Mater. Chem., 2005, 15, 2985 – 2988.
57. C.J. Brabec, J.A. Hauch, P. Schilinsky and C. Waldauf *"Production Aspects of Organic Photovoltaics and Their Impact on the Commercialization of Devices"* MRS January 2005.
58. N. Narihito and S. Koji *"The present state of the thermophotovoltaic system and its selective emitter materials technology"* Oyo Butsuri, Vol.76-3 Page 281-285 (2007).
59. Z. Bian and A. Shakouri "*Design of Heterostructures for High Efficiency Thermionic Emission*" MRS symposium F 2005.
60. D. Vashaee and A. Shakouri *"Improved Thermoelectric Power Factor in Metal-Based Superlattices"* Phys. Rev. Lett. 92, 106103 (2004).
61. R.K. Huang, R.J. Ram, M.J. Manfra, M.K. Connors, L.J. Missaggia, and G.W. Turner *"Heterojunction thermophotovoltaic devices with high voltage factor*" J. Appl. Phys. 101, 046102 (2007).

62. V.M. Andreev, A.S. Vlasov, V.P. Khvostikov, O.A. Khvostikova, P.Y. Gazaryan, S.V. Sorokina, and N.A. Sadchikov *"Solar Thermophotovoltaic Converters Based on Tungsten Emitters"* Journal of Solar Energy Engineering August 2007 Volume 129, Issue 3, pp. 298-303.
63. Stone, K.W. Fatemi, N.S. Garverick *"Operation and component testing of a solar thermophotovoltaic powersystem",* Photovoltaic Specialists Conference, 1996., Conference Record of the Twenty Fifth IEEE
64. P. J. Price *"Theory of Transport Effects in Semiconductors: Thermoelectricity"* Phys. Rev. 104, 1223 - 1239 (1956).
65. F.J. DiSalvo *"Thermoelectric Cooling and Power Generation"* Science 30 July 1999 Vol. 285. no. 5428, pp. 703 – 706.
66. J.R. Lim, J.F. Whitacre, J.P. Fleurial, C.K. Huang, M.A. Ryan, N.V. Myung *"Fabrication Method for Thermoelectric Nanodevices"* Advanced Materials Volume 17, Issue 12 , Pages 1488 – 1492.
67. R. Venkatasubramanian, E. Siivola, T. Colpitts & B. O'Quinn *"Thin-film thermoelectric devices with high room-temperature figures of merit"* Nature 413, 597 - 602 (2001).
68. G.Chen, M.S. Dresselhaus, G. Dresselhaus, J.P. Fleurial and T. Caillat *"Recent developments in thermoelectric materials"* International Materials Reviews, Volume 48, Number 1, February 2003 , pp. 45-66(22).
69. A. Schock, V. Sankarankandath, M. Shirbacheh "Requirements and designs for Mars Rover RTGs" Energy Conversion Engineering Conference, 1989. IECEC-89.
70. I. Prigogine *"Physica"*, 15 (1949), 272-284.
71. S.R. de Groot and P. Mazur "*Non-equilibrium Thermodynamics*" 1969.
72. I. Prigogine "Etude Thermodynamique des processus irreversibles" 1947.
73. L. Onsager *"Reciprocal Relations in Irreversible Processes"* Phys. Rev. 37, 405 - 426 (1931).
74. N. Oyama, T. Ohsaka, H. Yamamoto and M. Kaneko, *"Charge-Transfer Reactions in Pendant Viologen Polymers Coated on Graphite Electrodes and at Electrode/Pendant Viologen Polymer Film Interfaces"* J. Phys. Chem. 1986, 90, 3850-3856.
75. J. Lanzo, M. De Benedittis, B. C. De Simone and G. Chidichimo, *"Improvement of response times in electrochromic switchable nematic emulsions"*. Materials Letters, 2007, Vol. 61, pp. 3349-3351.
76. J. Lanzo , M. De Benedittis, B. C. De Simone, D. Imbardelli, P. Formoso, S. Manfredi, G. Chidichimo, *"Photoelectrochromic switchable nematic emulsions"*. Journal of material chemistry, 2007, Vol. 17, n. 14, pp. 1412-1415.
77. G. Chidichimo, M. De Benedittis, J. Lanzo, B. C. De Simone, D. Imbardelli, B. Gabriele, L. Veltri, G. Salerno, *" Solid Thermoplastic Laminable Electrochromic Film"*. Chemistry Of Materials, 2007, Vol. 19, n. 3, pp. 353-358.
78. H.L. Skriver and N.M. Rosengaard *"Surface energy and work function of elemental metals"* Phys. Rev. B 46, 7157 - 7168 (1992).
79. P. M. S. Monk, R.J.Mortimer, D.R. Rosseinsky, *"Electrochromism: Fundamental and applications"*, VCH 1995.

80. D.R. Li, H. Meng "*Organic Light-emitting Materials and Devices"*, CRC Taylor & Francis.
81. *"Physics Briefs"*, American Institute of Physics, 1979.
82. M. R. Bryce *"Recent progress on conducting organic charge-transfer salts*" Chem. Soc. Rev., 1991, 20, 355 – 390.
83. P. M. S. Monk *"The viologens"*, John Wiley & sons 1998.
84. E. De Castro *"Fondamenti di elettronica"*, UTET.
85. Sigma Aldrich website www.sigmaaldrich.com.
86. D. Mitrani, J.A. Tome, J. Salazar, A. Turo, M.J. Garcia, J.A. Chavez, ***"****Methodology for extracting thermoelectric module parameters*" Instrumentation and Measurement Technology Conference, 2004. Proceedings of the 21st IEEE.
87. P. Reddy,S.Y. Jang,R.A. Segalman,A. Majumdar, *"Thermoelectricity in Molecular Junctions"***,** Science, 2007, 315, 1568.
88. *Fenzi* industries, www.fenzigroup.it.

Appendices

A. Abbreviations

Ω	Ohm
A	Electron acceptor
AFC	Alkaline Fuel Cells
BAGD	Bisphenol-A-glycerolate(1-glycerol/phenol)diacrylate
BDT	Benzene-dithyol semiconductor molecules
BOS	Balance of system
C60	Fullerenes
CSP	Concentrating solar power systems
CTC	Charge-Transfer Complex
D	Electron donor
DMFC	Direct Methanol Fuel Cells
DOS	Electronic density of states
DSSc	Dye sensitized solar cells
EA	Electron affinities
EFM	Electromotive force
eV	Electron Volts
FCs	Fuel cells
FFC	Fossil fuels combustion
HOMO	Highest occupied molecular orbital
HOPVc	Organic/inorganic hybrid cell
IPVc	Inorganic photovoltaic cell
ITO	Indium Tin Oxide
LMW	Low molecular weight organic molecules
LUMO	Lowest unoccupied molecular orbital
MBE	Molecular beam epitaxy
MCFC	Molten Carbonate Fuel Cells
MDMO-PPV	Poly[2-methoxy-5-(3',7'-dimethyloctyloxy)-1,4-phenylene vinylene]
MEH-PPV	Poly[2-methoxy-5-(2'-ethyl-hexyloxy)-1,4-phenylenevinylene]
OMVPE	Vapor-phase epitaxy
OPVc	Organic photovoltaic cell
P3HT	Poly-3-hexylthiophene
PAFC	Acid Fuel Cells
PAN	Polyaniline
PC	Propylene carbonate
PCBZ	Polycarbazole
PEMFC	Proton Exchange Membrane Fuel Cells
PI	Ionisation potentials
POPV	Organic semiconductor polymers cell
PPV	Poly(phenylenevinylenes)
PT	Polythiophenes
PV	Photovoltaic systems

PVB	Poly(vinyl butyral-co-vinyl alcohol-co-vinyl acetate)
PVc	Photovoltaic cell
PVFM	Poly(vinyl formal)
QD	Quantum dot
RFC	Regenerative Fuel Cells
SE	Seebeck effect
SHS	Solar heating systems
SOFC	Solid Oxide Fuel Cells
SOFT	Single Organic Film Thermovoltaic
TDV	Thermoelectric device voltmeter
TE	Thermoelectric
TERs	3',4'-bis-(2-metossi-etil)-[2,2';5',2'']tertiophene and 3',4'-Bis[(Metossicarbonil)-metil]-[2,2';5',2"]tertiophene
Tg	glass transition temperature
TI	Thermionic devices
TPV	Thermophotovoltaic devices
TVC	Thermovoltaic celles
Varc	1-(11-(acryloyloxy)undecyl)-4,4'-bipyridin-1-ium bromide
Vet	1,1'-diethyl-4,4'-bipyridine-1,1'-diium diperchlorate
W	Watt
ZT	Figure of merit

Appendices

B. List of figures

C. List of tables

"Bisogna volere l'impossibile,
perché l'impossibile accada"
Eraclito
Efeso (550 a.C. – 480°.C.).

Alla fine di questo nuovo traguardo e con lo sguardo rivolto verso il futuro che mi attende, mai in passato più di oggi, voglio ringraziare le persone che, contribuendo a questo lavoro di tesi direttamente ed indirettamente, hanno contribuito a far crescere in me pensieri, opinioni, certezze, principi ed ideali che resteranno con me per sempre.
Le prime, troppo poche, parole vanno alla mia famiglia. In particolare al pensiero che loro hanno sempre avuto di me. In questi anni ho rivisto in loro e risentito nelle loro parole, come riflesse, le mie aspettative, i miei sogni ed la fiducia nelle mie potenzialità che tempo fa appartenevano soltanto al lontano mondo della mia adolescenza. Questi stimoli mi hanno permesso di capire cosa volevo dal mio lavoro e soprattutto dalla mia vita e se sono arrivato a qualche conclusione lo devo soprattutto a loro.
Se fin ora ho potuto apprezzare le gioie di ciò che mi circondava, anche quando il lavoro si faceva difficile e per certi aspetti deprimente, lo devo alla mia amata Simona. E' stata una complice nelle avventure, una compagna nelle disavventure ed una consigliera in ogni occasione; amica e confidente: la migliore amica che io abbia mai avuto e che mai avrò. La moglie che voglio accanto a me per il resto della mia vita.
Un ringraziamento particolare va al caro Prof. Giuseppe Chidichimo, sempre prodigo di insegnamenti sia nel lavoro di ricerca che nella vita. Lo considero il mio maestro oltre che il mio professore. Ha creduto in me, in ciò che facevo, molte volte più di quanto ci credessi io, mi ha insegnato a non abbattermi, ad non arrendermi, ad essere positivo sempre e comunque e che "quando bisogna fare le cose conviene farle bene, tanto il tempo necessario a fare una cosa bene o meno bene è sempre quello, è solo una questione di usare meglio la testa". A lui devo tutto il mio lavoro di tesi in questi anni.
Di grande sostegno è stata un'altra persona all'interno del gruppo di ricerca, la mia cara amica Patrizia. Con lei ho sempre potuto parlare di tutto apertamente e mi ha sempre fornito il sostegno che cercavo aiutandomi in ogni difficoltà.
Sento di ringraziare tutte le persone del gruppo di ricerca in cui ho lavorato: Daniela, Bruna, Maurizio, Jessica, Annaelia, Lucia, Daniela, Sabrina, Sabrina, Sasha e Lucia.
Inoltre voglio ringraziare il Prof. G.Salerno, già mio relatore della tesi di laurea, e collaboratori per quanto riguarda il sostegno durante le sintesi di composti organici e la progettazione e l'impiego di nuove molecole.
Infine, un ringraziamento speciale va ai miei due coordinatori di dottorato: al Prof. M.Longeri e al Prof. C.Versace, i quali hanno preso le difese di noi dottorandi sempre, comunque e a prescindere.

GRAZIE A TUTTI DI CUORE.